CHARACTERIZATION OF CONVENTIONAL HMA MIXTURES USING SIMPLE PERFORMANCE TESTING PROTOCOLS

Muhammad Junaid
(NUST201362903MSCEE15113F)

A thesis submitted in partial fulfillment of

the requirements for the degree of

Master of Science

in

Transportation Engineering

NATIONAL INSTITUTE OF TRANSPORTATION (NIT)
SCHOOL OF CIVIL AND ENVIRONMENTAL ENGINEERING (SCEE)
NATIONAL UNIVERSITY OF SCIENCES & TECHNOLOGY (NUST)
SECTOR H-12, ISLAMABAD, PAKISTAN
(2016)

Certified that the contents and form of thesis titled **"Characterization of Conventional HMA mixtures Using Simple Performance Testing Protocols"** submitted by Muhammad Junaid have been found satisfactory for the requirement of Master of Science degree.

Supervisor: _____

Dr. Muhammad Irfan, Ph.D.
Department of Construction Engineering & Management
College of Civil Engineering
National University of Sciences and Technology, Islamabad

Co-Supervisor: _____

Dr. Arshad Hussain, Ph.D.
Department of Transportation Engineering
School of Civil and environmental Engineering
National University of Sciences and Technology, Islamabad

CHARACTERIZATION OF CONVENTIONAL HMA MIXTURES USING SIMPLE PERFORMANCE TESTING PROTOCOLS

by

Muhammad Junaid

(NUST201362903MSCEE15113F)

A Thesis

of

Master of Science

Submitted to

Department of Transportation Engineering

National Institute of Transportation (NIT)

School of Civil and Environmental Engineering (SCEE)

National University of Sciences and Technology (NUST)

Islamabad

In partial fulfillment of the requirements for the degree of

Master of Science in Transportation Engineering

2016

DEDICATED

TO

MY LOVING PARENTS

WHO GAVE ME LOT OF INSPIRATION,

COURAGE &

SUPPORTED ME MORALLY &

FINANCIALLY FOR MY STUDIES

ACKNOWLEDGEMENTS

First of all, I am thankful to almighty Allah for making me able to complete this journey. After that I would like to thank my thesis supervisor Dr. Muhammad Irfan for his guidance during this project. I also thank my Co-Supervisor Dr. Arshad Hussain for his help and kind behavior during all phases of the lab work and also in analysis part of the thesis. Without his encouragement it would have been very difficult for me to complete my thesis.

I would also like to thank my committee members Dr. Tariq Mahmood and Dr. Bilal Khurshid for their help and gentle behavior. I am also grateful to Yasir Ali for his help in developing a research proposal for me and also for the efforts he made to improve my research paper before submission. I would also like to pay gratitude to staff of NIT Transportation lab Mr. Mehmmod, Mr, Hidayat and Mr. Iftikhar for their friendly behavior and for helping me in my lab work. I also appreciate Engr. Hmaza Masud and Engr. Muhammad Junaid for their help in this research.

Last but not the least I want to express my love for my father for an unconditional financial support during my MS studies. This would have been impossible without you.

TABLE OF CONTENTS

LIST OF ABBREVIATIONS

AASHTO – American Association of State Highway & Transportation Official

AC – Asphalt Concrete

ANOVA – Analysis of Variance

AMPT – Asphalt Mix Performance Tester

ASTM – American Society for Testing and Materials

G_{mb} – Mix Bulk Specific Gravity

G_{mm} – Mix Theoretical Maximum Specific Gravity

HMA – Hot-Mix Asphalt

LVDT – Linear Variable Differential Transformer

MEPDG – Mechanistic Empirical Pavement Design Guide

JMF – Job Mix Formula

NHA – National Highway Authority

LVDTs – Linear Variable Differential Transducers

NCHRP – National Cooperative Highway Research Program

NMAS – Nominal Maximum Aggregate Size

SGC – Superpave Gyratory Compactor

SHRP – Strategic Highway Research Program

SPT – Simple Performance Testing

VA – Volume of Air Voids

VFA – Voids filled with Asphalt

VMA – Voids in Mineral Aggregate

OBC – Optimum Binder Content

LIST OF FIGURES

LIST OF TABLES

ABSTRACT

In this research Simple Performance Testing of HMA mixes is carried out using Asphalt Mix Performance Tester (AMPT). The three candidate tests include dynamic modulus |E*|, flow number (FN) and flow time (FT) tests which are conducted on two wearing course gradations (SP A and NHA A) and two base course gradations (SP B and DBM). The bitumen binder used are of two penetration grades which are 40/50 and 80/100 grade. Dynamic modulus (E*) test was conducted on four different temperatures i.e. 4.4°C, 21.1°C, 37.7°C and 54.4°C and six different loading frequencies i.e. 25Hz, 10Hz, 4Hz, 1Hz, 0.5Hz and 0.1 Hz. Flow Number and Flow Time tests were conducted at a single temperature of 54.4ºC and a stress level of 300 Kpa. Optimum binder contents were obtained using Marshal Mix design method and the samples for performance testing were prepared using Superpave Gyratory Compactor (SGC) and then cored and trimmed to the specified dimensions. The |E*| test results were subjected to non-linear optimization technique to develop stress-dependent master curves which revealed that penetration grade of bitumen significantly influence the stiffness of mixtures. Two level factorial design of experiment technique was utilized to find the simultaneous effect of independent variables and their interaction on the response. Three factors were found to have a significant effect on the values of dynamic modulus i.e. temperature, frequency and binder viscosity. Mixture prepared using 80/100 pen grade binder were more temperature susceptible. Fatigue parameter was calculated using the dynamic modulus and phase angle values and the results revealed that fatigue parameter value is low for mixtures with 80/100 binder which means that mixtures with 80/100 binder are less fatigue susceptible. Performance modeling was also carried out to develop regression equations to predict the values of dynamic modulus using temperature, frequency, viscosity of the binder and NMAS as independent variables for both wearing and base course mixtures with a coefficient of determination (R^2) value of 0.84 and 0.86 respectively. Flow number and flow time results were also analyzed to determine the rutting susceptibility of mixtures. The mixtures prepared using 40/50 binder accumulated less strains as compared to the 80/100 binder making them less rut susceptible.

CHAPTER 1

INTRODUCTION

1.1 BACKGROUND

Transportation plays a leading role in the development and the socio-economic growth of any country no matter whether it is developed or developing. If the transportation facilities of a country are enhanced they will lead to rapid movement of goods and people resulting in increased economic growth rate and development of a country. Building new airports, roads and railways improves the existing transportation system and also provides massive employment opportunities. On the other hand, lack of transportation facilities may lead to delays and can become a barrier in the development and socio-economic growth of a country. Transportation modes include road transport, rail transport, space transport and pipeline transport etc.

Road transport is the major component of a transportation system. Asphaltic concrete pavements also known as flexible pavements are most commonly used form of the roads all over the world. Much importance is being given to constructing asphalt pavements which have extended life span and can provide the desired level of comfort and ease thus to serve the purpose for which they are intended. Cost-effective and acceptable design also plays an important role in hot mix asphalt (HMA) pavement structures. The main ingredients used in asphaltic concrete pavements are aggregates and bitumen binder upon which the response of pavements is mainly dependent. In order to achieve the desired performance, it is vital to build up a relationship between the ingredients of HMA and its performance.

Distresses associated with pavement structure includes rutting, fatigue cracking, stripping, ageing and raveling etc. Factors contributing to these distresses include severe loading, temperature, moisture, design deficiencies, poor construction practices and material specifications. Due to which pavements fail before finishing their service life and requires maintenance and rehabilitation which in turn causes enormous burden on nation's wealth. This premature failure of pavements is a global problem. So there is a need for the development and

improvement of mix design methodologies and testing technologies to characterize the HMA materials and enhance laboratory testing methods.

AASHO Road test was initiated after World War 2 because due to increased traffic demands, heavier loadings and high tire pressures, road pavements started to fail readily and a need was felt to design pavements structures based on pavement distresses and their responses so that pavement performance can be predicted before construction of the pavements and develop design of cost effective pavements which can fulfill their functions and are also aesthetic, comfortable, economic and environmental friendly. This was possible only by making a shift from the tradition of designing pavements based on experience and empiricism to pavements design based on evaluation of pavement distresses and responses based on laws on mechanics. This need was the basic motivation for the AASHO road test (Jenkins 2000).

It was a great effort to quantify the complex interaction between road pavement failure, traffic loading and material ingredients of the road such as aggregate and binders. The trial section was a close loop in Ottawa subjected to truck loadings. The resulting pavement distresses was recorded and analyzed so that existing design procedures can be modified and improved. The current empirical design methodology is based on AASHTO Road Test. It was revised and improved several times in 1961, 1972 and 1986. In 1986 version techniques were developed for advanced material characterization. In 1993, it was revised again to incorporate more consistency between flexible and rigid pavement. It was more focused on pavement rehabilitation process. Due to its empirical nature the use of 1993 AASHTO Design Guide is getting less popular day by day. It is completely empirical based on performance equations derived from the test conducted on one set of material, one environment and one test location.

The major step towards the mechanistically designed pavements was taken when AASHTO in collaboration with Federal Highway Authority and NCHRP started a project designated as NCHRP Project 1-37A in order to develop mechanistic empirical pavement design procedure.

A basic requirement for the M-E Pavement Design Guide is characterization of materials so that material input can be provided for the design process in addition to loading, traffic and environmental conditions. In order to fulfill this requirement FHWA and NCHRP started the

development and funding of research projects and recommended Simple Performance Test Protocols for characterization of HMA mixtures (Bhasin 2004).

Dynamic modulus is a major performance test for characterizing asphaltic concrete and can be performed over different temperatures in the range of (-10 to 60°C) and different loading frequencies (25 Hz to 0.01 Hz). It is an essential input parameter used in MPEDG software for the characterization of materials and aids pavement structural design process and can be used to develop models for the prediction of pavement response. Along with dynamic modulus flow number and flow time are also used to fully recognize the visco-elastic nature of asphalt mixtures (Witzak 2002).

The flow number is carried out at a single temperature and a single effective stress level. It is used to evaluate pavement rutting performance. While performing this test, repeated load is applied axially on the specimen with 0.1 sec of loading time after 0.9 sec of rest period or dwell period which allow recovery of the elastic strains. And the load cycle at which tertiary flow just begins is designated as flow number. The difference between flow time and flow number is changed loading pattern. In flow time test static load is applied axially on the sample and the strains are measured for a definite time period or until failure. This test is also used to predict rutting performance and visco-elastic behavior of asphaltic concrete mixtures under static stresses.

1.2 PROBLEM STATEMENT

Pakistan produces an overall transport demand of more than 239 billion passengers-km and 153 billion tons-kilometer per year. Most of which is achieved by using road transportation system. Roads infrastructure of Pakistan is extensive and diverse consisting of motorways, highways, local roads and streets serving over 180 million people. But it is still in its development phase and needs a lot of improvement in terms of new roads construction and rehabilitation of existing roads. A significant percentage of total GDP is spent every year on the construction, maintenance and rehabilitation of roads to provide adequate level of service and level of safety and mobility to road users. The total length of Motorways and National Highway is 5,950 miles, only 3.65% of the total roads but move 80% of total traffic load of Pakistan. Due to such heavy demand pavements fail to complete their service life and the result is premature

failure which is a global problem and a matter of great concern for road engineers and scientists. Another reason for premature failure of flexible pavements in Pakistan is use of structural design approach based on the 1993 AASHTO design guide and Marshall Mix design procedure for bituminous mixture designs which are empirical.

Premature failure of flexible pavements within few years of construction is a global problem. The first significant step taken to solve this problem was the development of the AASHTO 2002 Mechanistic-Empirical Pavement Design Guide (M-EPDG) and software (M-EPDS) as part of NCHRP Project 1-37A. In order to improve mix design technology of Pakistan and apply the new ME pavement design guide in road design projects it is necessary to characterize the materials and mixtures so we can have a material database for the M-EPDG software. Present study involves the characterization of mixtures using Simple Performance testing for the implementation of M-EPDG approach. In NIT studies has been conducted recently under National Road Research Project involving characterization of the HMA and SMA mixtures based on their stiffness, fatigue and rutting performance. This study is carried out to bridge the gaps of testing plan of these studies and also augment the findings of these studies.

1.3 OBJECTIVES OF THE STUDY

The objectives of this research are as follow:

i) To characterize and compare the mixtures with different penetration grade bitumen binder based on their stiffness parameter (Dynamic Modulus and Development of Master Curves).

ii) To estimate the resistance to fatigue of different asphalt concrete mixtures (Calculation of Fatigue Parameter)

iii) To evaluate and compare the rutting susceptibility of HMA mixes using repeated axial load test (Flow Number test) and static creep loading test (Flow Time Test)

1.4 SCOPE OF THE THESIS

In order to achieve above mentioned objectives a research methodology was developed and planned. A detail study of already carried out research on simple performance testing worldwide basis and also the level of research already carried out in Pakistan was done to get familiar with the simple performance testing, its background, its use in new ME design guide and background of MEPDG. In this study three simple performance tests i.e. dynamic modulus, flow number and flow time test will be performed on specimens composed of four different gradations, two of wearing course and two base course and two bitumen binders of different penetration grades i.e. NRL 40/50 and ARL 80/100 and a single sourced aggregate i.e. Margalla aggregate which is primarily lime stone. Marshal mix design method was employed for the determination of optimum binder contents. And using these optimum binder contents laboratory specimens were prepared for the performance testing according to the specification and then trimmed and cored to meet the desired dimensions. The dynamic modulus test was carried out at four different temperatures and six different frequencies whereas the flow number and flow time tests were conducted at a single stress level of 300kpa and a temperature of 54.4°C. Dynamic Modulus test results were used to develop master curves using non-linear optimization technique in excel with the help of solver add on. Fatigue parameter was developed for the mixtures using dynamic modulus and phase angle and results were compared to determine which mixture is more susceptible to fatigue cracking. Two level factorial design was also conducted using Minitab 15. Flow Number and Flow Time results were compared to evaluate or asses the rutting performance of the mixtures. Test matrix adopted for this study is shown in the Table 1.1.

Table 1.1: Test Matrix

Test		Dynamic Modulus Test																							FN & FT
Temperature		4.4°C						21.1°C						37.8°C						54.4°C						54.4°C
Loading Frequency(hz)		0.1	0.5	1	5	10	25	0.1	0.5	1	5	10	25	0.1	0.5	1	5	10	25	0.1	0.5	1	5	10	25	Stress= 300 KPa
Materials		Margalla Aggregate/ NRL 40/50 & ARL 80/100																								
AWC	NHAA	√	√	√	√	√	√	√	√	√	√	√	√	√	√	√	√	√	√	√	√	√	√	√	√	√
	SP A	√	√	√	√	√	√	√	√	√	√	√	√	√	√	√	√	√	√	√	√	√	√	√	√	√
ABC	SP B	√	√	√	√	√	√	√	√	√	√	√	√	√	√	√	√	√	√	√	√	√	√	√	√	√
	DBM	√	√	√	√	√	√	√	√	√	√	√	√	√	√	√	√	√	√	√	√	√	√	√	√	√
Total		48 Specimens (03 replicates for each test)																								

1.5 ORGANIZATION OF REPORT

This research thesis consists of five chapters and an appendix portion. Chapter one consists of introduction to simple performance testing, introduction to various mix design methodologies, problem statement and research objectives. Second chapter consists of literature review of already carried out research on simple performance testing and how to develop the dynamic modulus master curves and dynamic modulus prediction models. This chapter also covered a detailed literature on flow number and flow time, their mechanism and work done by various researchers. Chapter three explains the detailed methodology of the research i.e. selection of materials and mix design process, preparation of specimens for the performance testing and testing procedures and equipment's in details. Chapter four consists of results and analysis of the test data. Master curves, factorial deign of experiment, comparison plots etc. are a part of this chapter. The last chapter summarizes the report along with conclusions and recommendations.

CHAPTER 2

LITERATURE REVIEW

3.1 INTRODUCTION

Due to increased traffic volumes, severe loading of vehicles, adverse environmental conditions, poor construction practices and out dated mix design methodologies, flexible pavement failure soon after the construction, before completion of their design life has become a major problem for road stack holders which are mainly road users, road agencies and government. In order to solve this global problem of premature pavement failure pavement researchers and engineers by AASHTO and NCHRP started a project aiming to shift mix design methodology from empirical to mechanistic phase and the research project was designated as NCHRP 1-37A. They recommended three candidate tests termed as simple performance tests SPTs for HMA characterization. Dynamic modulus |E*| test is most important among them because it is used as a primary material input in mechanistic empirical design guide software for characterization of materials. The following section will give an introduction of MEPDG for flexible pavements, different efforts carried by states to develop a catalog of E* values of locally used HMA mixes. Past researches carried out by different researchers internationally and in Pakistan and different dynamic modulus predictive models.

3.2 MECHANISTIC EMPIRICAL DESIGN FOR FLEXIBLE PAVEMENTS

For many years 1993 AASHTO Pavement design guide is used for structural design of pavements which consists of pavement design equations which are empirical in nature and are based on AASHO road test conducted in 1950 (AASHTO 1993). However due to many limitations its use is getting less popular day by day. Some of its disadvantages include,

1. Increased traffic: Since 1950 and after World War 2 pavements are receiving an enormous amount of traffic and which is continuously increasing day by day. Nowadays pavements are designed for up to 200 million ESALs whereas the design equations of 1993 AASHTO Design Guide are developed based on a traffic of 2

million ESALs. So in order to design new roads based on 1993 AASHTO Pavement Design Guide an extrapolation is needed for using equations based on 1950 AASHO Road Test.

2. Environmental Conditions: AASHO Road test was conducted at a single location so it don't take into account the variations of environmental and climatic conditions of different locations into its design equations. Only it allows seasonal adjustment of subgrade resilient modulus and layer drainage coefficients.
3. Material Deficiencies: In AASHO Road Test only one type of materials were used to construct road base and sub base however, in different areas of the world different materials are used to build these pavement layers and variation in pavement materials can significantly affect the pavement performance which is not accounted in empirical equations of AASHO Road test.
4. Test Duration: The AASHO Road Test was carried out for two years and didn't take into account the long term binder aging affects and climatic effects on pavement materials.

Due to advancement in material characterization and testing techniques NCHRP was able to come up with a more sophisticated pavement design guide known as mechanistic empirical pavement design guide releasing its first version in 2004 which was later on updated and modified to current AASHTOware ME design software (Schwartz 2011). ME Design consists of two parts mechanistic and empirical. Mechanistic part consists of the models that are used to predict pavement response in terms of stresses, strains and deformations. These responses are then used to predict pavement distresses. In ME design software it is necessary to input material, climate and traffic data. Three levels of material input can be used in ME design software based on the level of accuracy required, importance of the work and money involved in the project (AASHTO 2008).

Level 1 input: level 1 input data is acquired by conducting laboratory testing or field testing. It has highest level of accuracy and the least uncertainty.

Level 2 input: data is acquired from agency data base or derived from a limited testing program or may also be derived from correlations with the field data. This is usually used for the

projects with resources that are not enough to obtain a level 1 input in the laboratory or from the field.

Level 3 input: It has the minimum level of accuracy. It may consist of values selected by the software user based on experience or can be obtain by calculating the average value for the region. Pavements designed using this level of input have more chances of premature failure due to less accurate material input.

In ME design software individual layer input can be divided into three parts i.e. asphalt mix input, binder input and asphalt general input. For example, if we are carrying out a level 1 input then asphalt mix input we need to conduct dynamic modulus testing in a laboratory at different temperatures and different frequencies to characterize asphalt mixture. And these results are used to develop master curves along with shift factors

The NCHRP 1-47 research team tested the sensitivity of pavement responses and distresses to E* results. They found that pavement response is very sensitive to E* results except thermal cracking (Schwartz 2011). So it is very important to accurately determine E* values for correct performance prediction. But it is very difficult for transportation agencies to carry out a full level 1 input testing for all their mixtures. Solution to this problem is that agencies should carry out dynamic modulus testing for typical asphalt mixes and develop a data base of material input. This data base can be used to check and calculate the difference between laboratory E* results and predicted E* values in Level 2 and Level 3 input.

3.3 EFFORTS OF DIFFERENT STATES FOR IMPLEMENTATION OF MEPDG BY DEVELOPING A DATABASE OF E* RESULTS

This section summarizes various efforts made by the transportation agencies in characterizing the HMA mixtures typically used in the respective states. The major test conducted was dynamic modulus. The basic objective was to create a database of E* values which constitutes level 1 input for MEPDG and also to assess the accuracy of Witzak and Hirsh prediction models which are used in level 2 and 3 design input.

New Jersey: New Jersey department of transportation funded a research project involving characterization of HMA mixes using E* test, developing a database of E* values for the state and checking the accuracy of Witzak and Hirsh models against the tested E* values. the test

matrix included 21 HMA mixes which were dense graded and prepared using two bitumen binders one modified and one unmodified. The unmodified binder was PG 64-22 and the modified binder was PG 76-22. The NMAS of mixtures was ranging from 9.5 mm to 25mm. After conducting the tests and analyzing the results they concluded that Witzak model has a better predictive ability as compared to Hirsh model. The average difference in the values of tested and predicted dynamic modulus was 10.5% by Witzak model and that was 12.6% by Hirsh model. In case of comparison between the two binders, PG 64-22 produced better results in case of predicted E* values as compared to PG 76-22 because dynamic modulus prediction equations are developed for unmodified binders (Bennert 2009).

Virginia: Virginia CTIR carried out dynamic modulus testing on 18 HMA mixes consisting dense graded, gap graded, base mixes and stone mastic asphalt mixes. The test mixtures were acquired from the 7 districts of Virginia. Dynamic modulus testing was carried out over a range of temperatures and frequencies. Five testing temperatures and six loading frequencies were used to develop the master curves. The results were also used to compare the predicted E* values with measured E* values. Witzak Equation was used for prediction of dynamic modulus values. There were cases in which Witzak model over predicted the dynamic modulus values 190% higher than that measured using laboratory testing and sometimes it under predicted the values by 85% of that of measured dynamic modulus. It was found that much difference was observed between the measured and predicted dynamic modulus when testing was performed at low temperature and higher frequencies (Apeagyei 2011).

North Carolina: Kim et al conducted E* testing on 42 HMA mixes prepared using different aggregate sources, gradations, binder sources and optimum binder contents. The testing was carried out at different temperatures and different loading frequencies in accordance with AASHTO TP 62-03 except he reduced the number of testing temperatures from five to four and increased loading frequencies. He used these results to develop master curves and shift factors used as a level 1 input in MEPDG. The difference was compared for measured E* with predicted E* and found that prediction capability of Witzak equation was higher especially when testing temperature was low. He also concluded that binder variables such as its source, its grade and it content bear greater effect on dynamic modulus values as compared to aggregate variables. He also tried calibration of the prediction models in another study using data from previous project (Kim 2005).

Mississippi: Mississippi DOT funded a research study for characterizing commonly used HMA mixtures. Test matrix consists of a total of 25 mixes fabricated using different NMAS i.e. 9.5, 12.5 and 19mm and with three bitumen binders with different performance grades PG 76-22, PG 67-22 and PG 82-22. Testing was carried out in accordance with AASHTO 62-03 without any exception (White 2007).

3.4 PAST RESEARCHES ON SIMPLE PERFORMANCE TESTING

Papzian was the first who in 1962 developed an advanced method for defining the response of linear viscoelastic materials. He investigated the viscoelastic behavior of asphalt mixture using the complex modulus testing method. For this purpose, he performed testing on several test samples under controlled temperature and frequency and viscoelastic behavior of hot mix asphalt was studied by means of algebraic coefficients linking stress to strain which are complex functions of frequency, and equations were formed which state viscoelastic stress-strain laws in the frequency domain, as well as in the time domain (Papzian 1962).

Kallas in 1970 observed that considerable variations turn into more obvious with the increase in temperature chiefly associated to phase angle (Kallas, 1970).

Bonnaure et al. (1977) performed testing in which dynamic load were applied to trapezoidal specimens and the modulus of these specimen was determined from a graph of load applied and resulting deformations. He concluded that stiffness of hot mix asphalt is significantly affected by loading time and temperature. It had a negative relation i.e. E* value reduces with an increase in the loading time or temperature. In addition, they also revealed that E* curves from various temperatures and loading times could be superimposed. This has now turned into an incredibly helpful tool in the shape of master curves.

By making use of the bi-modular study method, together with the modulus determined both in tension and compression the researchers were able to bring more accuracy in the prediction of hot mix asphalt properties. (Witczak and Root, 1974; Khanal and Mamlouk, 1995).

Lekarp et al. (2001) conducted triaxial test on three unbound granular materials to find the effect of grading materials with different nominal maximum aggregate sizes. From the results he concluded that nominal maximum aggregate size plays important role in structural response of the unbound materials. And if nominal maximum aggregate size is decreased it will directly

affect the permanent deformation properties and resilient strain properties of the HMA mixes. However, he was unable to find the nature of these impacts due to complexity of the different materials and inconsistency of the results.

Uzan et al. (2003) characterized HMA mixes based on their rutting performance using a mechanistic empirical procedure. Dynamic modulus and repeated load tests were conducted at various temperatures and confining pressures to check material sensitivity against testing conditions. He found that material properties were very sensitive to testing temperature and confining pressure. He also developed a master curve based on Fillers–Moonan–Tschoegl (FMT) equation.

Mu-yu L& Shao-yi (2003) took two factors rutting and cracking and developed an optimization model, using genetic algorithms for solution of that model. It was a new idea for HMA structural optimization.

Amit et al. (2003) carried out a study in which nine HMA mixes were acquired from state Departmental of Transportation and have changing levels of field performance. The research also included testing of three lab prepared specimens. Three simple performance test protocols were used for mixture characterization. From this research they arrived at the conclusion that slope of flow time (creep load) and flow number (repeated load) values demonstrated a strong correlation with the APA‟s rut depth. And if we compare them the correlation of APAs rut depth with the flow time slop was stronger than that of with flow number.

Bonaquist et al. (2004) carried out a research study to develop an instrument for conducting three SPT tests. The study was extremely successful and at the end of the project they develop full specifications of the instruments for both the manufacturers and the users. Two instruments were developed for SPT testing one was Interlaken SPT system and the other was Shedworks SPT system. An evaluation study was carried out to check the suitability of these two instruments for SPTs. The findings suggested that both the units were user friendly and meeting the requirements with certain common deficiencies. In case of dynamic modulus results, there was some variability in the results that was found to be due to variability of deformation measuring devices that were glued to the test specimen placed in the environmental conditioning system. The level of variability for flow number results by the two instruments was not

significant. On the basis of the findings of the evaluation study Shedworks SPT system was found to be more suitable for SPT testing. The study resulted in the development of AMPT that is Asphalt Mix Performance Tester.

Bahia et al. (2005) used two aggregate gradations commonly used in Wisconsin. Aggregate was acquired from four different sources. The output achieved from the uniaxial repeated creep test was the flow number, and from the results it was clear that asphalt mixtures showed tertiary creep failure. The results also showed that a strong relation exists between resistance to permanent deformation and traffic force index.

Mohammad et al. (2005) performed four tests including dynamic modulus and flow number on six plant-prepared hot mix asphalt mixtures. From the results they arrived upon the conclusion that results from flow number tests were pretty consistent with the In-situ performance of those mixes selected for the study. Additionally, they were able to find a strong correlation between flow number. a and b-values determined from secondary portion of accumulated strain vs cycles curve. These parameters were used for the analysis of a flow number test, particularly when the tertiary flow zone was not attained. It was also found that rut depths found by using Hamburg Wheel Tracking test and by flow number test had a strong correlation.

Romanoschi et al. (2005) picked up four superpave mixtures commonly used in base course of pavements in Kansas with the objective to characterize and evaluate the mixtures dynamic modulus, their bending stiffness and resistance to fatigue cracking. After analyzing the results dynamic modulus was found to be a poor indicator of the mixture's fatigue resistance. Mixtures with lower amount of air voids shown more resistance to fatigue cracking as compared to those with higher amount of air voids because low air voids content leads to higher values of dynamic modulus. The predictive ability of the Witzak model was also evaluated in this study and it was found that it strongly under estimated the dynamic modulus for all the four mixtures under study. In most cases measured E* was twice the Predicted E*. Keeping the temperature and frequency constant a comparison of E* and bending stiffness revealed that E* is twice the bending stiffness of the HMA mixtures.

Muhammad et al. (2006) characterized asphalt mixes based on their rutting performance using dynamic modulus, flow number and Hamburg wheel tracking test. Sensitivity analysis was carried out using MEPDG software to check dynamic modulus role in rutting performance prediction of pavements.

Mohammad et al. (2006) carried out a research using thirteen (13) plant manufactured asphaltic mixes. They tested these hot mix asphalt mixtures by conducting repeated load test (FN) and static creep test (FT) HWTT and |E*| test. From the tests results they arrived at the conclusion that the rut resistance parameters from the FT, FN and |E*|test were capable of differentiating among mixtures based on their design traffic.

Cross et al. (2007) conducted dynamic modulus test on various mixtures prepared using different types of aggregate and bitumen binders. Testing was conducted at five different temperatures and six different loading frequencies were selected for application of sinusoidal loading. The testing of dynamic modulus at lower temperature of -10 °C was observed to be difficult and intensive process due to development of frost on the test frame including test specimens and LVDTs. After analyzing E* testing results he reported that loading frequency and testing temperature were the major factors having a significant effect on the values of E*.

Garcia & Thompson (2007) Conducted a study that comprised of three different stages for the evaluation of E* prediction equations. The mixtures used for the study were taken from Illinois DOT. Objective of the study was to develop modulus-temperature generic equations that can be used for design of roads. Currently used E* prediction models were also evaluated and Hirsh model was found to be best predicting the dynamic modulus values with high precision and low error. To eliminate or minimize these errors a database of correction factors was developed and the amount of error was significantly reduced when these correction factors were applied to the Hirsch model.

Flintsch et al. (2007) conducted HMA testing to characterize HMA mixes for implementation of MEPDG in Virginia. Dynamic modulus test was conducted along with creep compliance test and indirect tensile test for evaluation of thermal cracking in surface, intermediate and base layers. Resilient modulus test was also conducted to correlate dynamic modulus with resilient modulus. Based on the test results he found that dynamic modulus test can

best characterize the HMA mixes at different temperatures and frequencies. Also dynamic modulus results were affected by mix characteristics such as NMAS, binder content, aggregate type etc. He also found that dynamic modulus was reasonably predicted by level 2 prediction equations with some differences. But the results produced by indirect tensile strength test and creep compliance test were non repeatable due to some reasons. Phase angle values generally increased with increased temperature, but at high temperature and low frequency the decrease was observed in phase angle values due to aggregate interlock dominant behavior.

Wu et al. (2007) conducted dynamic modulus test to evaluate and characterizes the HMA mixes modified with different fibers such as cellulose, polyester and mineral fibers. Dynamic modulus and phase angle values were found at various temperatures and frequencies for modified and control HMA mixes and it was observed that HMA mixes modified with different additives produced higher dynamic modulus values as compared to control mixes. Using dynamic modulus results he developed dynamic modulus master curves using time temperature superposition principle based on nonlinear regression. He also calculated fatigue and rutting parameters and comparison with control mix revealed that these properties were improved by using fiber additives.

Sugandh et al. (2007) evaluated the ability of flow number test to detect the existence of modifier in HMA mixtures and to assess the changes in the performance of HMA mixes which occurred due do the addition of modifier. Four modifiers were used for designing HMA specimens for performance testing. Flow number test was conducted at a static stress level of 210 kpa at a temperature of 54.4ºC. After analyzing the results, it was concluded that flow number test was able to detect the existence of modifier in case of rutting susceptibility of the mixtures but it failed in case of fatigue.

Abdo et al. (2009) conducted a research study involving testing of 17 HMA mixtures using dynamic modulus test for developing a prediction model that uses HMA mix parameters for estimating dynamic modulus. He reported dynamic modulus results were significantly affected by the variations of bitumen grade and its percentage and also by the aggregate gradation. Further, regression analysis was used for the development of the model which resulted in R^2 value of 0.94.

Ceylan et al. (2009) employed advanced neural network methodology instead of regression modelling for prediction of dynamic modulus. The new ANN methodology is used to solve complex problems. The ANN predictive model was developed using latest E* data base. The predictive capability of the new ANN models was found to be higher as compared to the existing predictive models based on regression equations. He suggested that this technique due to its higher predictive accuracy will result in better material characterization and may reduce chances of premature pavement failures.

Bonaquist tested twelve (12) laboratory prepared HMA mixes commonly used in Wisconsin prepared using aggregate from different sources and binders of different grades for E* and permanent deformation. Specimens were tested at three different temperatures that are 4ºC, 20ºC and 35ºC and three frequencies were selected for application of sinusoidal loading that were 0.1 Hz, 1 Hz and 10 Hz. He determined the sensitivity of AMPT results when mix design factors were changed and concluded that E* and flow number results are significantly affected by change in binder or gradation. His results were used to develop a data base of E* and master curves for use in MEDG related efforts (Bonaquist 2010).

Kaloush et al. (2010) conducted tests on 94 hot mix asphalt mixes and obtained a large number of flow number test results. These results were used to build up a flow number prediction model. Their model showed good accuracy with an R^2 of .62. Researchers stated that their model is applicable to broad array of temperature, stress condition and mixture types. Furthermore, it is also essential to point out here that the inconsistency inside replicates used in their research was reasonably high.

Wassage et al. (2010) conducted two tests on HMA mixes. One was repeated creep test, a new test method to check the elastic response of modified bitumen binders and behavior of HMA mixes was modelled using linear and nonlinear rheological modeling. The second test was repeated load permanent deformation test recommended by NCHRP as a candidate member of SPTs. The accumulated strains in the material due to cyclic loading were evaluated and viscoelastic theory was used to describe HMA behavior under haversine pulse loading.

Ahmed et al. (2011) conducted a study using densely graded HMA mixtures produced by superpave and marshal mix design method and using granite aggregate of Klang, Malaysia to assess the rutting resistance by using dynamic modulus test. Test results were obtained for

different temperatures and frequencies so that data at different temperatures can be shifted with respect to loading frequency to develop a master curve that was used as a comparison of stiffness between the mixtures and it was revealed that mixtures designed using superpave mix design had higher stiffness as compared to that of marshal mix design method. Rutting resistance of mixtures was also evaluated using HWTT and an effort was made to develop a relationship between the results of dynamic modulus at higher temperatures and rut depths obtained by HWTT. Strength of the correlation was higher at a frequency of 5Hz and test temperature ranging between 40^{O}C and 50ºC and it was concluded that rutting resistance of HMA mixtures can be evaluated by using dynamic modulus test.

Hafeez et al. (2011) conducted a research study in which E* was used to check the rutting and fatigue susceptibility of asphalt mixtures modified using hydrated lime. Three different bitumen binders that are PG70, PG64 and PG58 were tested in DSR for determination of shear modulus and phase angle and a particular aggregate gradation was used for designing of HMA mixtures for performance testing. Two performance tests were considered in this study which are resilient modulus test and dynamic modulus test. Dynamic modulus was determined at three temperatures and six frequencies whereas resilient modulus was conducted at three temperatures. From the results of dynamic modulus, it was concluded that at 25^{O}C dynamic modulus values were mostly dependent on bitumen binder's viscosity whereas at 55ºC it was mostly effected by shear modulus (G*) of the binder. It was also noted that asphalt mixtures modified with hydrated lime presented an increase in dynamic modulus values but this increase was dependent on testing temperature, loading frequency and binder type for all the mixtures. In case of phase angle values, it was found that it increased with decreasing frequencies reaching to a maximum value at 0.5Hz and then it stared decreasing with decreasing frequency. Rutting and fatigue factors was also calculated and the results for different HMA mixtures under study were compared and it was reported that it is more convenient to characterize HMA mixtures based on rutting parameter instead of dynamic modulus alone. Results of resilient modulus were correlated with dynamic modulus and a good correlation was developed depicting that at a frequency of 5 Hz dynamic modulus is equal to 0.96 times resilient modulus value.

John & Dallas (2011) evaluated the capability of flow number and flow time test to assess the rutting susceptibility of airport pavements that are designed to take higher tire pressures as compared to normal road pavements and the results of the study were compared to

rut depths obtained by conducting tests on APA. Aggregate used for design of specimens were of lime stone, granite and chert gravel. A total of twenty-six specimens were produced using a single binder that is PG 64-22 and fine and coarse gradations. After analyzing the results, they came to the conclusion that mixture containing a rich amount of natural sands as higher as 30% sand is more prone to rutting as compared to mixtures with lower amount of sand. Tertiary flow state was achieved in less than 10 seconds in case of flow time test whereas in flow number test the time taken for starting of tertiary flow stage was 60 cycles. A correlation was found between the secondary flow part of the flow time test and results achieved through APA having a higher value of R^2 representing higher strength of the correlation. Similar correlation was produced between flow number and APA test results but having comparatively low R^2. After ranking the HMA mixtures on the basis of their rutting susceptibility it was found that the order of the mixtures is same for both flow time and flow number test.

Miljković and Radenberg (2011) reported that excessive rutting can cause troubles in terms of safety, ease, and overall pavement life-cycle cost. HMA rutting vulnerability is relying on constituent materials and their content. As an addition to superpave mixture volumetric design Simple Performance Tests (SPT) were suggested to get a better idea of the HMA properties.

Apeagyei et al. (2012) developed a technique to develop master curves without conducting dynamic modulus testing at highest and lowest temperatures as required by AASHTO TP-62. This technique was named as abbreviated testing temperature (ABBREV) resulted in time saving due to reduced testing temperatures. Dynamic modulus results at highest and lowest temperatures were predicted using regression models. Master curves were developed using combination of predicted and measured dynamic modulus values.

Hefeez et al. (2012) conducted a research study for prediction of performance of HMA mixes from the characteristics of bitumen binder. For this purpose, four different type of HMA mixtures were used prepared from two aggregate gradations and two bitumen binders. Aggregate gradations were Class A and Class B of National Highways Authority Specifications. Testing was performed by applying a sinusoidal uniaxial stress at six different frequencies and three temperatures and two parameters were measured which are dynamic modulus and phase angle. From the results it was noted that HMA behavior was significantly related to temperature and frequency. Frequency was directly related to dynamic modulus at a constant temperature

whereas temperature was inversely related to dynamic modulus. Master curves were developed at a reference temperature of 25^{O}C using TTS. It was found that HMA mixtures with coarse particles and polymer modified binder showed higher dynamic modulus values for all frequencies and using master curves one can easily predict HMA behavior from bitumen binder.

Shen et al. (2012) carried out dynamic modulus performance testing using specimens representing the seven asphalt plants of Washington State. After analyzing the results, he suggested the use of Hirsch Model and a modified flow number prediction model for conventional dense graded asphalt mixtures of Washington State. Moreover, he also reported that air voids significantly affect both the dynamic modulus and the flow number. Increasing the percentage of air voids will also increase the dynamic modulus and flow number values. They also managed to locally calibrate a model for predicting flow number values for Washington State. The model was able to predict flow number values using volumetric parameters, temperature and type of bitumen binder. They were able to develop a model which predicted reasonably well for conventional mixes but was not applicable in case of highly polymer modified mix.

Walubinta et al. (2012) conducted a comparison study to evaluate the capability of three HMA performance tests that are dynamic modulus test, RLPD test and HWTT to characterize HMA mixtures based on their rutting susceptibility. These tests were performed in the laboratory and the results were compared to the field performance of the mixtures under study. Aggregate used for preparation of test mixtures were of different types such as granite, lime stone and quartzite which were used to form different type of gap graded, fine graded and dense grade HMA mixtures. After analyzing the results, it was reported the HMA stiffness represented by its dynamic modulus is more effected by bitumen binder a higher loading frequencies as compared to lower loading frequencies and effect of gradation can be seen more clearly at higher temperatures. comparison of dynamic modulus results to that of flow number results revealed that stiff mixtures are more rut resistant due to their lower accumulated strains. It was concluded that dynamic modulus results are completely correlated with the HMTT results for capturing the rutting suseptibility of HMA mixtures and also were more effected by a change in bitumen binder grade and its percentage as compared to RLPD test. This may be due to the fact that RLPD test a rest period between the applications of loads for the recovery of strains whereas

dynamic modulus and HWTT don't allow such a rest period. It was also revealed that superpave mixtures were stiffer as compared to conventional mixtures. This was more pronounced at higher temperatures. Falling Weight Deflectometer (FWD) was used to measure field response of the mixtures. The COV for HWTT was low representing it lower variability as compared to dynamic modulus and RLPD test and it was designated as the best and reliable test for routine assessment of the HMA mix rutting susceptibility but the major problem with this test was that it can't be used for generation of input data of the materials used in HMA for the ME Design software. Whereas dynamic modulus test and RLPD tests were recommended for use in structural design of HMA pavements. While dynamic modulus test proved to be best suited for characterizing HMA mixtures in case of producing material input data for new ME design it was found that it under estimate the stiffness of coarse graded dense gradations. It was also reported that use of stiff binder, coarser aggregate gradations and low bitumen binder percentages results in higher values of dynamic modulus.

Yu et al. (2012) conducted a study to develop material input database to support the implantation of MEPDG in Washington state and dynamic modulus test was performed on commonly used HMA mixes prepared in laboratory and specimens obtained by coring from the field in Washington state. He tried to correlate mix field performance with laboratory results obtained at a range of temperatures and frequencies. And on the basis of results of dynamic modulus he made recommendations of HMA mixtures that can be used in Washington State for better performance.

Yu and Shen (2012) carried out dynamic modulus testing on HMA mixes containing granite aggregate because of its abundance in Korea. Four HMA mixes were evaluated containing aggregate gradations with two different NMAS and two different. Asphalt binders at a temperature range of -10 to 55. They also compared laboratory results with the values found by using dynamic modulus predictive equations and found that predicted values were lower than the actual values at high testing temperatures and vice versa. He reported that softest binder resulted in HMA mixes with lowest dynamic modulus and as the stiffness of the binder increases dynamic modulus values increases.

Seo et al. (2103) carried out a dynamic modulus study using experimental results and numeric simulations to relate loading frequency with vehicular speeds by using pulse duration

along the depth results due to vertical compressive stress pulse. He found that dynamic modulus can predict HMA pavement performance with varying speeds. He used a falling weight deflecto--meter to estimate in-situ dynamic modulus of undamaged pavements and developed a factor for their conversion and found that it was in agreement with the trends generally found by field measurements.

Ameri et al. (2014) evaluated and compared several methods to find flow number parameter which is an indicator of rutting performance of HMA pavements and onset of tertiary flow. Permanent deformation data from twelve (12) different mixtures was obtained and after the comparison on the basis of variability in flow number values he recommended franken model as best method to find flow number with limited variability.

Wen et al. (2014) conducted a research study on reclaimed asphalt shingles (RAS) which is used to cut the cost of bitumen binder and also is considered environmental friendly. The effect of RAS on the performance of HMA is that its addition results in an increased stiffness of HMA according to some previous researches (Williams 2011). This study was conducted to check the effects of RAS on the performance and behavior of HMA in terms of permanent deformation or rutting, cracking due to fatigue or from high or low temperatures also called thermal cracking. Performance testing was done on specimens cored from field. Different tests were performed to characterize the HMA mixtures including dynamic modulus and flow number tests and it was concluded that addition of RAS resulted in increased resistance to rutting, fatigue behavior and resistance to thermal cracking didn't showed any significant improvement.

Khosravifar et al. (2015) used time temperature superposition principle to construct master curves for repeated load permanent deformation test on three temperatures low, medium and high as recommended by NCHRP. He conducted dynamic modulus and repeated load axial deformation tests to find temperature shift factors using the results of dynamic modulus and apply these shift factors to the results of permanent deformation repeated load test to achieve a smooth master curve and avoid time consuming material characterization. This confirmed to that time temperature superposition was also valid for results of permanent deformation repeated load test. The master curve was constructed on a plot of cumulative strain vs reduced loading cycles.

Nega et al. (2015) tested seven asphalt mixtures produced in laboratory with different polymer modified binders. Dynamic modulus test was used as a performance indicator and also

the temperature susceptibility of the dynamic modulus results were found. Effect of confining pressure was also evaluated. Master curves were generated using the laboratory testing results and a very good correlation was found for each polymer modifier and between binder viscosity and temperature.

Yu et al. (2015) conducted repeated load triaxle test which was modified to check high temperature pavement performance of asphalt pavements. It was able to simulate confinement and temperature gradient as in actual pavements. A three-layer test specimen was prepared and was tested to evaluate the effect of different elements such as binder, temperature and mix type. This test can be performed at RLT test apparatus with little modifications to test the high temperature performance of three-layer asphalt mixes using flow number test. Main disadvantage of this test was that some extra effort was needed to create specimens for the testing.

3.5 PAST RESEARCHES ON SIMPLE PERFORMANCE TESTING IN NIT NUST

Ali et al. (2015) carried out a study to perform the dynamic modulus test on various commonly used mixtures in collaboration with National Highway Authority (NHA). Tests were carried out on four wearing course gradations and four base course gradations at four different temperatures and six different frequencies. The binder used was ARL 60/70 and the aggregate source was Margalla aggregate. Development of master curves was also a part of this study. Regression models were also developed for prediction of dynamic modulus for base and wearing course mixtures with R^2 values of 0.77 and 0.82 respectively. The study also reported that the temperature and frequency were the most significant factors affecting the dynamic modulus while other factors like optimum bitumen binder, voids in mineral aggregate and voids filled with asphalt and specific gravity had no significant effects on dynamic modulus values.

Irfan et al. (2016) picked up seven plant produced mixtures from road agencies of Pakistan. Loose samples were reheated and compacted using SGC and then subjected to dynamic modulus test. He also analyzed the phase angle results and reported that the phase angle starts increasing with the increasing temperature but after reaching a peak limit, the values again start declining due to reliance of the material over the binder stiffness at low temperature and aggregate interlocking at higher temperature. He also evaluated dynamic modulus prediction models

namely Witzak and Hirsch dynamic modulus prediction models for their regional application and comes to the conclusion that both models under predict the dynamic modulus (Waraich, 2012).

Farhan in 2013 performed flow number and flow time test on the four wearing course gradations and four base course gradations at a single stress level of 300kpa and 54.4°C. He then applied the data smoothening technique to correct the results obtained from AMPT. It was also observed that all the mixtures undergo tertiary flow state in flow number test but tertiary strains were not observed in the flow time test. He ranked the mixtures according to their rutting resistance based on flow number and flow time test results and reported that NHA A gradation performed the best among all other gradations of wearing course and DBM performed well and show more rutting resistance in base course gradations (Gul 2013).

Salman in 2014 evaluated various stone mastic asphalt mixes formed in the laboratory by conducting simple performance tests on AMPT. He reported the significant factors affecting the pavement performance for their performance for dynamic modulus, flow tests and other factors that significantly influence the performance of pavement. Test temperature and frequency was reported as main significant factors affecting the value of dynamic modulus. The power and polynomial models for prediction of values flow number were evaluated for their potential applicability (Salman 2014)

3.6 DYNAMIC MODULUS PREDICTION EQUATIONS

As determination of dynamic modulus is a laborious work requiring extensive laboratory work, time and also lots of experience is required. The equipment's used for the determination of dynamic modulus are costly and difficult to operate. So to make the determination dynamic modulus easy task road scientists have developed the dynamic modulus prediction equations. Witzak and Bari (2006) has listed the dynamic modulus predicting models from a number of researches that is shown in Table 2.1.

Table 3.1: A list of E* prediction models (Bari & Witczak, 2006)

S. No	Prediction Equation	Year of Publishing
1	Van der Poel Model	1954
2	Shook and Kallas Mode	1969
3	Witczak's Early Model 1972	1972
4	Bonnaure Model	1977
5	Witczak and Shook's Model	1978
6	Witczak's 1981 Model	1981
7	Witczak, Miller and Uzan's Model	1983
8	Witczak and Akhter's Model	1984
9	Witczak, Leahy, Caves and Uzan's Model	1989
10	Witczak and Fonseca's Model	1996
11	Andrei, Witczak and Mirza's Revised Model	1999
12	Hirsch Model of Christensen, Pellinen and Bonaquist	2003

3.6.1 WITZAK PREDICTION MODEL

Witzak revised regression model is considered as a good model to predict dynamic modulus values and is very popular. This dynamic modulus prediction model uses the HMA volumetric properties to predict the dynamic modulus values. The data set used for this model consisted of results of 2800 mixtures. The required dynamic modulus testing was carried out in asphalt institute laboratory, Federal Highway Administration and University of Maryland.

$$\log E^* = -1.249337 + 0.029232\,(p_{200}) - 0.001767\,(p_{200})^2 - 0.00284\,(p_4) - 0.05809Va$$
$$- 0.80228\,\frac{Vb_{eff}}{Vb_{eff} + Va}$$
$$+ \frac{3.871977 - 0.0021P_4 + 0.003958\,P_{38} - 0.000017\,P_{(38)^2} + 0.00547\,P_{34}}{1 + e^{[(-0.6033130 - 0.313351\,\log f - 0.393532\,\log \eta)]}}$$

Where,

E*= Dynamic Modulus (10^5 Psi)

η= bitumen viscosity in poise

p_{38}= cumulative % retained on 3/8 in sieve

f= frequency (Hz)

V_a= % Air Voids

p_{200}= % passing #200 sieve

p_4= cumulative % retained on #4 sieve

p_{34}= cumulative % retained on 3/4 sieve

Vb_{eff}= effective binder content (% by volume)

3.6.2 HIRSCH PREDICTIVE MODEL

Christensen et al. (2003) introduced a regression equation for prediction of E*. That regression equation was based on a law stated by Hirsch for composite mixes i.e. a composite mix is composed of more than one constituent material and HMA is also a composite material so this law can also be applied to the HMA. 18 mixes and over 200 data points were used for the development of Hirsch model. This model is simpler than Witzak model due to less number of variables included. The Hirsch model is shown by the following equation,

$$|E^*| = P_c\left[42000000\left(1-\frac{VMA}{100}\right)+3|G^*|_b\left(\frac{VFA\times VMA}{10000}\right)\right]+\frac{(1-P_c)}{\left[\frac{1-\frac{VMA}{100}}{4200000}+\frac{VMA}{3VFA|G^*|}\right]}$$

Where,

$$P_C = \frac{\left(20+\frac{VFA\times 3|G^*|_b}{VMA}\right)^{0.58}}{650+\left(\frac{VFA\times 3|G^*|_b}{VMA}\right)^{0.58}}$$

Where,

|E*|= Dynamic Modulus in lb/in^2

VFA = voids in aggregate filled with asphalt, %

$|G^*|_b$= dynamic shear modulus of bitumen binder inlb/in^2

VMA= voids in mineral aggregate, %

3.7 SUMMARY

This chapter includes background of new MPEDG and factors contributing to its development, simple performance test protocols consisting of three simple performance tests that are E*, FN and FT tests are discussed. The efforts made by different states of America to implement the new mechanistic empirical pavement design guide are also discussed. Dynamic modulus test is used for the characterization of the stiffness and viscoelastic behavior of hot mix asphalt mixtures. It also includes review from the past researches on flow number and flow time. History of mechanistic empirical pavement design is also briefly discussed in this chapter. Dynamic modulus prediction equations from the past researches are also a part of this chapter. But the two important dynamic modulus prediction models that are Witzak and Hirsch are described in details. An overview of level of research carried out internationally and at national level is also part of this chapter. Effects of various factors effecting the value of laboratory determined dynamic modulus, flow number and flow time like testing temperature, loading frequencies or loading time, particle size distribution, optimum binder content, nominal maximum aggregate size and binder viscosity and its penetration grade studied by various researchers are also included in this chapter.

CHAPTER 3

RESEARCH METHODOLOGY

4.1 INTRODUCTION

This chapter describes the methodology adopted for this research study in detail. Aggregate and bitumen binder selection, mix design method, specimen fabrication, conditioning time for the specimens, testing method and testing equipment's are discussed. Two wearing course gradations (NHA A and SP A) and two base course gradations (DBM and SP B) were tested using simple performance testing protocols. The aggregate was acquired from a single source that is Margalla quarry situated in Islamabad Pakistan and two binders having different penetration grades were used that are NRL 40/50 and ARL 80/100. Optimum bitumen content was determined using Marshal Mix design method. Superpave Gyratory Compactor was used for the fabrication of specimens for the performance testing, fabricated specimens were then cored and trimmed to the dimensions specified for performance testing using core cutter and saw cutter. Performance testing was performed using Asphalt Mix Performance Tester (AMPT). The dynamic modulus test is a nondestructive test so same specimen were used for the dynamic modulus and flow number test and separate specimens were used for the flow time test.

The research methodology is better explained with the help of flow chart shown in Figure 3.1. It shows that the research started with the selection of materials and desired gradations and binders were planned. The next step was the mix design process and determination of OBCs. After The determination of OBCs samples were prepared for performance testing using SGC. After preparation the specimens were cored and sawn according to the specifications. After conditioning the samples for required time period performance tests were performed and the results were obtained in the form of excel sheets that were used for further analysis.

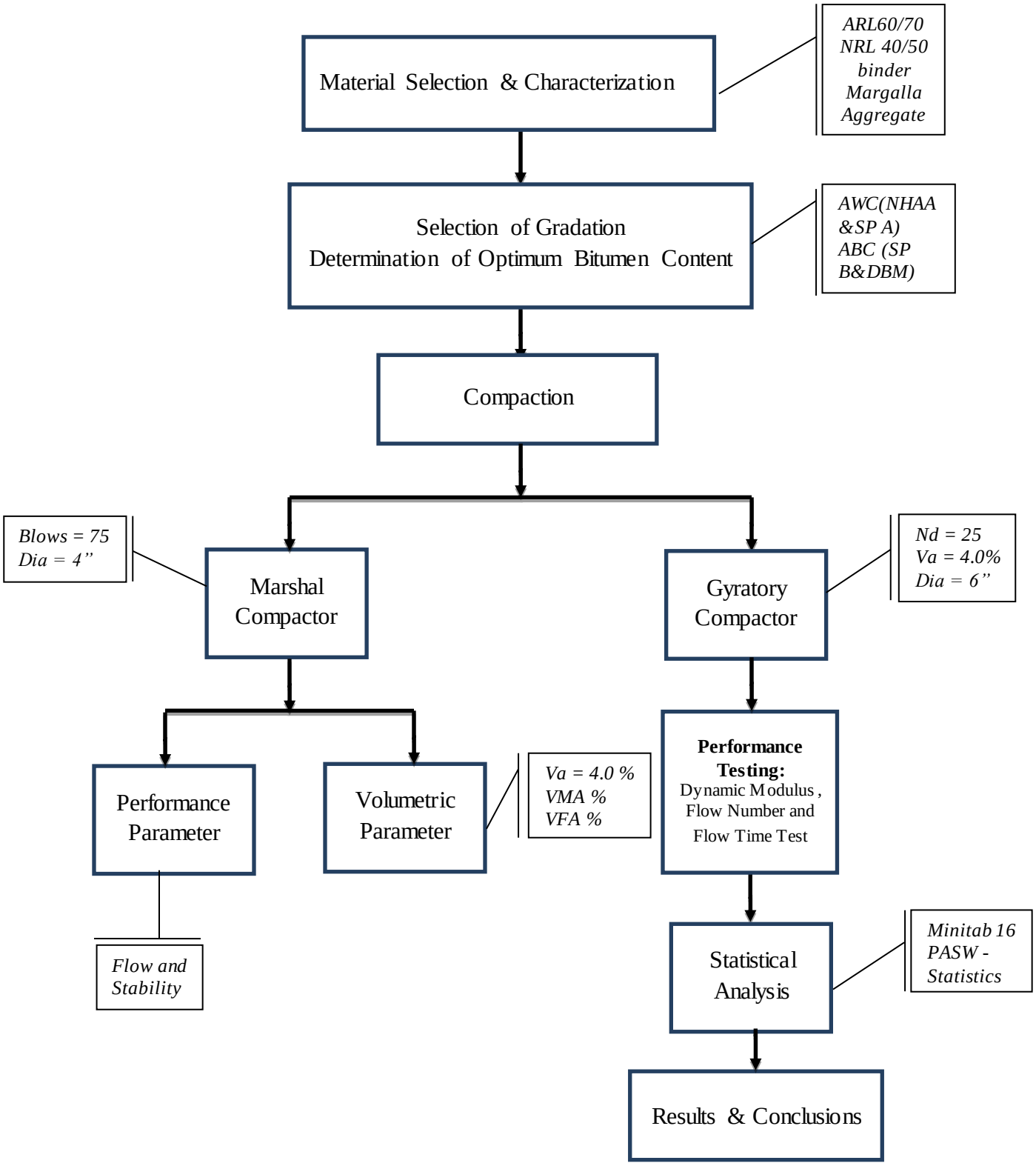

Figure 4.1: Research Plan

4.2 AGGREGATE AND BINDER SELECTION

The aggregate used for the preparation of samples was lime stone and was acquired from a single source i.e. Margalla quarry situated near Islamabad. The bitumen binders were of two penetration grades; one was from National Refinery Limited (NRL) and was of 40/50 penetration grade. The other bitumen binder used in this research was from Attock Refinery Limited (ARL) and was of 80/100 penetration grade.

4.3 GRADATION

Accurate proportioning of different sizes of aggregate according to the gradation specification is vital. This study focuses on testing two (02) wearing course gradations and two (02) gradations for base course. The wearing course gradations selected for this study are NHA A and SP A while the base course gradations are SP B and DBM. Aggregate gradations are shown in tabulated form in Table 3.1 and plotted on a 0.45 power chart as shown in Figure 3.2.

Table 4.1: Gradations

Sieve Size	Gradation			
	Cumulative Percentage Passing (%)			
	NHA A	SP A	SP B	DBM
37.5 mm	100.0	100.0	100.0	100.0
25.4 mm	100.0	100.0	95.0	95.0
19 mm	95.0	100.0	85.0	83.0
12.5 mm	76.0	94.0	60.0	70.0
9.5 mm	63.0	87.0	47.0	63.0
6.4 mm	51.5	74.0	35.0	57.0
4.75 mm	42.5	65.0	30.0	52.0
2.36 mm	29.0	37.0	20.0	39.0
1.18 mm	20.0	21.0	15.0	28.0
0.6 mm	13.0	14.0	12.0	20.0
0.3 mm	8.5	9.0	8.0	14.0
0.15 mm	6.0	7.0	6.0	9.0
0.075 mm	5.0	5.0	4.0	5.5
Pan	0.0	0.0	0.0	0.0

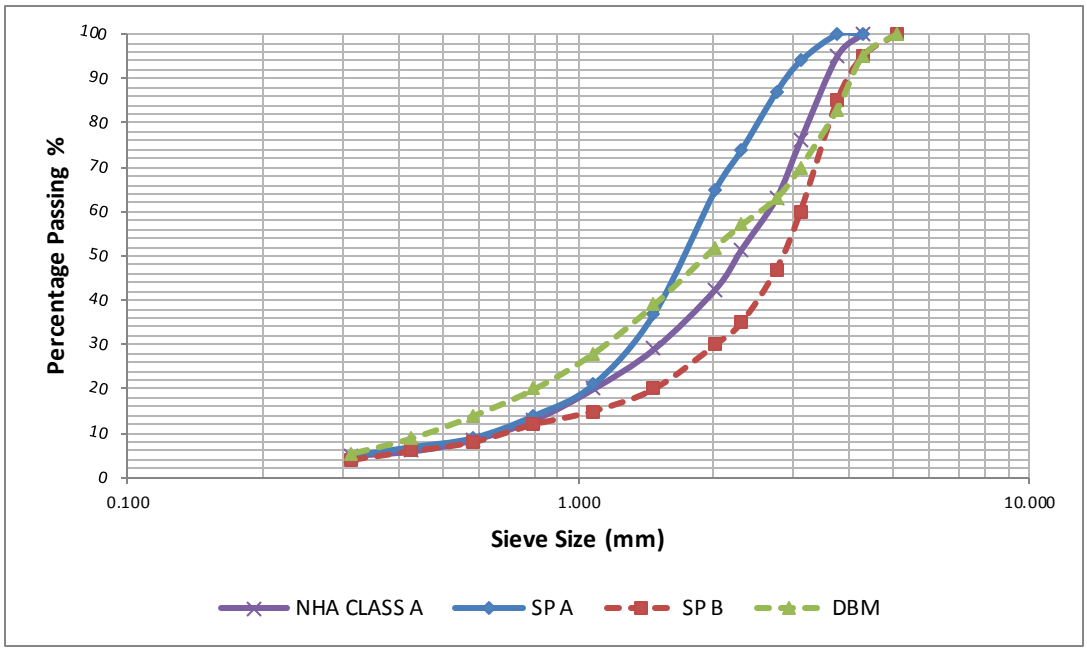

Figure 4.2: Gradation Chart

4.4 OPTIMUM BINDER CONTENT DETERMINATION

One of the initial steps in preparation of specimens for performance testing is determination of Optimum Binder Content (OBC). Marshal Mix design method was used for the determination of OBCs.

4.4.1 Sample Preparation for Determination of Optimum Bitumen Binder

Specimens were fabricated according to the specification ASTM D6929, "Standard Practice for the Preparation of Specimens using Marshall Apparatus" for both wearing course and base course mixtures. 4-inch diameter specimens were used for the wearing course and 6-inch diameter specimens were used for the base course mixtures. Figure 3.3 represents specimen prepared for Marshall Mix Design for both wearing and base course mixtures. Triplicate specimen were prepared for each binder percentage.

4.4.2 Volumetric Properties

. Table 3.2 and 3.3 represents the job mix formula and volumetric properties in detail for wearing course mixtures whereas Table 3.4 and 3.5 represents the same for base course mixtures.

Table 4.2: OBC Determination for Wearing Course Mixtures

Gradation	Binder	A.C. %	Stability (kn)	Flow mm	Gmb	Gmm	Va (%)	VMA (%)	VFA (%)	OBC (%)
NHA A	40/50	3.5	10.733	2.011	2.34	2.50	6.1	13.61	55.1	3.9
		4	11.822	2.309	2.36	2.46	3.8	13.07	70.9	
		4.5	10.551	2.540	2.37	2.45	3.2	13.26	75.8	
		3.9	11.75	2.291	2.36	2.46	4.0	13.09	69.4	
	80/100	3.5	7.121	2.283	2.40	2.51	4.3	11.40	62.1	3.7
		4	8.046	3.055	2.41	2.50	3.5	11.49	69.4	
		4.5	6.805	3.101	2.40	2.47	2.9	12.31	76.2	
		3.7	7.75	2.68	2.40	2.50	4.0	11.32	64.6	
SP A	40/50	5	10.725	2.454	2.33	2.48	5.9	14.85	60.2	5.5
		5.5	14.193	2.637	2.33	2.43	4.0	15.22	73.7	
		6	10.449	3.384	2.34	2.43	3.8	15.52	75.5	
		5.5	14.193	2.637	2.33	2.4	4.0	15.22	73.7	
	80/100	4	7.330	2.342	2.31	2.44	5.1	14.83	65.4	4.6
		4.5	9.261	2.560	2.32	2.42	4.3	14.91	71.0	
		5	7.086	2.590	2.32	2.40	3.1	15.36	79.4	
		4.6	9.16	2.58	2.32	2.41	4.0	15.04	73.4	

Table 4.3: Job Mix Formula for wearing course mixtures

Parameters	Gradations			
	NHA A		SP A	
	40/50	80/100	40/50	80/100
Optimum Binder Content(%)	3.9	3.7	5.5	4.6
VMA (%)	13.09	11.32	15.22	15.04
VFA (%)	69.44	64.66	73.71	73.40
Stability (KN)	11.75	7.75	14.19	9.16
Flow (mm)	2.291	2.68	2.637	2.58

Table 4.4: Mix Design for Base Course Mixtures

Gradation	Binder	A.C. %	Stability (kn)	Flow mm	Gmb	Gmm	Va (%)	VMA (%)	VFA (%)	OBC (%)
SP B	40/50	3.0	24.87	6.070	2.352	2.482	5.23	12.95	60.01	3.4
		3.5	21.65	5.773	2.357	2.450	3.76	13.21	71.51	
		4.0	18.72	5.600	2.361	2.439	3.21	13.52	76.21	
		3.4	**22.00**	**5.501**	**2.356**	**2.451**	**4.0**	**13.16**	**69.62**	
	80/100	3.0	21.059	5.963	2.39	2.50	4.41	11.55	61.81	3.3
		3.5	25.059	6.034	2.41	2.50	3.63	11.26	67.76	
		4.0	24.242	7.618	2.42	2.51	3.32	11.36	70.77	
		3.3	**24.77**	**5.98**	**2.40**	**2.50**	**4.0**	**11.45**	**65.07**	
DBM	40/50	3.5	33.592	5.176	2.334	2.521	7.34	13.73	46.51	4.4
		4.0	37.027	7.319	2.343	2.483	5.50	13.85	60.29	
		4.5	31.32	9.512	2.366	2.462	3.81	13.46	71.68	
		4.4	**32.500**	**9.00**	**2.361**	**2.459**	**4.0**	**13.55**	**70.48**	
	80/100	3.5	32.512	5.972	2.370	2.51	5.52	12.40	55.48	4.3
		4.0	33.250	7.178	2.375	2.50	5.01	12.67	60.45	
		4.5	24.606	7.580	2.41	2.49	3.20	11.85	73.00	
		4.3	**28.81**	**7.52**	**2.393**	**2.493**	**4.0**	**12.30**	**67.50**	

Table 4.5: Mix Design for Base Course Mixtures

Parameters	Gradations			
	SP-B	DBM	SP-B	DBM
	40/50	40/50	80/100	80/100
Optimum Binder Content(%)	3.9	5.5	3.4	4.4
VMA (%)	13.09	15.22	13.16	13.55
VFA (%)	69.44	73.71	69.62	70.48
Stability (KN)	11.75	14.19	22	32.5
Flow (mm)	2.291	2.637	3.4	9.00

Figure 4.3: Samples Prepared for Wearing and Base Course OBC

4.5 PERFORMANCE TESTING

Three simple performance tests consisting of Dynamic Modulus |E*| test, Flow Number test and Flow Time test were carried out. These performance tests are discussed in detail in the following sections.

4.5.1 Dynamic Modulus Test

This test is used to characterize hot mix asphalt by evaluating its visco-elastic behavior and stiffness properties. This test is performed by applying a haversine stress pattern and from the induced strains dynamic modulus is calculated. It is the absolute value of complex modulus mathematically,

$$|E*| = \frac{(\sigma_o)}{(\varepsilon_o)} \qquad (3\text{-}1)$$

Where,

|E*| = Dynamic Modulus

σ_o = max stress that is applied dynamically

ε_o = max strain that is produced axially

Complex modulus consists of a real and an imaginary part. The real part represents the elastic stiffness of hot mix asphalt and the imaginary part describes of HMA viscosity. These components are mathematically written as under,

$$E = E' + iE^{"} \quad (3\text{-}2)$$

Where,

E = Complex Modulus

E' = Elastic Stiffness

E"= viscous modulus

For perfectly elastic materials, viscous modulus is zero i.e. E"=0, so the above equation becomes:

$$E = E' \quad (3\text{-}3)$$

From above equation it is evident that when E" =0, the dynamic modulus is equal to elastic modulus as shown below:

$$E^{*} = \sqrt{(\frac{\sigma^{o}}{\varepsilon^{\varphi}}\cos\phi)^{2} + (\frac{\sigma^{o}}{\varepsilon^{\varphi}}\sin\phi)^{2}} = \frac{\sigma^{o}}{\varepsilon^{\varphi}} \quad (3\text{-}4)$$

Where,

E* = dynamic modulus expressed in lb/seq in

σo = peak dynamic stress (psi)

ε_o= Peak Recoverable Axial Strain (με)

φ = phase angle (radians)

Phase angle shows the viscoelastic characteristics of the mixture. It is the angle by which the compressive dynamic stress is ahead of induced axial strains (Witczak 2002).

$$\theta = \frac{T_i}{T_p} \times 360 \quad (3\text{-}5)$$

Where,

Θ = Phase Angle

Ti = lag between a cycle of strain and stress in seconds

Tp = stress cycle in seconds

In a perfectly elastic material Θ= 0º and for perfectly viscous material Θ= 90°.

Dynamic modulus is described by angular velocity ϕ and time t shows that the phase angle presents the time dependence of hot mix asphalt as shown in Figure 3.4. Equation 3-6 shows the relation between angular frequency and the loading frequency.

$$\omega = 2\pi f \quad (3\text{-}6)$$

Where,

f = loading frequency (Hz)

ω= angular frequency (rad/sec)

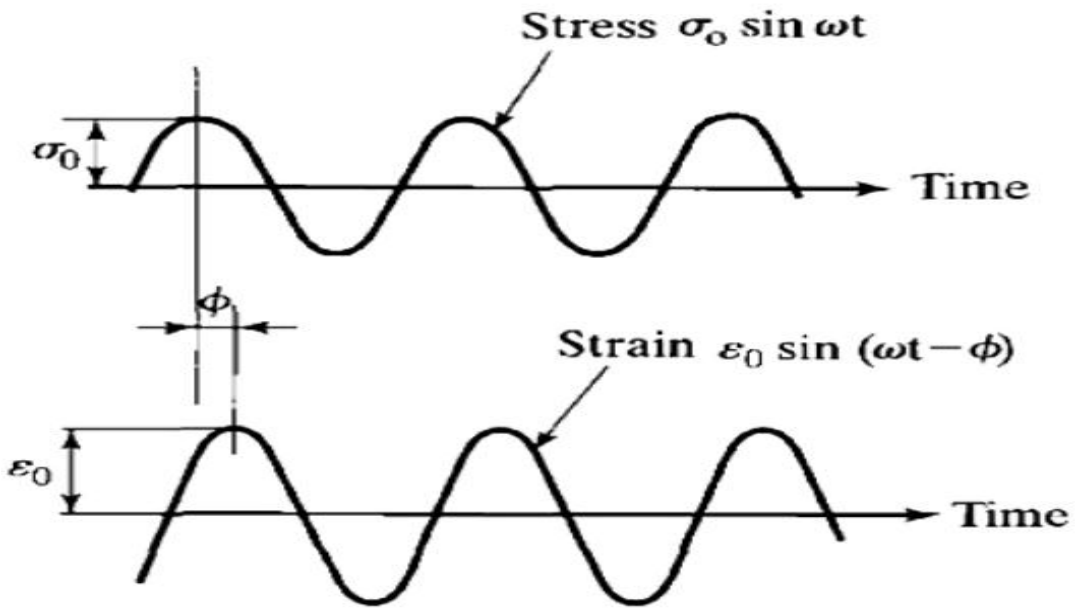

Figure 4.4: Dynamic Modulus Test Mechanism (Huang 2004)

In Asphalt Mix Performance Tester, we select the frequency and temperature at which the test is conducted and test results are obtained in the form of dynamic modulus and phase angle. A typical software output for dynamic modulus test is shown in Figure 3.5.

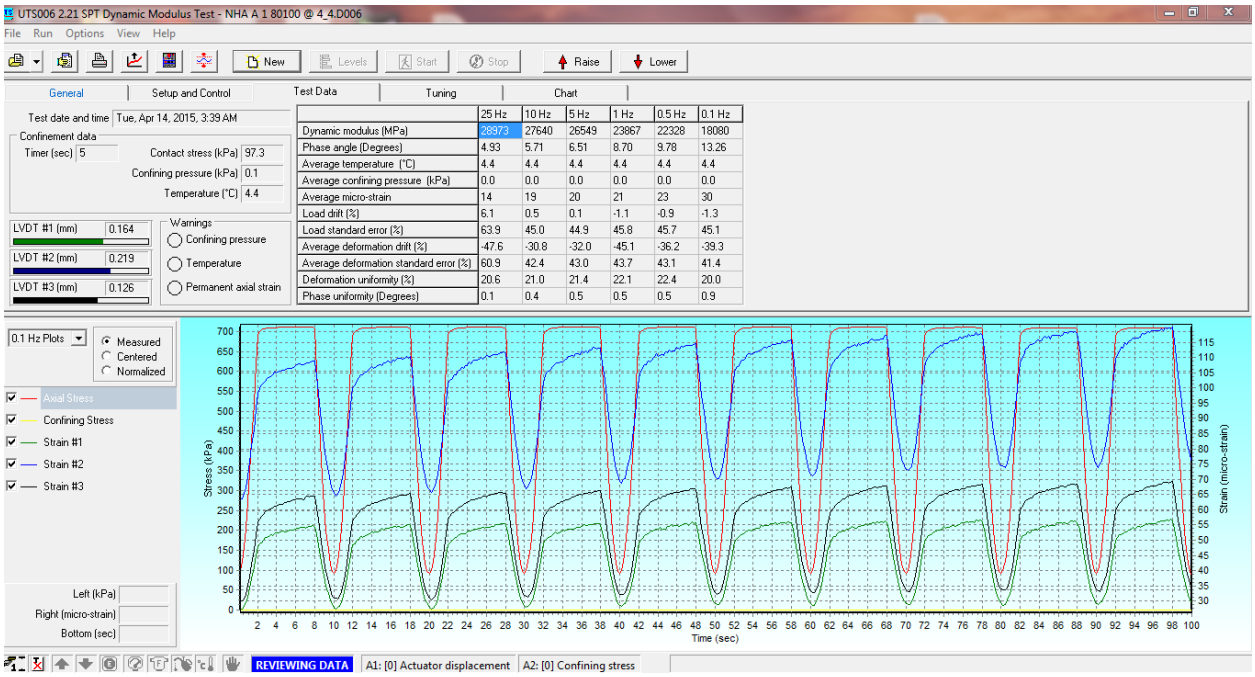

	25 Hz	10 Hz	5 Hz	1 Hz	0.5 Hz	0.1 Hz
Dynamic modulus (MPa)	28973	27640	26549	23867	22328	18080
Phase angle (Degrees)	4.93	5.71	6.51	8.70	9.78	13.26
Average temperature (°C)	4.4	4.4	4.4	4.4	4.4	4.4
Average confining pressure (kPa)	0.0	0.0	0.0	0.0	0.0	0.0
Average micro-strain	14	19	20	21	23	30
Load drift (%)	6.1	0.5	0.1	-1.1	-0.9	-1.3
Load standard error (%)	63.9	45.0	44.9	45.8	45.7	45.1
Average deformation drift (%)	-47.6	-30.8	-32.0	-45.1	-36.2	-39.3
Average deformation standard error (%)	60.9	42.4	43.0	43.7	43.1	41.4
Deformation uniformity (%)	20.6	21.0	21.4	22.1	22.4	20.0
Phase uniformity (Degrees)	0.1	0.4	0.5	0.5	0.5	0.9

Figure 4.5: Dynamic Modulus Software Output

AASHTO standard for dynamic modulus is TP 62-07(AASHTO, 2007) which is now very popular method for laboratory evaluation of dynamic modulus. In this method a sinusoidal axial compressive stress is applied to the specimen and resulting strain is measured and dynamic modulus is calculated. This test is performed at six different frequencies (0.1, 0.5, 1, 5, 10, and 25 Hz) and four different temperatures (14, 40, 70, 100 and 130 ºF). Strains are measured using LVDTs attached to the specimen.

4.5.2 Developing Dynamic Modulus |E*| Master Curves for HMA mixes.

Master curves are used as a material input in the MEPDG software for the structural design of pavements. They are developed by the application of time-temperature superposition (TTS) principle to E* test results. According to this principle, data at various temperatures and frequencies is shifted to a reference temperature and various curves are merged to form a smooth curve that is called a master curve. This is done by nonlinear optimization technique to minimize sum of square error using excel solver add on. Time-temperature principle is appropriate for the materials that are thermo-rheological and Hot mix asphalt mixtures are assumed to be thermo-rheological (Ekingen 2004).

Data at different frequencies and temperatures is shifted with the help of a shift factor a(T). Reduced frequency *fr* can be determined by dividing the actual frequency by the shift factor a (T) as represented by equation 3-7,

$$f_r = \frac{f}{a(T)} \quad (3\text{-}7)$$

Where,

f_r = Reduced frequency

f = Actual frequency

a(T)= shift factor

Sigmoidal function is used for the representation of Master curves due to its S-shape and two asymptotes. Equation 3-8 represents a sigmoidal function.

$$\left[\log|E^*| = \delta + \frac{a}{1+e^{\beta+\gamma(\log Tr)}}\right] \quad (3\text{-}8)$$

Where,

δ= minimum |E* |

δ+ a= maximum |E* |

β,γ = shape parameters as shown in Figure 3.6

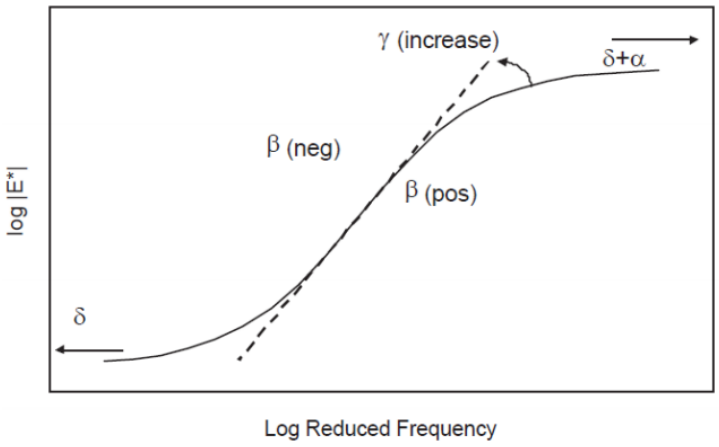

Figure 4.6: Master Curve Shape Parameters (Witzak 2002)

The shift factor can be written as shown in the following equation 3-9:

$$a(T) = \frac{t}{tr} \quad (3\text{-}9)$$

Where,

a(T)= shift factor

T = reduced time

tr= reference temperature

t = time of loading

For increasing the accuracy, a 2nd order polynomial equation between the logarithm of the shift factor and the temperature is used as shown in equation 3-10:

$$\log a(Ti) = aT_i + bT_i + c \quad (3\text{-}10)$$

Where,

a (T_i)= shift factor

T_i = temperature of interest

a, b, c =coefficients

4.5.3 Flow Time Test

The Flow Time (FT) test is also called as static creep test. It is used by researchers to evaluate the basic characteristics of asphaltic concrete related to rutting performance. This is usually achieved by applying a static stress level to the sample and induced deformations are determined. These induced strains are used to assess the visco-elastic behavior of HMA. The test seeks the visco-elastic behavior of an HMA specimen due to a static stress level. The induced compliance, D(t), can be determined by dividing the induced strain by applied stress.

$$D(t) = \frac{\varepsilon_t}{\sigma_o} \quad (3\text{-}11)$$

Where,

ε_t = measured strain

σ = applied stress

When compliance is plotted against time on a log-log scale, the resulting graph is divided into three flows; first one is primary flow, secondary flow and tertiary flow presented in Figure 3.7.

4.5.3.1 Primary Zone:

Primary zone is observed at the start of the test when the strain rate lessens rapidly under static load and becomes stable.

4.5.3.2 Secondary Zone:

Secondary zone is the strain rate stays nearly unchanged.

4.5.3.3 Tertiary Zone:

Tertiary Zone is where the strain rate again starts increasing rapidly.

A graph containing log of compliance as ordinate and log of time as abscissa can be used to determine flow number because the point where rate of change is minimum is clearly visible in this graph. It is the point where tertiary flow zone starts.

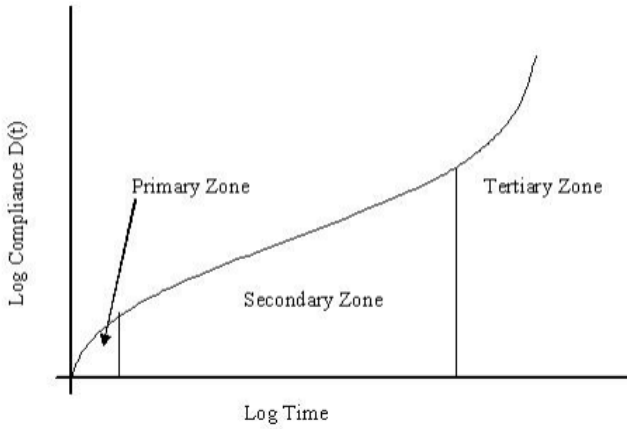

Figure 4.7: Flow Zones (Witzak 2002)

In general, the overall compliance in the secondary zone at any specified time, D(t), can be articulated as a power function as follows:

$$D(t) = at^m \tag{3-12}$$

Where,

t = time (sec) and

a, m = regression constants

In order to determine the regression constants a log-log scale graph of compliance vs time was plotted in the secondary zone. As shown below in Figure 3.9,

$$\log D(t) = m \log t + \log a \tag{3-13}$$

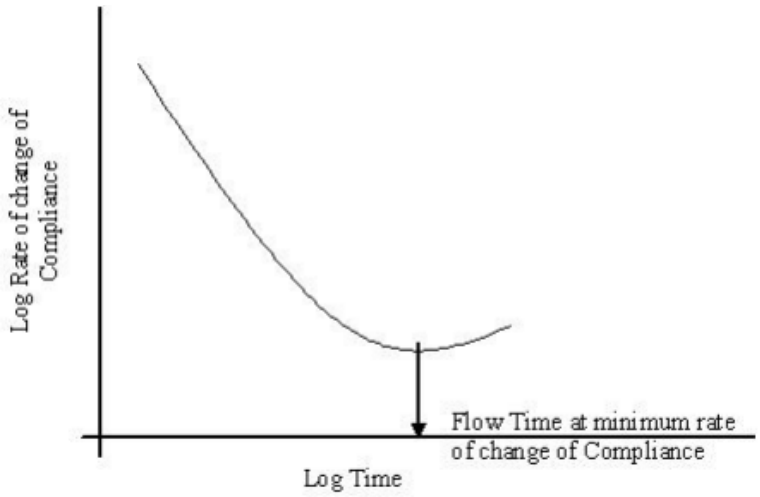

Figure 4.8: Flow Time Determination (Witzak 2002)

When conducting a flow time test on Asphalt Mix Performance Tester we select a stress level and a temperature at which test is performed, test termination strain and test termination cycle. A typical software snap while conducting a flow time test is given in Figure 3.9.

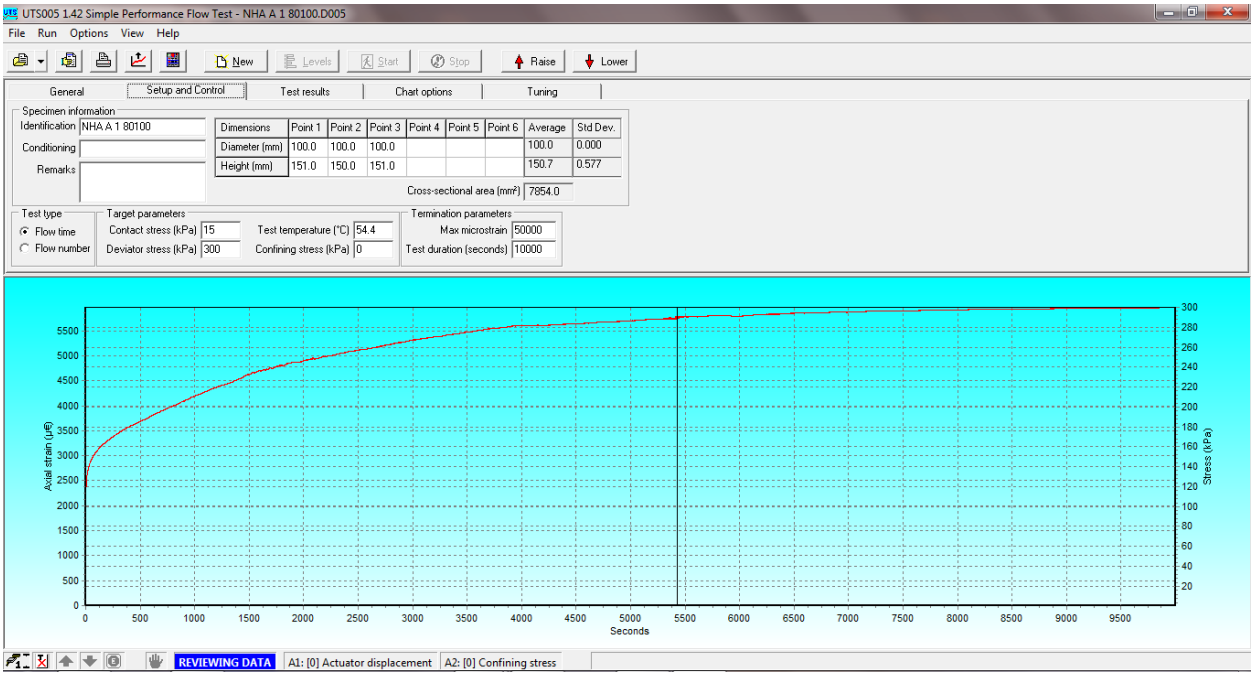

Figure 4.9: Flow Time test

4.5.4 Flow Number Test

The flow number (FN) test measures basic characteristics of an HMA mix related to pavement resistance to permanent deformation (rutting) performance. This is achieved by applying a predefined dynamic stress level is on to the HMA specimen with a loading period of 0.1 s pursued by a rest phase of 0.9 s at a given temperature.

As shown in Figure 3.10 three flow zones can be seen, primary, secondary and tertiary zones. In primary zone the strain rate increases slowly and reaches to point where strain rate becomes nearly constant. From this point secondary flow zone starts with a stable strain rate. After some time, the strain rate again starts increasing rapidly, and the zone of tertiary flow starts. When the applied stress level is low it is very common to observe only primary and secondary flow zones only. Tertiary flow zone is mostly seen when the applied stress level is high.

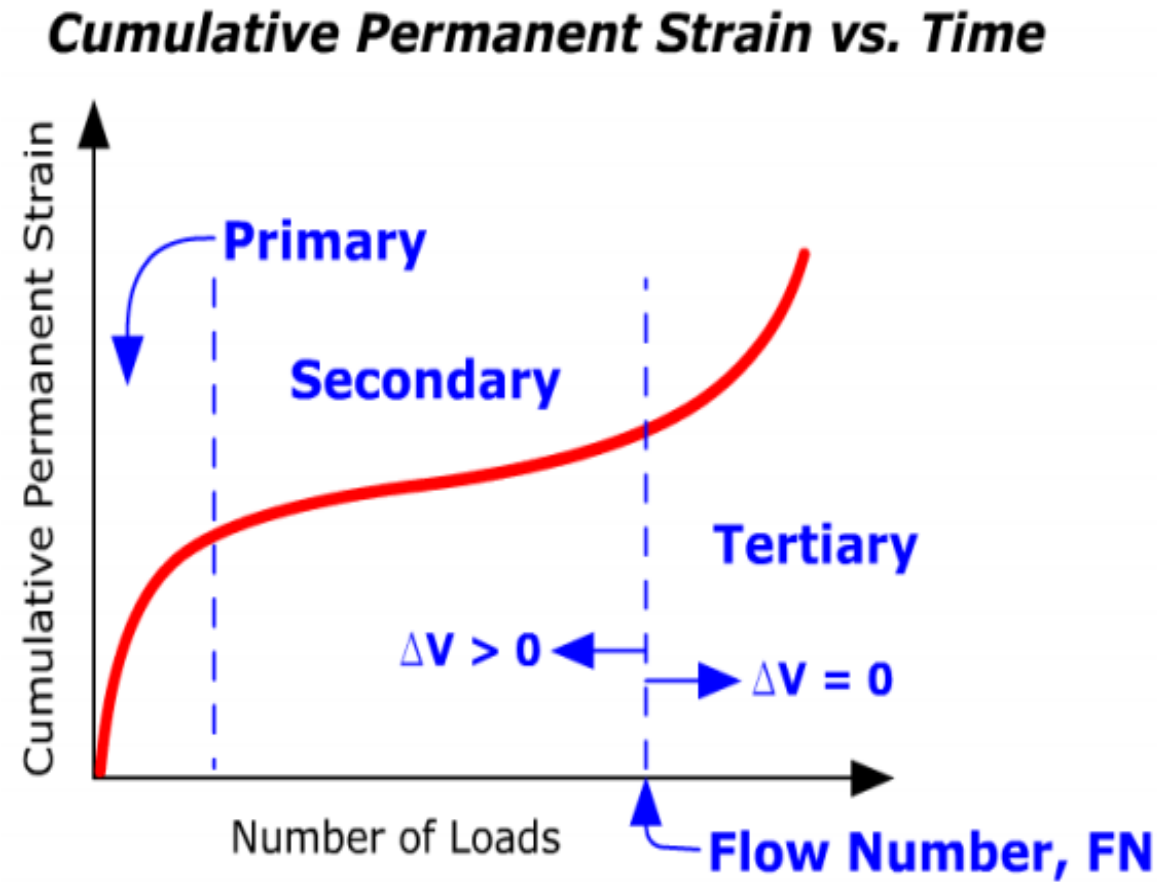

Figure 4.10: Flow Number, Flow Zones (Witzak 2002)

During the test the strain data is recorded and can be exported as an excel file. The following Equation 3-14 represents a typical model in which permanent strains are represented as a function of loading cycles.

$$\varepsilon_p = xN^y \quad (3\text{-}14)$$

Where,

ε_p = permanent strain,

x,y = model parameters

N = number of load cycles at which ε_p recorded

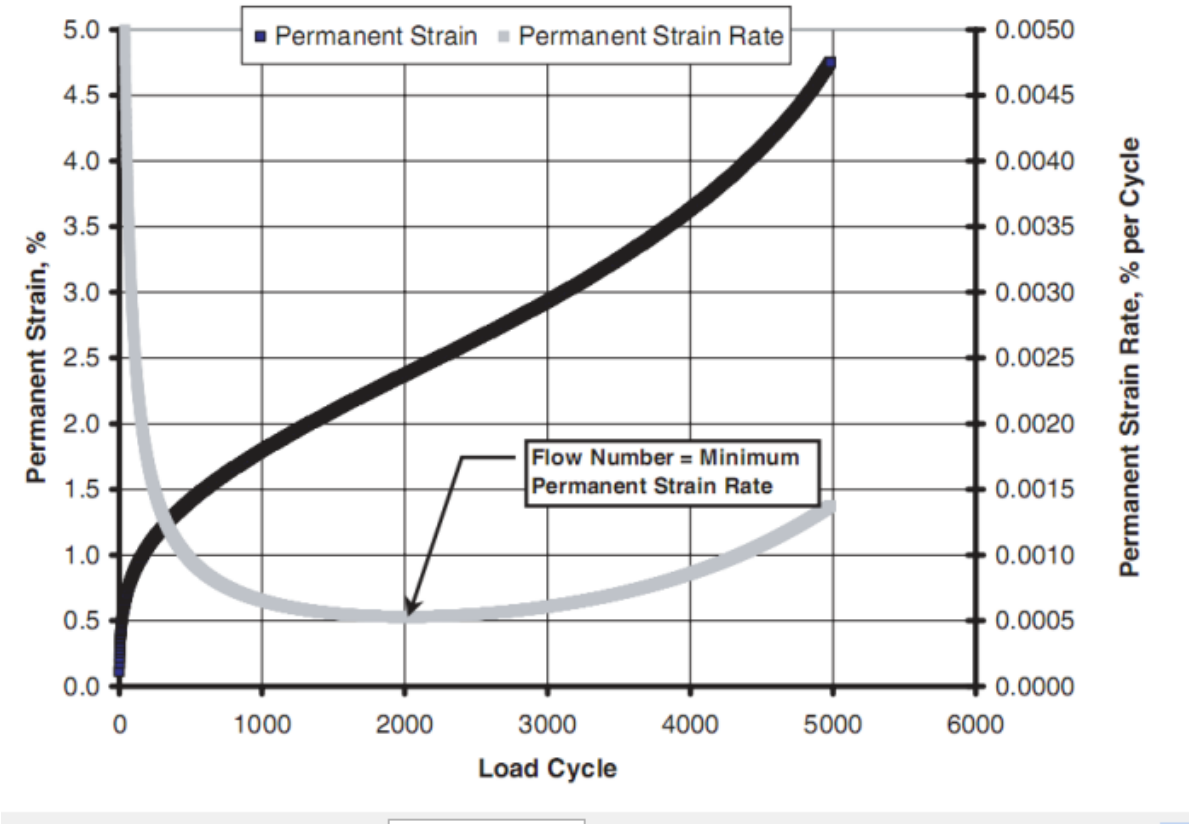

Figure 4.11: Flow Number Cycle (Bonaquist 2011)

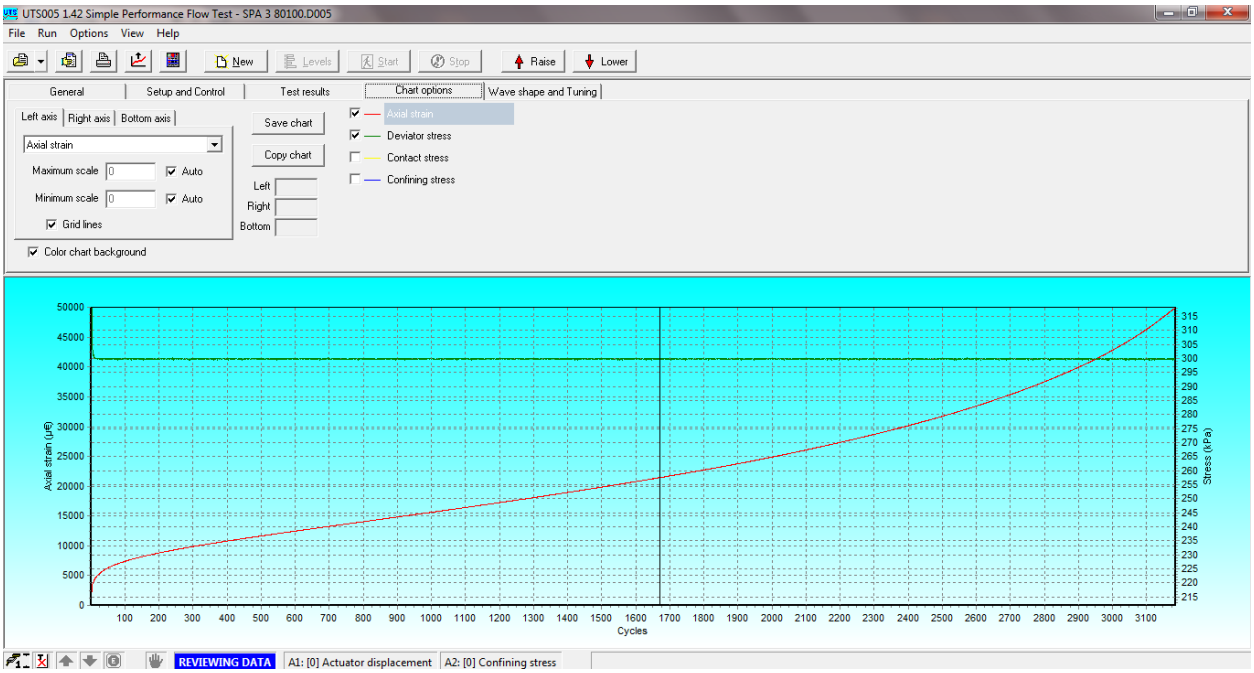

Figure 4.12: Flow Number test on IPC Global Software

A typical snapshot for flow number test is presented in Figure 3.12 showing the accumulation of strains with loading cycles.

4.6 PREPARATION OF SAMPLES FOR SIMPLE PERFORMANCE TESTING

The sieved aggregate was weighted according to the specified gradations. The bitumen was used according to their calculated OBCs. The method of specimen preparation for all the three simple performance tests is and is designated as ASTM D3496-99. The height of the specimen was kept approximately 170mm and diameter was kept 150mm and for each test triplicate specimens were fabricated. To avoid mixing of the specimens each specimen were labeled with a distinct name comprising name of the gradation, the binder type used and the specimen number.

Superpave Gyratory Compactor (SGC) was employed to fabricate HMA specimens in accordance with AASHTO 62-07. Standard required that the prepared specimens for the SPTs should have L/D of 1.5, where L is specimen height and D is diameter. This was achieved by core the sample with the help of core cutter machine a reducing the diameter to 150mm. the height was also reduced to 170mm and the edges were trimmed using an electric sawing cutter.

Figure 4.13: Samples Prepared Using SGC

Figure 4.14: Cored and Trimmed Specimens ready for Testing

A total of forty-eight (48) specimens were prepared as shown in Figure 3.13 which were trimmed and cored as shown in Figure 3.14. During the preparation of the specimens, care was taken to ensure that all the specimens meet the specification requirement and compacted enough to ensure the desirable air voids content.

It was necessary for the dynamic modulus test to fix the gauge points also called studs on to the sample so that LVDTs can be attached. This was done using a gauge fixing machine and epoxy glue shown in Figure 3.15. After fixing the studs with the help of glue the sample was left for 45 minutes so that it should develop enough strength to carry the weight of LVDTs and clamps during the test. Clamps are used to for the adjustment of LVDTs on to the sample. These LVDTs measure the strains during the test. After the conditioning of the sample the sample is placed in the environmental chamber. When the test is carried out at higher temperature the glue some time softens and studs starts losing up. So it is needed to take great care while conducting the test at higher temperatures.

Figure 4.15: Stud Fixing Machine without and with Sample

4.7 LABORATORY TESTING

The dynamic modulus |E*| test, flow number (FN) test and flow time (FT) tests were performed according to the specifications given in Appendix A, B and C of NCHRP Report 465.

4.7.1 Testing equipment

The equipment used for simple performance tests is known as Asphalt Mix Performance Tester formally known as Simple Performance Tester shown in Figure 3.16. It is a very popular machine among the transportation agencies and laboratories around the world for testing the asphalt concrete specimens. Its outputs are used as an input in the structural design of the pavements and also it is used to predict the quality of the in service roads. It is comparatively easy to operate and a compact machine. It can be adjusted in comparatively lesser space.

It has an in built refrigerator with is used for cooling purpose and is turned on when test is to be conducted at low temperatures. It also has a heating unit which is used to raise the temperature of the environmental unit whenever it is necessary to carry out the test at high temperatures. AMPT apply the axial loading by hydraulically driven actuator and confining pressure is applied by air pressure produced by an air compressor. Temperature is controlled digitally by an environmental chamber and the specimen is placed in integrated triaxial cell.

Figure 4.16: Simple Performance Tester

It is capable of conducting the test over a range of temperatures and frequencies. These testing temperatures and frequencies are entered into the AMPT software. This machine has built in testing modules for performing different tests such as dynamic modulus test and flow tests. Each test required its out input parameters that are entered into the software according to the desired testing conditions e.g. deviator stress, confining pressure and frequencies and temperature etc. Test data is recorded in the computer hard disk and can be exported to excel file where further analyses can be performed.

4.8 SUMMARY

Prior to carrying out laboratory testing and preparing the specimens for performance testing, optimum binder content was determined using standard marshal and modified marshal method for wearing course and base course mixtures respectively. It was found that OBC was higher for stiffer binder as compared to softer binder. Marshal stability and flow tests were performed as a performance parameter for mixtures and the values were checked against the recommended values as prescribed by the highway agencies. After the determination of optimum binder content, specimens were prepared for carrying out three performance tests using Superpave Gyratory Compactor (SGC). A total of forty-eight samples were prepared so that each of the three performance test can be carried out on triplicate specimens. Dynamic modulus tests were performed on six loading frequencies and four testing temperatures. Whereas flow number and flow time tests were performed at a single effective temperature of 54.4ºC and a static stress level of 300 Kpa. In order to achieve standard sized specimens cutting and coring was done to reduce the length and diameter of the specimens to 6 inch and 4 inch respectively. For dynamic modulus tests it was necessary to fix the studs on to the samples for attaching the LVDTs so that strains on different points on the specimen can be measured for the determination of dynamic modulus. The tests were conducted using the Asphalt Mix Performance Tester (AMPT) formally known as simple performance tester of HMA developed as a part of NCHRP 9-29 project and the results were extracted both on the form of excel sheets and software output. These excel sheets were used for the further analysis of the results which mainly include master curves development and two factorial DOE.

CHAPTER 4

LABORATORY DATA INVESTIGATION AND INTERPRETATION OF RESULTS

5.1 INTRODUCTION

The results of simple performance tests are analyzed using different techniques presented in this chapter. Softwares used for analysis includes Microsoft excel, SPSS PSAW and MINITAB. Results are presented in the forms of tables and graphs and are divided into three parts, E* test, FN test and FT test results for the HMA mixes with both soft and stiff bitumen binder.

5.2 DYNAMIC MODULUS TEST RESULTS

Dynamic modulus |E*| results are tabulated in the Appendix A for all four testing temperatures and six loading frequencies. From the results it was evident that for all asphalt mixtures the dynamic modulus values decreases with an increase in temperature as expected. This can be better visualize by isochronic curves shown in Figure 4.1 and 4.2 for wearing and base course mixtures respectively. Isochronic curves are drawn at a single frequency and different temperatures. These curves depicted a drop in dynamic modulus values with increasing temperature. This is because as the temperature increases the stiffness of the mix decreases and more strains are produced in response to the same applied stress resulting in a decreased dynamic modulus value. This decrease in dynamic modulus values was more rapid for mixtures fabricated with 80/100 pen grade binder as compared to mixtures with 40/50 pen grade binder. This is clearly because of the higher stiffness of the 40/50 binder. The decrease in values of dynamic modulus for 40/50 pen grade binder is almost linear but in case of 80/100 binder a sudden decline in |E*| values is observed as the temperature the temperature rises from 4.4ºC to 21.1ºC. This may be due to the fact that 80/100 pen grade softens more rapidly as it comes to higher temperatures. Another noticeable observation can be seen at highest test temperature that is 54.4ºC. At 54.4ºC the curves for both the binders come closer so that the difference in dynamic modulus values decreased for both binders at higher temperature. This may be due to the reason

that at higher temperature both the binders soften enough that dynamic modulus values depend only on aggregate interlock and effect of binder stiffness is decreased at higher temperature.

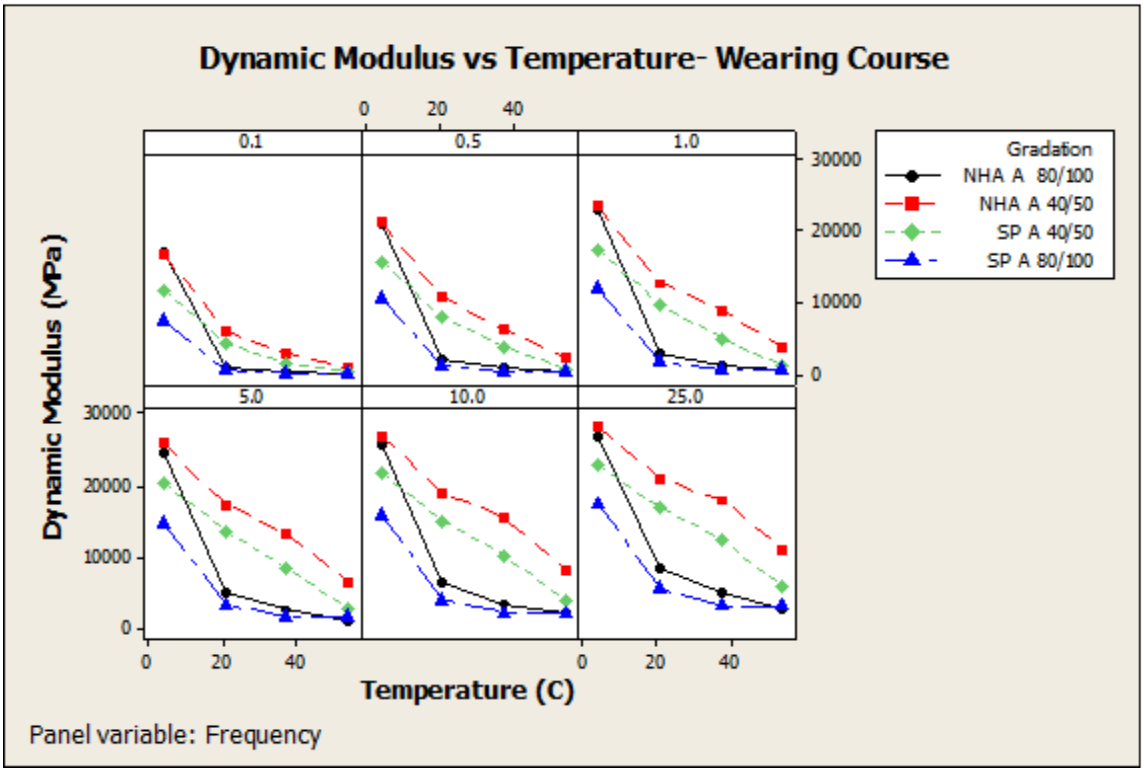

Figure 5.1: Isochronal Curves for Wearing Course

It was also noted that dynamic modulus test results are more sensitive at higher temperature and have higher coefficient of variation than at lower temperatures for almost all the mixes. So it is necessary to take great care and avoid errors while conducting the dynamic modulus test at higher temperatures.

Dynamic Modulus values were increased with increased loading frequency because as the frequency increases, loading time decreases producing lesser strains due to linear visco-elastic nature of hot mix asphalt in which stress strain relationship also depends on loading duration. This effect is shown with the help of isothermal curves representing dynamic modulus loading frequency relationship at constant temperature. Figure 4.3 and 4.4 represents isothermal curves for wearing and base course respectively. It can be seen that dynamic modulus value rises with increasing frequency. The trend is almost similar for both the binders with 40/50 pen grade binder producing higher dynamic modulus values at all the frequencies as compared to asphalt concrete mixtures produced with 80/100 pen grade binder

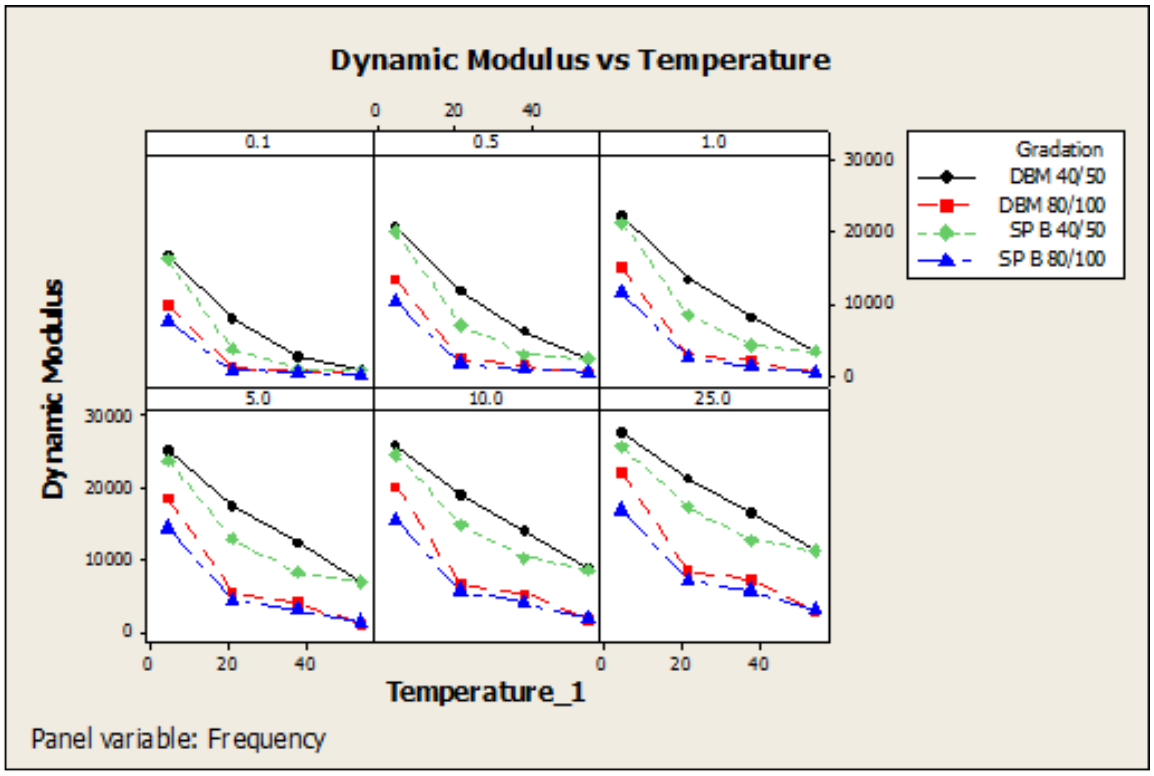

Figure 5.2: Isochronal Curves for Base Course Mixtures

After comparison of |E*| values for both the binders a comparison of aggregate gradation revealed that in case of wearing course gradations, the Pakistan's National Highways Authority (NHA) Class A gradation is producing higher dynamic modulus values irrespective of the binder grade at all temperatures and loading frequencies as compared to Superpave A gradation while in case of base course gradation European DBM gradation is stiffer than Superpave B gradation. This also validate the previous studies carried out recently in NIT involving comparison of gradations (Ali et al. 2015).

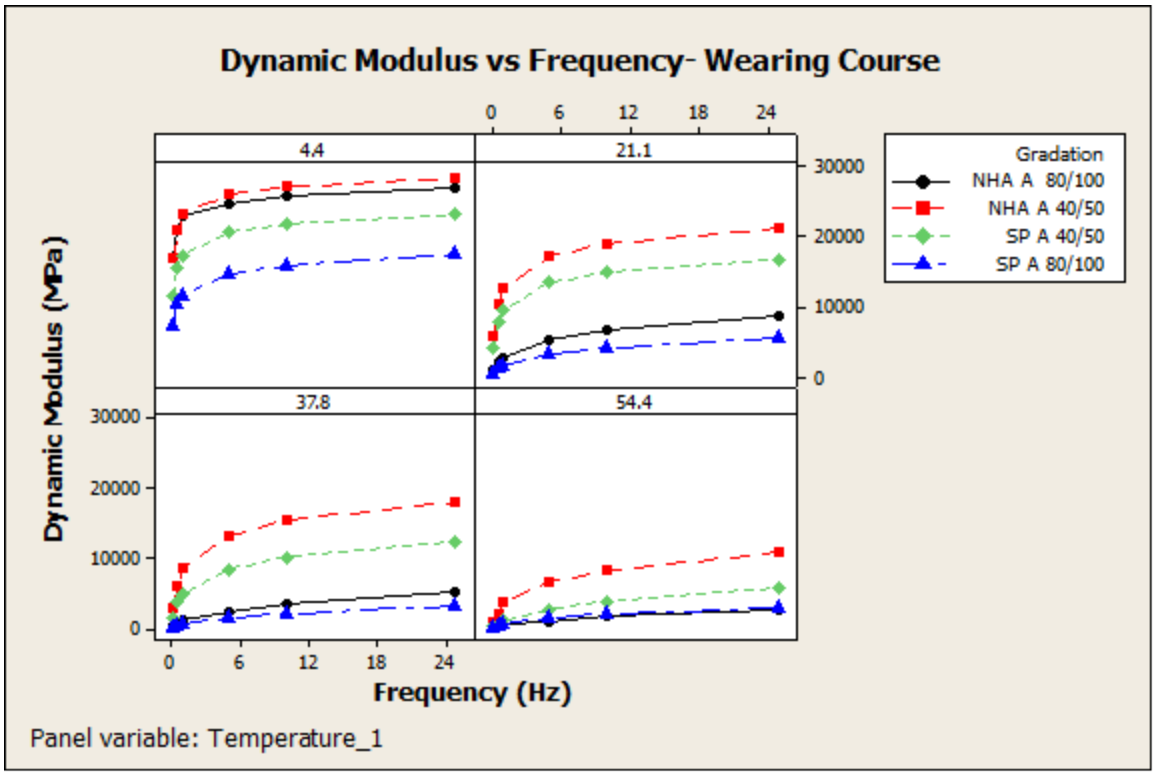

Figure 5.3: Isothermal Plot for Wearing Course Mixes

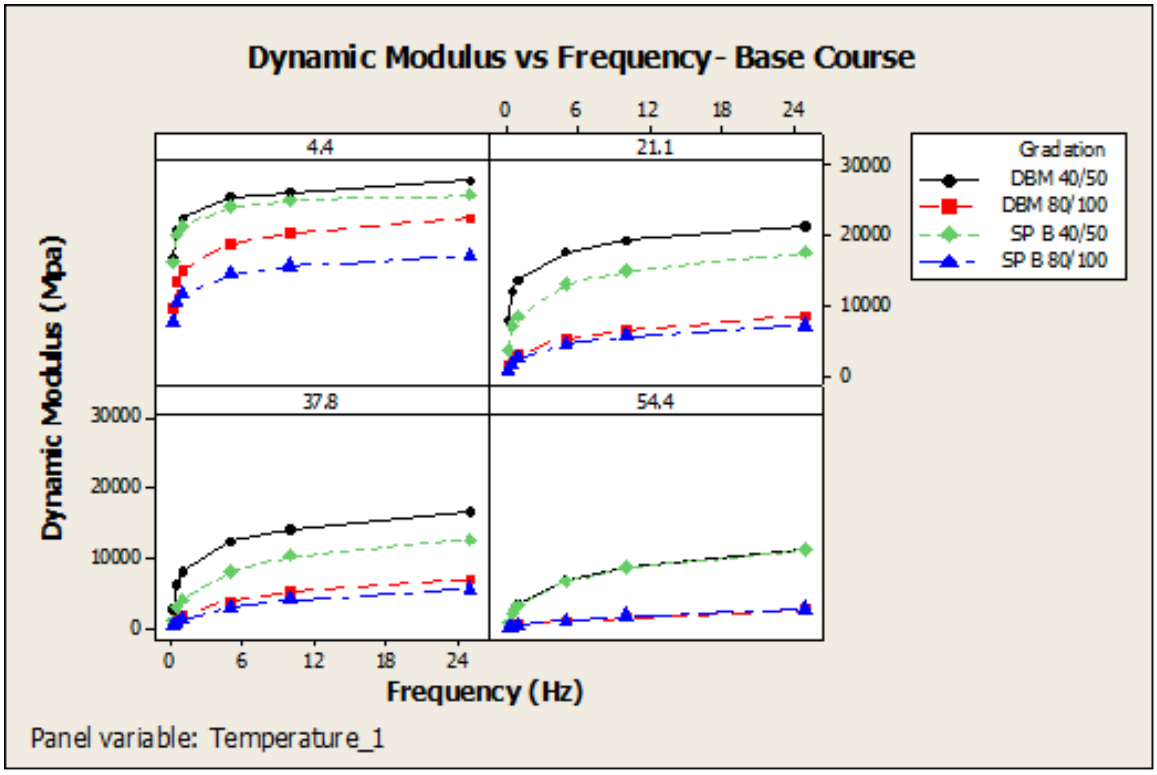

Figure 5.4: Isothermal Plots for Base Course Mixtures

5.3 MASTER CURVES DEVELOPMENT

Master Curves were developed using the dynamic modulus test results which are helpful in determining pavement behavior while designing process and are used as a material input in Mechanistic-Empirical Pavement Design Guide (MPEDG) software. These curves are developed using time-temperature superposition principle by the help of Master solver excel sheet which is produced as a part of NCHRP Project 9-29 (Bonaquist 2008). It is developed by using the concept of minimizing the sum of square of errors using the MS Excel solver add in tool to best fit the curve. This excel tool utilizes the sigmoidal function to build the master curves. For development of master curve, a reference temperature is selected for example I our case this reference temperature is 21.1°C and data at other temperatures is shifted with respect to reduced frequency until they all merge into a single smooth function. The amount of shift represented by shift factor shows the temperature dependency of the material. Figure 4.5 and 4.6 presents master curves for wearing and base course mixtures.

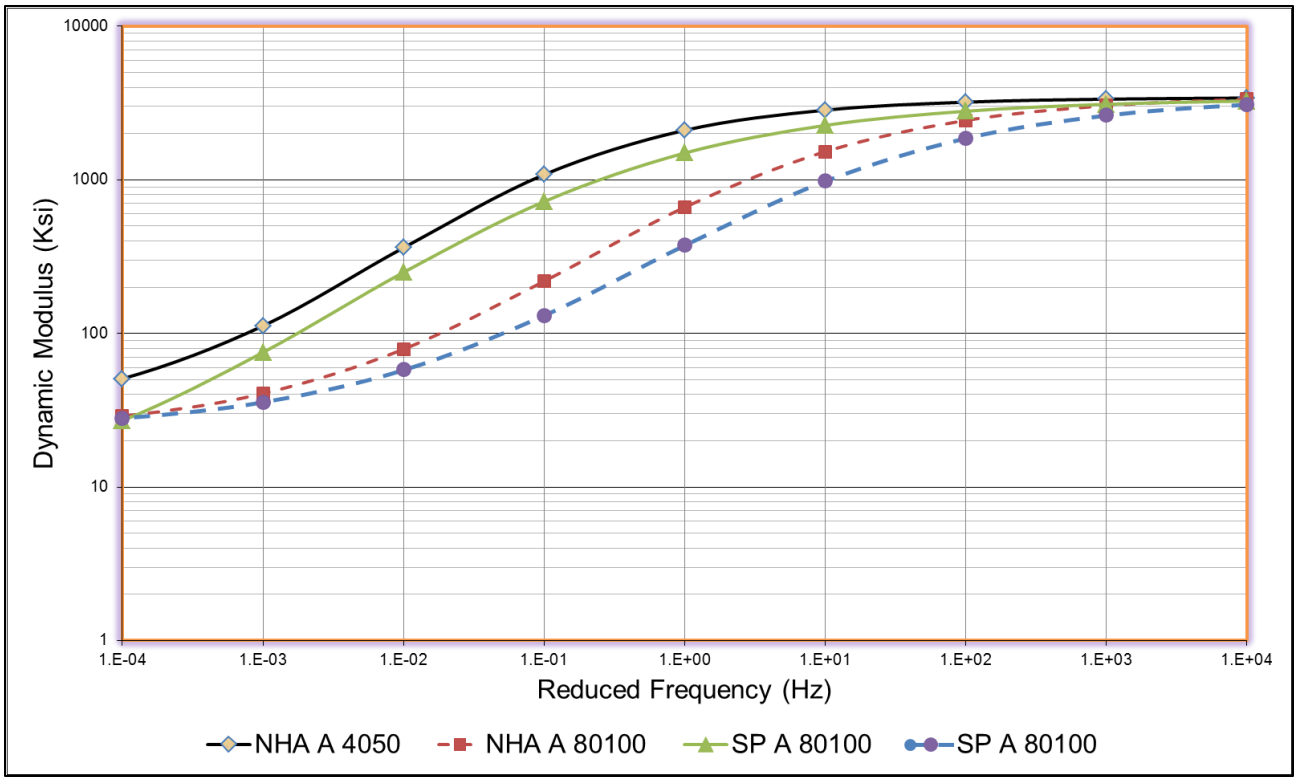

Figure 5.5: Master Curves for Wearing Course Mixtures

At low temperature presented by higher reduced frequency, master curves for almost all the mixtures merge at a single point irrespective of the binder penetration grade and gradation.

This may be explained by the reason that at lower temperature mix stiffness is dictated by binder stiffness while at high temperature; mix stiffness is dictated by the aggregate interlocking (Pellinen & Witczak 2002). At low temperature both binders are stiffer and stiffness of mixture

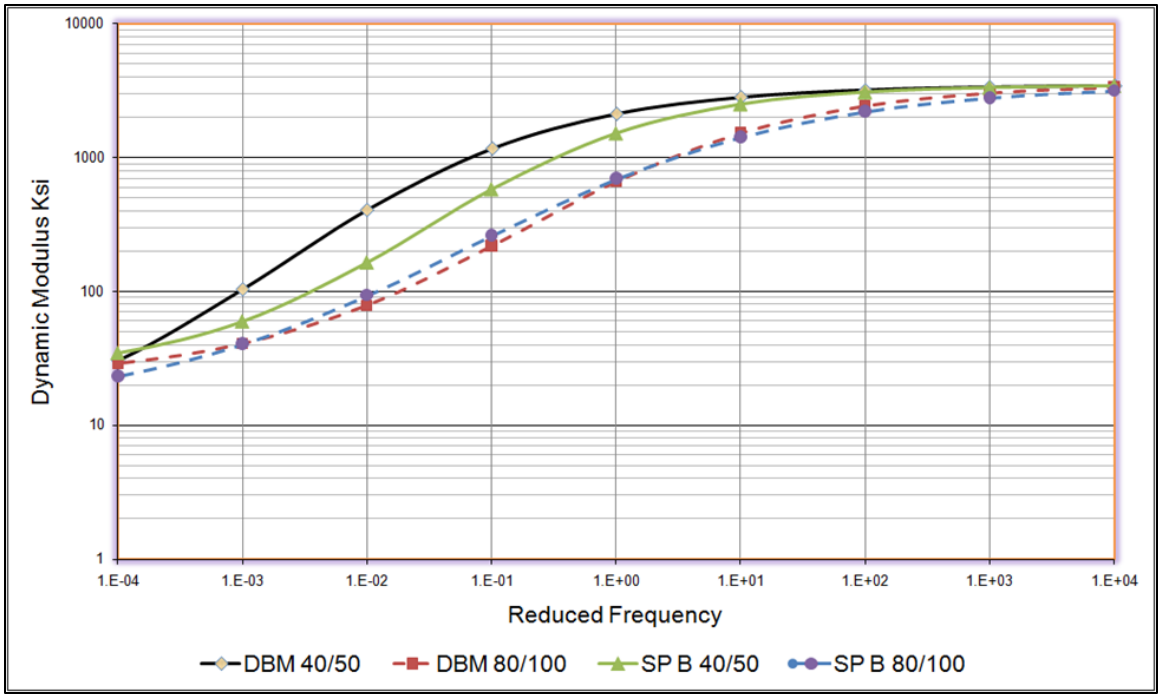

Figure 5.6: Master Curves for Base Course Mixtures

depends on stiffness of the binder resulting in merging of master curves at low temperature. But as the temperature increases shown by frequency decrease in master curves a drop in dynamic modulus master curves can be seen. This drop is 1st observed in mixtures with 80/100 pen grade binder as the stiffness of softer binder decreases more rapidly due to increase in temperature. As the highest test temperature reaches the master curves are merged once again. But this time this merging of the master curves is attributed to aggregate gradation and aggregate interlock. Because at higher temperature both the binders are soften enough that their role in mixture stiffness is limited by the aggregate interlock and gradation with higher aggregate interlocking are showing higher stiffness as compared to aggregate gradations with lower aggregate interlocking properties. At intermediate temperatures mix stiffness is governed by combined interaction of binder's stiffness and aggregate gradation.

5.4 DESIGN OF EXPERIMENT

Design of experiment technique was incorporated to evaluate the effects and interaction of different variables on dynamic modulus results of tested HMA mixtures. This was done with the help of Minitab 15 and a two level factorial design was selected to analyze the results. It is called two level design of experiment because it has two levels low level and high level. After initial trial and error procedure all the insignificant variables were eliminated including NMAS, Optimum bitumen content (OBC), VFA and VMA etc. and only three variables are selected for carrying out two level factorial design of experiment. These variables are frequency, temperature and binder viscosity. Theses variables along with their units, abbreviations and levels are presented in Table 4.1.

Table 5.1: Design of Experiment

Factors	Abbreviation	Units	Low level	High level
Frequency	Freq	Hz	0.1	25
Temperature	Temp	°C	4.4	54.4
Binder Viscosity	BV	cp	212.5	485.8

Table 4.2 presents the estimated main effects and the interaction effects as a result of the factorial design. From the effect of a variables we can determine how average response of dependent variable changes as the level of dependent variable changes from high to low or from low to high. It's an estimate of strength of significance of an independent variable. Greater the absolute value of the effect of a variable, greater will be its significance. The sign of effects shows the nature of the effect. A positive sign shows a direct relationship of independent variable with the dependent variable i.e. value of dependent variable increases as the value of independent variable increase. A negative sign shows the negative relation i.e. the increase in value of independent variable will result in a decrease in dependent variable.

Table 5.2: Estimated Effects of Dynamic Modulus for Wearing Course mixes

One Factor			Two Factors			Three Factors		
Main factors	**Effects**	**p-value**	**Interaction**	**Effects**	**p-value**	**Interaction**	**Effect**	**p-value**
Temp	-16737	0	Temp* freq	-1557	.098	Temp*	-963	.301
Freq	7185	0	Temp*BV	-53	.949	freq* BV		

BV	6526	0	Freq*BV	2284	.001

Similarly for Base course mixtures

Table 5.3: Estimated Effects of Dynamic Modulus for base Course Mixtures

One Factor			Two Factors			Three Factors		
Main factors	**Effects**	**p-value**	**Interaction**	**Effects**	**p-value**	**Interaction**	**Effect**	**p-value**
Temp	-18695	0	Temp* freq	-1667	.097	Temp*	-973	.311
Freq	6543	0	Temp*BV	-64	.900	freq* BV		
BV	5748	0	Freq*BV	3675	.001			

It is clear from Table 4.2 and Table 4.3 that testing temperature, frequency and binder viscosity significantly affect F value of dynamic modulus in case of both wearing and base course mixtures. However, if we evaluate the strength of the effects, temperature effect is stronger than frequency and its sign is negative meaning that it inversely effects the value of dynamic modulus i.e. by increasing dynamic temperature value of dynamic modulus decreases. And frequency and binder viscosity have a positive sign meaning that by increasing testing frequency and binder viscosity value of dynamic modulus increases.

ANOVA is used to compare various variables and groups of variables for their significance. ANOVA stands for Analysis of Variance.

Table 5.4: ANOVA for Dynamic Modulus of Wearing Course Mixes

Source	DF	Seq SS	Adj MS	F	P
Main Effects	3	14311355645	3992146780	232.58	0.000
2-Way Interactions	3	244722446	78432625	4.57	0.004
3-Way Interactions	1	18138234	18138234	1.06	0.305
Residual Error	280	4806014536	17164338		
Pure Error	240	1723649873	7181874		
Total	287	19380230861			

Table 5.5: ANOVA for Dynamic Modulus of Base Course Mixes

Source	DF	Seq SS	Adj MS	F	P
Main Effects	3	13847844887	3839415447	396.82	0.000
2-Way Interactions	3	345401645	71527531	6.89	0.000
3-Way Interactions	1	70431112	70431112	6.78	0.010
Residual Error	280	2906953408	10381976		
Pure Error	240	678934068	2828892		
Total	287	17170631052			

Table 4.4 and Table 4.5 represents that the ANOVA for the dynamic modulus of both the wearing and base course mixtures. Degree of freedom value is 03 in both the tables which means that 03 independent variables are used to explain the dependent variable. For wearing course mixes the three-way interaction is not significant while for base course mixes it is slightly significant. Significant of an effect can be easily judged by its p-value. P-value less than 0.05 represent a significant effect.

An easy way to determine whether a factor or interaction is significant or not is cumulative normal probability plots as presented in Figure 4.7 and 4.8 for wearing course and base course mixtures respectively.

Red square dots represent significant factors while black round dots represent insignificant factors. Distant from the reference line shows strength of the relation while direction shows the nature of the relation whether the effect is positive or negative. We can see that effect of temperature on value of dynamic modulus is most significant and is negative i.e. increasing temperature will decrease the value of dynamic modulus as discussed earlier. Effects of frequency and binder's viscosity are also significant and of nearly same strength and showing a positive relationship with the values of Dynamic Modulus. Two-way interaction effect of binder viscosity and frequency is slightly significant as the point lies closer to the line. The cumulative normal probability plot for base course is similar to the wearing course. The only difference is that three-way interaction effect of temperature, frequency and binder viscosity showing a little significance in base course normal plot but are insignificant in wearing course normal plot.

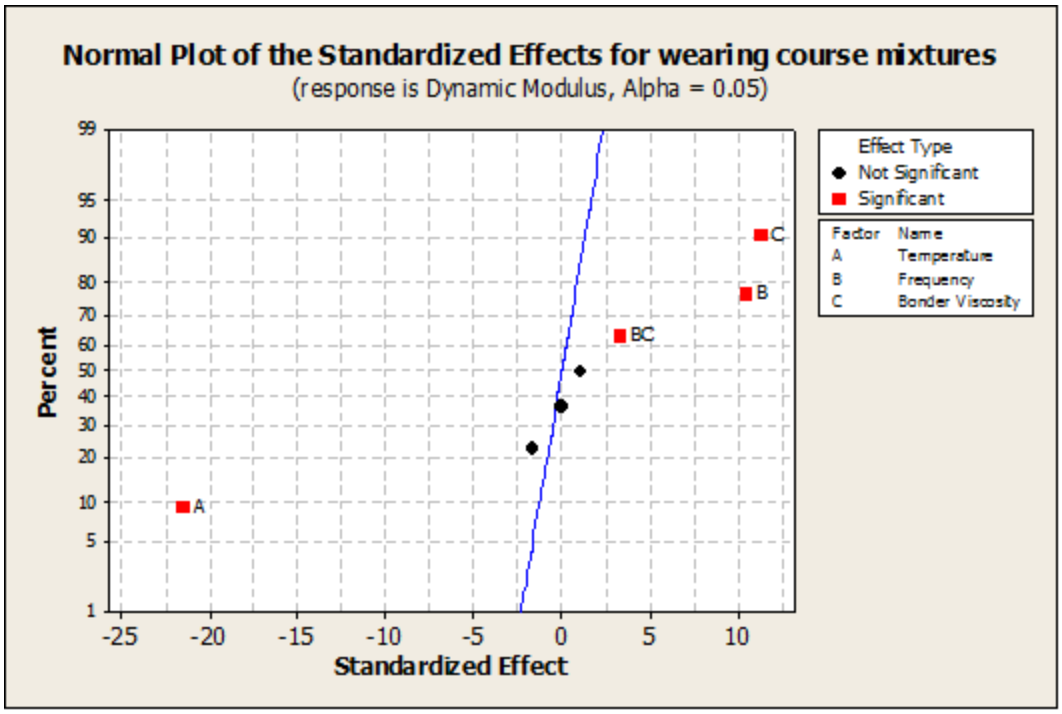

Figure 5.7: Normal Pot- Wearing Course

The next are main effects plots. In these plots main effect of a predictor variable is

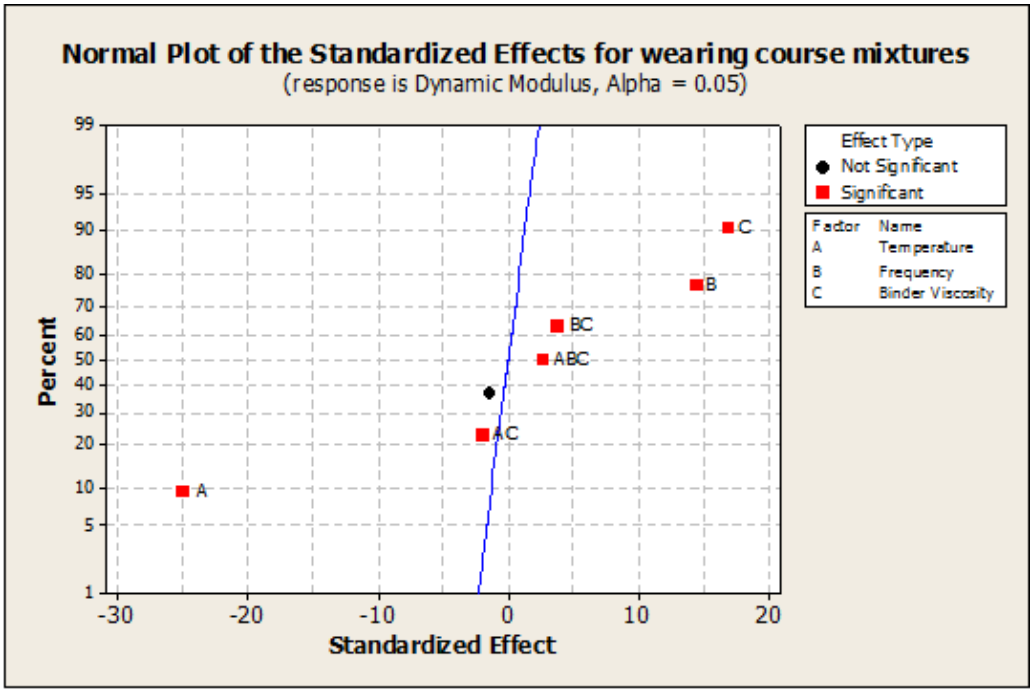

Figure 5.8: Normal Plot for Base Course Mixtures

plotted against its high and low values and slop of the resulting line represents the strength and nature of the relation. Figure 4.9 shows the main effect plot for the wearing course mixes. Dependent variable i.e. dynamic modulus is plotted on the y-axis and independent variables i.e. temperature, frequency and binder viscosity are plotted on x-axis in three separate panels. The sharp slope of the temperature line represents its greater effect on dynamic modulus value and the direction in which the line is inclined clearly shows its negative relation with the dynamic modulus i.e. increasing temperature will decrease the dynamic modulus values. The lines for both frequency and binder viscosity are positively sloped and frequency line having a slope slightly greater than that of binder viscosity line, which means that increasing the binder's viscosity or loading frequency will increase the dynamic modulus values.

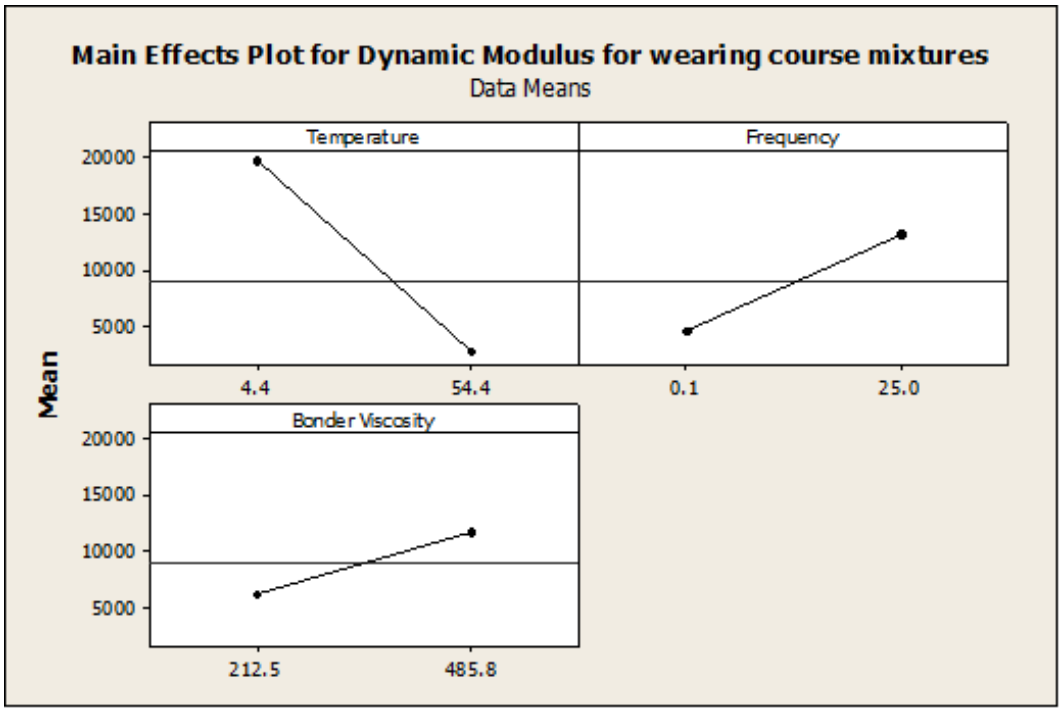

Figure 5.9: Dynamic Modulus Main Effect Plots- Wearing Course

Main effects plot of base course mixtures also show similar kind of trends and behavior and represented by Figure 4.10.

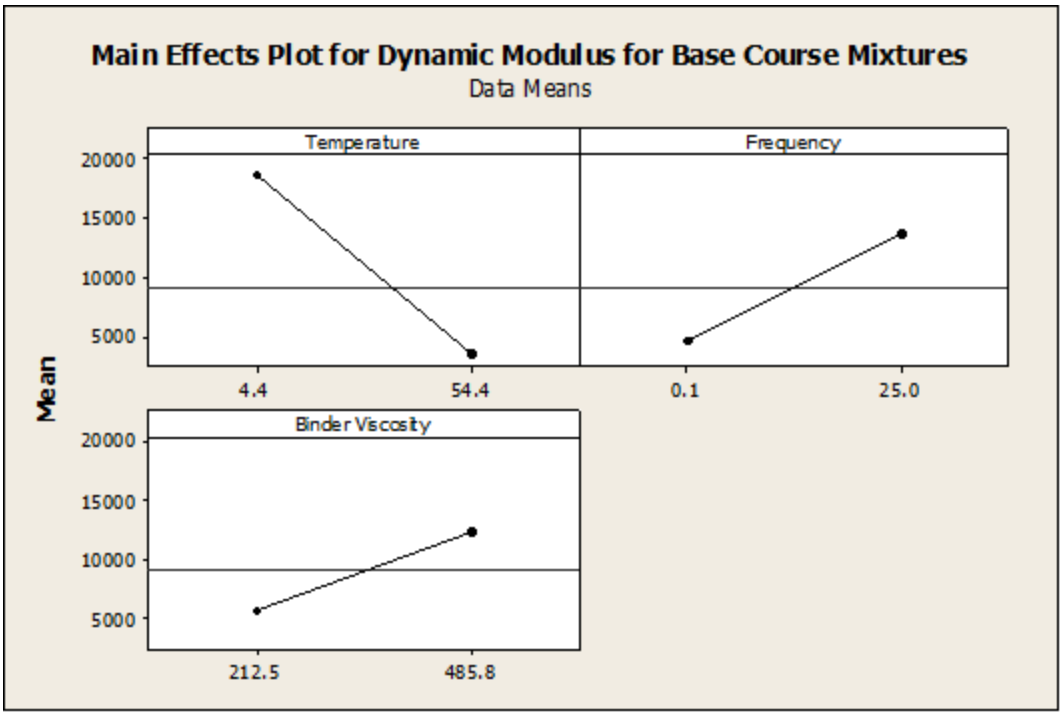

Figure 5.10: Dynamic Modulus Main Effect Plots- Base Course

Figure 4.11 and 4.12 represents the interaction plots. In interaction plots we can visualize that how high and low levels of a factor are effecting the level of the other factors. Parallel lines mean no or little interaction. But as the lines become more and more unparalleled the degree of interaction increases.

Figure 4.11 shows the interaction plots for wearing course mixtures. If we take a look at the temperature-binder viscosity relationship the interaction lines are completely parallel representing that no significant interaction lies in between the testing temperature and binder viscosity also discussed in effects and interaction tables. But if we analyze the plots of temperature-frequency and frequency-binder viscosity relationship, the lines are slightly unparalleled showing that a relationship exist that is not significant.

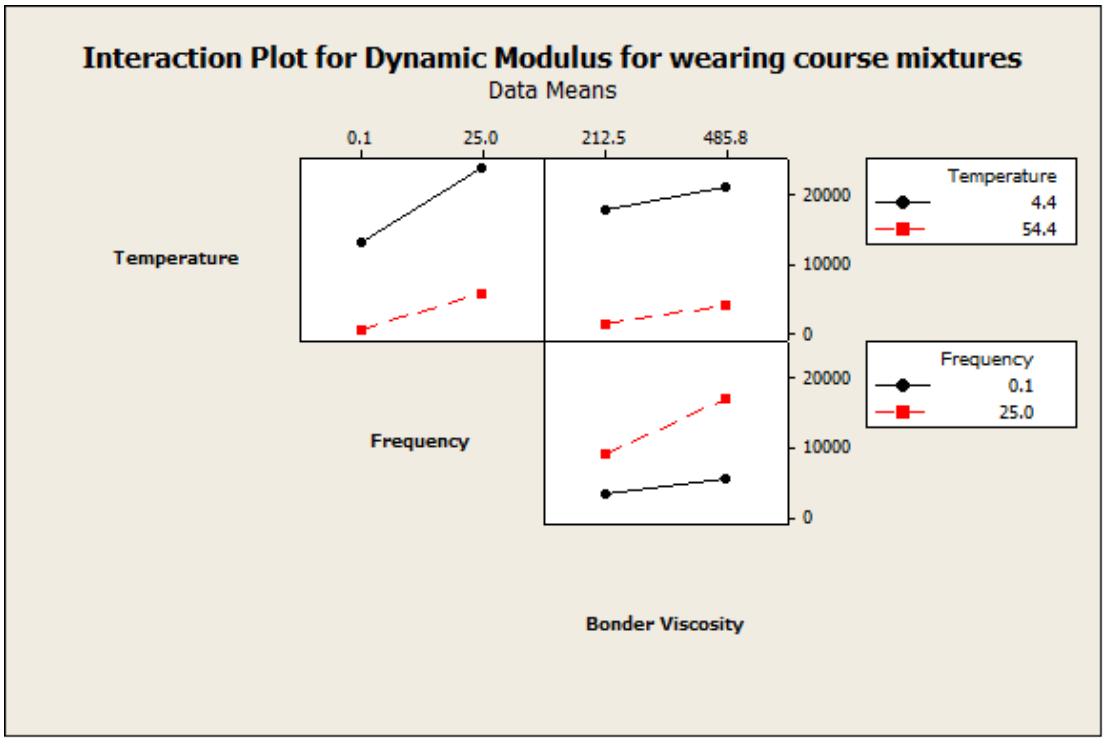

Figure 5.11: Dynamic Modulus Interaction Plots- Wearing Course

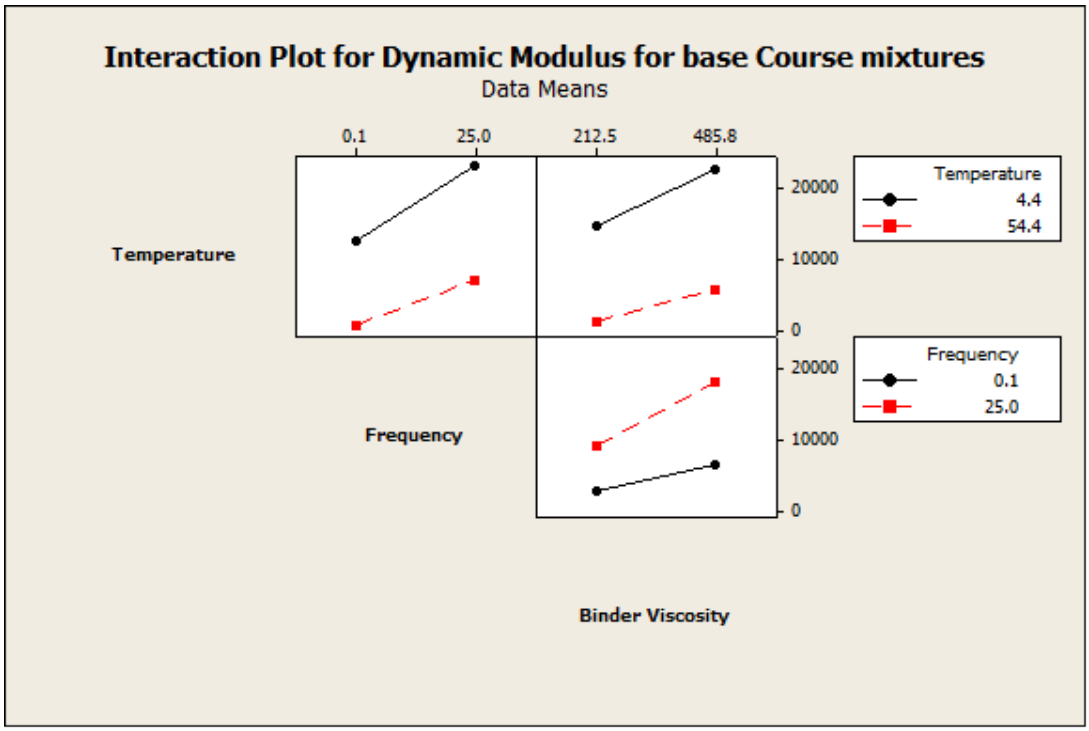

Figure 5.12: Dynamic Modulus Interaction Plots: Base Course Mixture

The interaction plot for dynamic modulus of base course mixtures is presented in Figure 4.12. The interaction effects are nearly same as the in the wearing course mixtures.

A pareto chart contains a reference line which is the line of significance. Any effect extending beyond the reference line is significant. Greater the length of bar for an effect greater is the magnitude of that effect and vice versa. It only shows absolute value of the effects. Figure 4.13 shows Pareto chart of standardized effects for wearing course mixtures. Length of temperature bar is greater than other bars showing the greater magnitude of the standardized effect of the temperature. Then are the viscosity and frequency bars representing their relative effects. It can be seen that there is no much difference between the standardized effect of the viscosity and the temperature as shown by their nearly equal bars. The combined two-way effect of the frequency and binder viscosity is also significant to a little extent as represented by smaller bar.

The two-way standardized effect of temperature-binder viscosity and three way standardized effects of temperature-frequency-binder viscosity are insignificant as their representative bars don't cross the reference line.

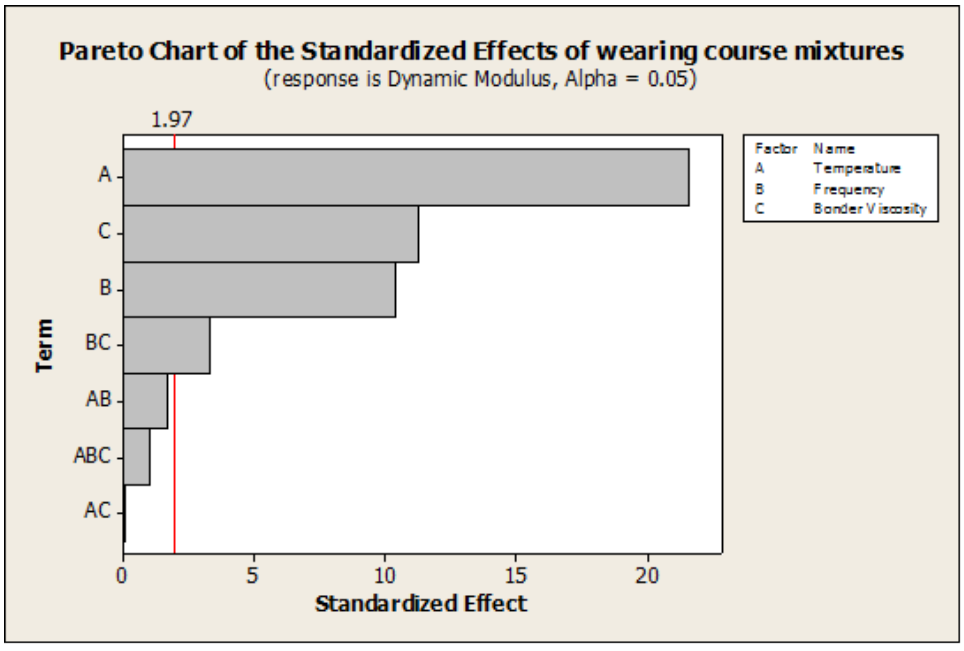

Figure 5.13: Pareto Chart of the Standardized Effects- Wearing Course

Figure 4.14 shows Pareto chart of standardized effects for base course mixtures.

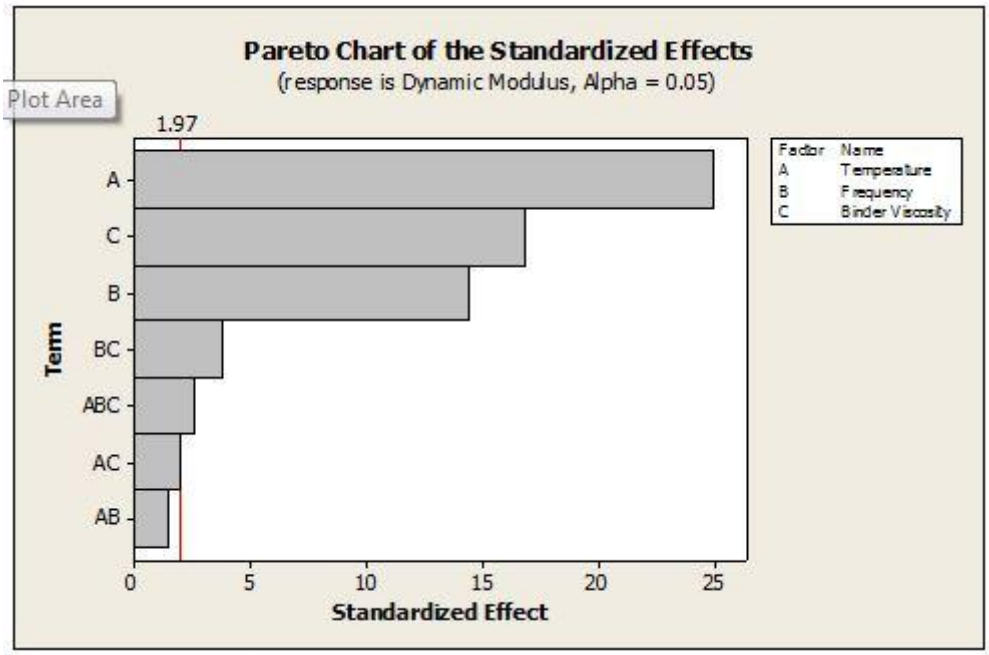

Figure 5.14: Pareto Chart of Standardized Effects-Base Course

5.5 PERFORMANCE MODELING

The performance is assessment of the response of HMA paved surface when open to the elements like climate conditions, traffic loading and temperature etc. it is important to predict pavement response at designing phase so that we can make all efforts such as improved materials, improved designs and improved specifications to elongate the life span of the pavement. This can be achieved by developing pavement performance models to foresee distresses like rutting and fatigue etc. in the pavement before construction of the pavement. In new mechanistic empirical pavement design guide material response and its behavior to applied load is modelled using dynamic modulus. So dynamic modulus is very important input parameter in pavement design but determination of dynamic modulus in laboratory is a laborious and time taking procedure. So predictive models are developed to predict dynamic modulus based on some independent variables. In our case, the dependent variable is dynamic modulus which is predicted using three independent variables that are temperature, frequency and type of bitumen

Dynamic modulus $|E|^* = f$(temperature, frequency, Binder Viscosity)

Model was developed using hit and trial method using the laboratory test results of dynamic modulus. Various functional forms were checked and finally Cobb Douglas functional form was selected due to its higher coefficient of determination (R^2) value. And also to keep the things simple.

The general generic form of Cobb Douglas model is shown below

$$Y = a \times X^{\beta i}$$

Where i= Number of Variables=1, 2, 3, 4…….N

For wearing course mixtures performance modeling was done using four predictor variables i.e. temperature (T in °C), frequency (F in Hz), viscosity of the binder (V in centipoise) and NMAS (Nominal Maximum Aggregate Size) (S in mm). So functional form becomes as follow

$$|E^*| = \alpha \times T^{\beta_1} \times F^{\beta_2} \times V^{\beta_3} \times S^{\beta_4}$$

For base course mixtures only three predictor variables are used because NMAS is constant for all base course gradations. So for base course the functional form is reduced and can be written as shown in equation

$$|E^*| = \alpha \times T^{\beta_1} \times F^{\beta_2} \times V^{\beta_3}$$

The estimated parameters for both wearing and base course are represented in table 4.6 and 4.7 respectively. α, β1, β2 and β3 are the regression coefficients,

Table 5.6: Model Summary- Wearing Course

Parameter	Estimate	Std. Error	t-Stat	R^2 (%)	95 % confidence Interval	
					Lower Bound	Upper Bound
A	261.907	91.491	2.86	84.2	81.816	441.999
β_1	-0.552	0.019	-29.05		-.591	-.514
β_2	0.134	0.010	13.40		.115	.154
β_3	0.453	0.042	10.79		.369	.538
β_4	0.852	0.084	10.14		.687	1.018

The above table shows the estimated parameters and their respective t-stat. all the parameters are significant at 95% confidence interval as evident from their t-stat values. The coefficient of determination R^2 value is 84.2% which means that independent variables are explaining the 84.2% variation in the values of dependent variable. The model summary for base course mixtures is represented in table 4.7

Table 5.7: Model Summary- Base Course

Parameter	Estimate	Std. Error	t-Stat	R^2 (%)	95 % confidence Interval	
					Lower Bound	Upper Bound
A	495.522	123.956	3.997564	86.7	251.534	739.51
β_1	-0.492	0.016	-30.75		-0.523	-0.46
β_2	0.144	0.009	16		0.126	0.161
β_3	0.718	0.041	17.5122		0.637	0.8

Coefficient of determination R^2 value is 86.7%. All the parameters are significant at 95% confidence level because their t-stat value is greater than 2.308.

5.6 FATIGUE PARAMETER

In general, fatigue is process in which pavement weakens and develop cracks due to the repeated traffic loading. As pavement is exposed to recurring traffic loading and unloading, if loading go beyond certain limit, crack initiates at top and bond between binder and aggregate reduces. This results in propagation of cracks. E* and phase angle (ϕ) results can be combined to calculate fatigue parameter which is used to estimate the fatigue susceptibility of HMA mixes.

Fatigue Parameter= $|E^*| x \sin\phi$, where $|E^*|$ is dynamic modulus and ϕ is phase angle. It has an inverse relationship with resistance to fatigue cracking. Higher value of fatigue parameter represents lower resistance to fatigue cracking and vice versa (Ye et al. 2009). Figure 4.15 represents the fatigue parameters of wearing course mixes at 21 °C temperature and six different frequencies i.e. 25, 10, 5, 1, 0.5, 0.1 Hz. Fatigue parameter was calculated at 21^{O}C because at higher temperatures HMA pavements are more prone to rutting instead of fatigue. HMA layers are more susceptible to fatigue at medium temperatures.

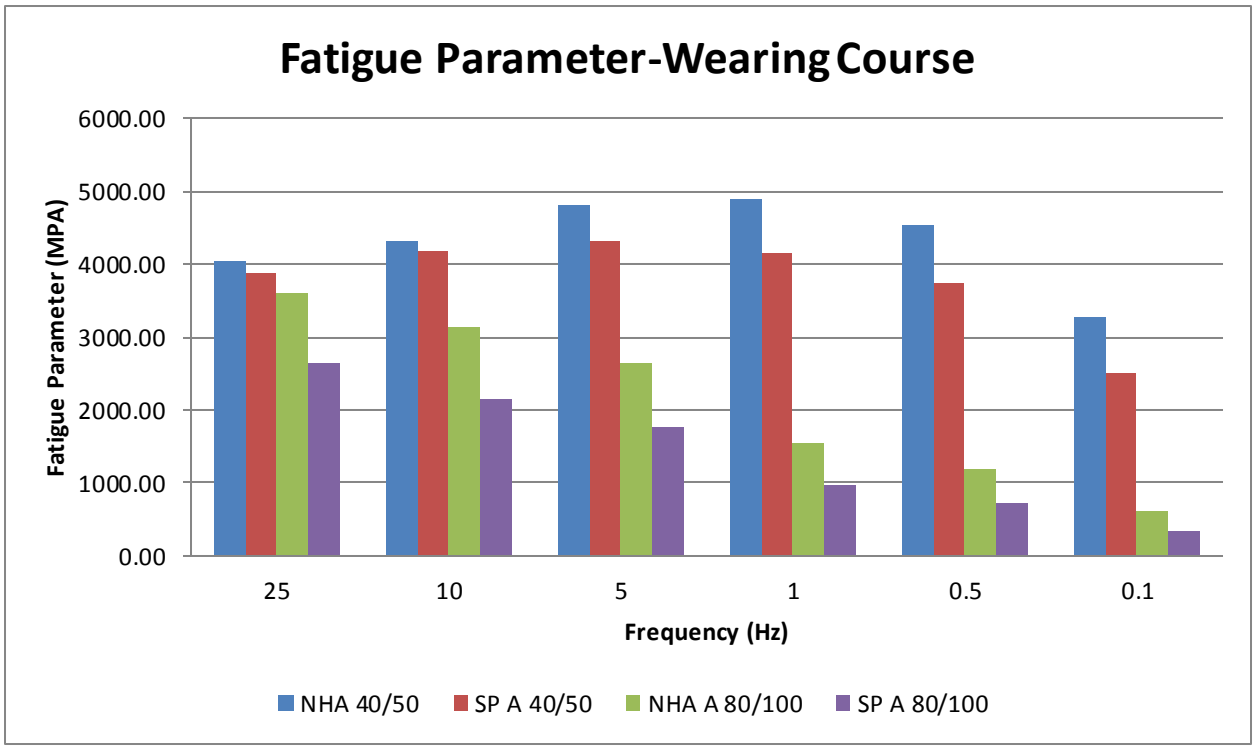

Figure 5.15: Fatigue Parameter- Wearing Course

. From the Figure it is clear that gradations with 80/100 binder show the smaller fatigue parameter than gradations with 40/50 binder. This is because of lower stiffness of the HMA mixes fabricated using 80/100 binder. This lower stiffness leads to the improved flexibility/ductility resulting in lower dynamic modulus values. As fatigue parameter is product of dynamic modulus and sine of phase angle, lower dynamic modulus leads to lower fatigue parameter which shows higher fatigue resistance of the mixtures. And if we compare the two gradations SP A has a low fatigue parameter showing its high resistance to fatigue than NHA A gradation. This may be because NHA A gradation is dense and stiffer and more prone to fatigue cracking as compared to SP A in which fines content is more, reducing the mix stiffness and its fatigue susceptibility. Figure 4.16 represents a comparison between the base course gradations for the two binders. Here again gradations with 80/100 produces a lower fatigue parameter depicting its higher fatigue resistance as compared to mixes with 40/50 pen grade binder. And individually fatigue parameter of SP B is smaller than DBM. And from the figures it is also obvious that as the frequency decrease fatigue parameter also decreases. Because lesser the number of load repetitions, lower will be the chance of fatigue cracking.

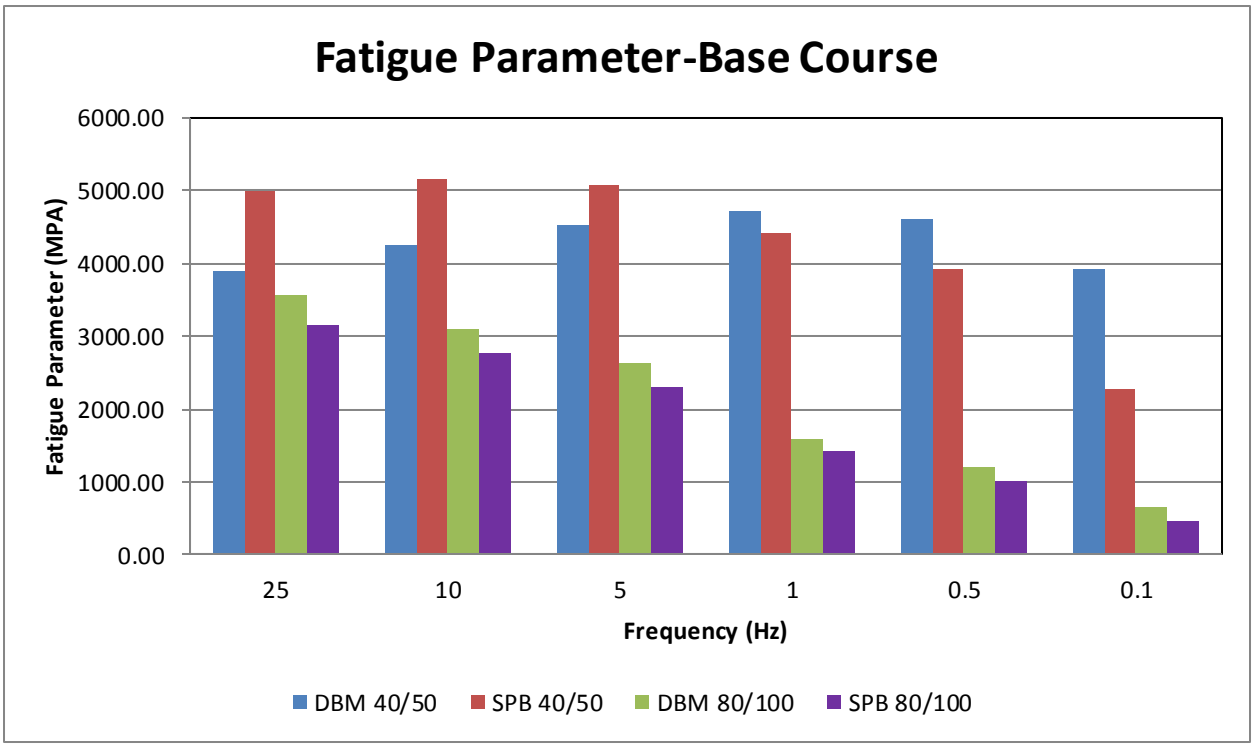

Figure 5.16: Fatigue Parameter- Base Course

5.7 PHASE ANGLE RESULTS

Phase angle is the angle measured in degrees by which the axial strain lags behind the vertical compressive stress. For perfectly elastic material phase angle is equal to zero and for perfectly viscous materials it is equal to 90 degrees. So in order to characterize a linear viscoelastic material it is vital to measure its phase angle along with its dynamic modulus. Phase angle is obtained as an output while conducting dynamic modulus test. As dynamic modulus test was conducted at various temperatures and frequencies phase angle results were also obtained for various temperatures and frequencies. In order to analyze phase angle results scatter plots are developed relating phase angle to dynamic modulus for different mix types and temperatures. From the scatter plots presented in Figure 4.17 it can be observed that phase angle generally decreases with increasing dynamic modulus value. This is because higher dynamic modulus values are obtained at low temperatures and at low temperature HMA mixes are stiffer as compared to high temperatures and load induced strains take less time to recover. But as the temperature is increased, HMA mix stiffness decreases, its behavior changes from elastic part towards more viscous part resulting in increased phase angle values and decreased dynamic modulus values. This behavior is observed up to a temperature of 37.8°C. After 37.8°C the

phase angle value starts decreasing with increasing temperature. This may be due to the reason that when temperature is increased to 54.4ºC, the binder becomes softer and less viscous and the phase angle is controlled by the aggregate behavior.at low temperature and higher frequency the phase angle is directly proportional to temperature. this direct relation can be explained by the fact that binder is stiffer at low temperature governing behavior of HMA due to which phase angle of binder is low causing phase angle of HMA to be low. At higher temperature, binders become softer and aggregate interlock dominates the behavior of HMA (Pellinen and Witczak, 2002).

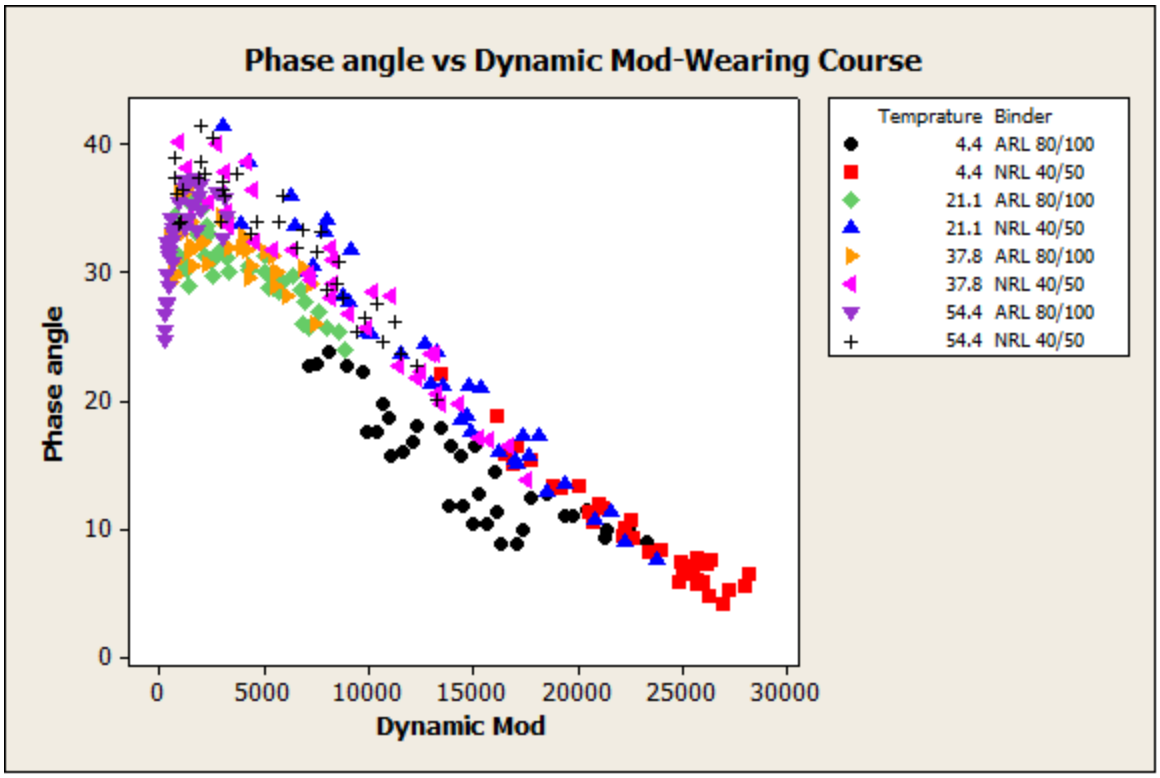

Figure 5.17: Phase Angle Vs Dynamic Modulus- Wearing Course

The scatter plots presented in Figure 4.17 and 4.18 for wearing and base course mixes augment the findings of Witzak and Pellinen. At low temperature which is 4.4ºC, mixes with 80/100 pen grade binder produces higher phase angle values as compared to mixes with 40/50 binder. This is because 40/50 binder is stiffer than 80/100 binder so the induced strains taking less time to recover. At 21.1ºC, behavior remain same for mixes with 40/50 pen grade binder i.e. increase of phase angle with increasing temperature but in case of 80/100 pen grade binder some mixes were observed which show a decrease in phase angle values at lower frequencies pointing

towards the above mentioned finding that at higher temperatures and lower frequencies aggregate interlock overpowers the binder stiffness. At 37.7ºC, trend remain the same as that on 21.1ºC for mixes with both the binders. At 54.4ºC, the behavior of softer 80/100 pen grade binder is totally overpowered by aggregate interlocking effect governing the phase angle values that are decreasing at a significant rate with the frequency drop. But the stiffer 40/50 pen grade binder is still showing the directly proportional values of phase angle with the temperature increase. Even at 54.4ºC, only few mixes are showing a decrease in phase angle values at lower frequencies. In short words, we can say that mixes with 40/50 pen grade binder at 54.4ºC are behaving nearly similar to mixes with 80/100 binder at 21.1ºC in case of phase angle values.

Same trend can be seen for the base course gradations shown in Figure 4.18.

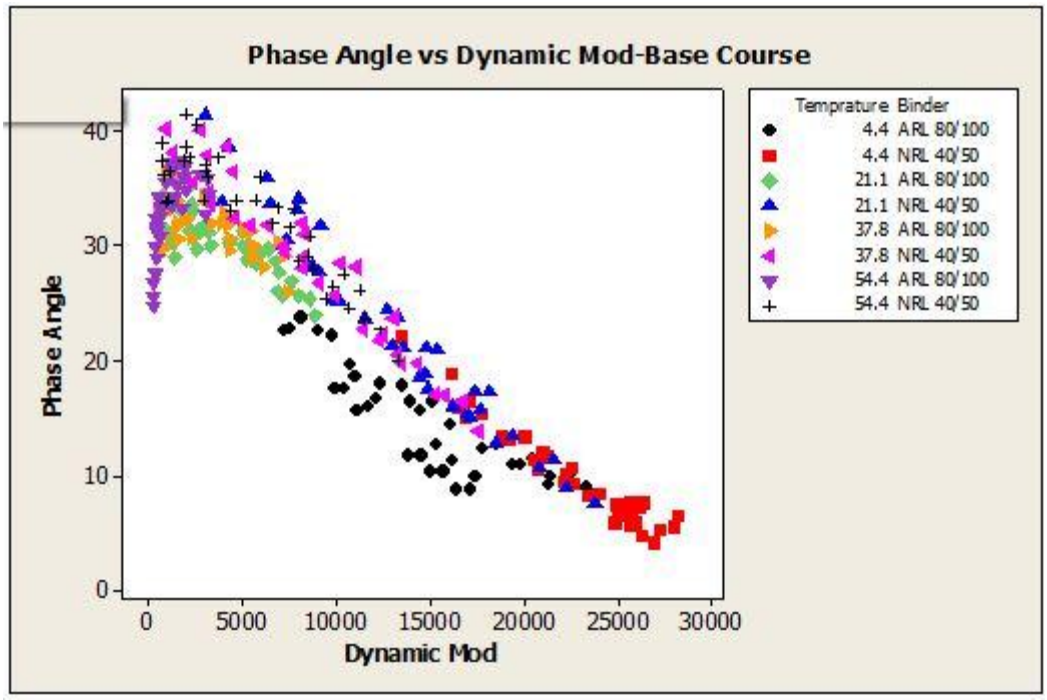

Figure 5.18: Phase Angle Vs Dynamic Modulus- Base Course

5.8 TWO FACTORIAL DESIGN FOR PHASE ANGLE

Two level factorial design was also adopted for phase angle results the factors were kept the same as that for dynamic modulus. The tabulated effects and ANOVAs are represented in the following tables.

Table 5.8: Estimated effects for Phase Angle-Wearing Course

One Factor			Two Factores			Three Factors		
Main factors	**Effects**	**p-value**	**Interaction**	**Effects**	**p-value**	**Interaction**	**Effect**	**p-value**
Temp	23.172	0	Temp* freq	-3.490	.003	Temp*	-1.909	.097
Freq	-7.843	0	Temp*BV	0.538	.576	freq* BV		
BV	-6.081	0	Freq*BV	-4.270	.000			

Above Table 4.8 shows temperature has direct relationship with the phase angle value as represented by its positive sign and its effect is greater than other frequency and binder viscosity. Two-way interaction effects of temperature and binder viscosity is insignificant because its p-value is greater than 0.005. Three-way interaction effect of temperature, binder and frequency is also insignificant. Table 4.9 represents estimated effects for phase angle of dynamic modulus for base course mixtures.

Table 5.9: Estimated effects for Phase angle og Dynamic Modulus- Base Course

One Factor			Two Factores			Three Factors		
Main factors	**Effects**	**p-value**	**Interaction**	**Effects**	**p-value**	**Interaction**	**Effect**	**p-value**
Temp	20.739	0	Temp* freq	2.706	.016	Temp*	-4.741	000
Freq	-8.423	0	Temp*BV	0.550	.557	freq* BV		
BV	-6.046	0	Freq*BV	-4.804	.000			

It is same as that for wearing course mixtures except that the three way interaction effect of temperature, frequency and binder is coming significant unlike the wearing course mixtures.

ANOVA for both the wearing course and the base course is represented in Table 4.10 and Table 4.11 respectively.

Table 5.10: ANOVA for Phase Angle--Wearing Course

Source	**DF**	**Seq SS**	**Adj MS**	**F**	**P**
Main Effects	3	22109.9	6445.10	246.73	0.000
2-Way Interactions	3	976.4	301.29	11.53	0.000
3-Way Interactions	1	72.5	72.54	2.78	0.097
Residual Error	280	7314.2	26.12		
Pure Error	240	1398.3	5.83		
Total	287	30471.3			

Table 5.11: ANOVA for Phase Angle-Base Course

Source	**DF**	**Seq SS**	**Adj MS**	**F**	**P**

Main Effects	3	14311355645	3992146780	232.58	0.000
2-Way Interactions	3	244722446	78432625	4.57	0.004
3-Way Interactions	1	18138234	18138234	1.06	0.305
Residual Error	280	4806014536	17164338		
Pure Error	240	1723649873	7181874		
Total	287	19380230861			

In ANOVA table the significance of a factor is represented by its higher F and lower P values. From the above ANOVA tables for both wearing and base course it is clear that main effects are greatly significant then 2-way interactions which are slightly significant then 3-way interactions are insignificant.

These interactions can also be represented using normal probability plots. The distance from the reference line represent the strength or magnitude of the effect and its direction shows the nature of the relation whether it is direct or inverse. The normal probability plots of the phase angle for both the base course and wearing course are shown in Figure 4.19 and Figure 4.20 respectively

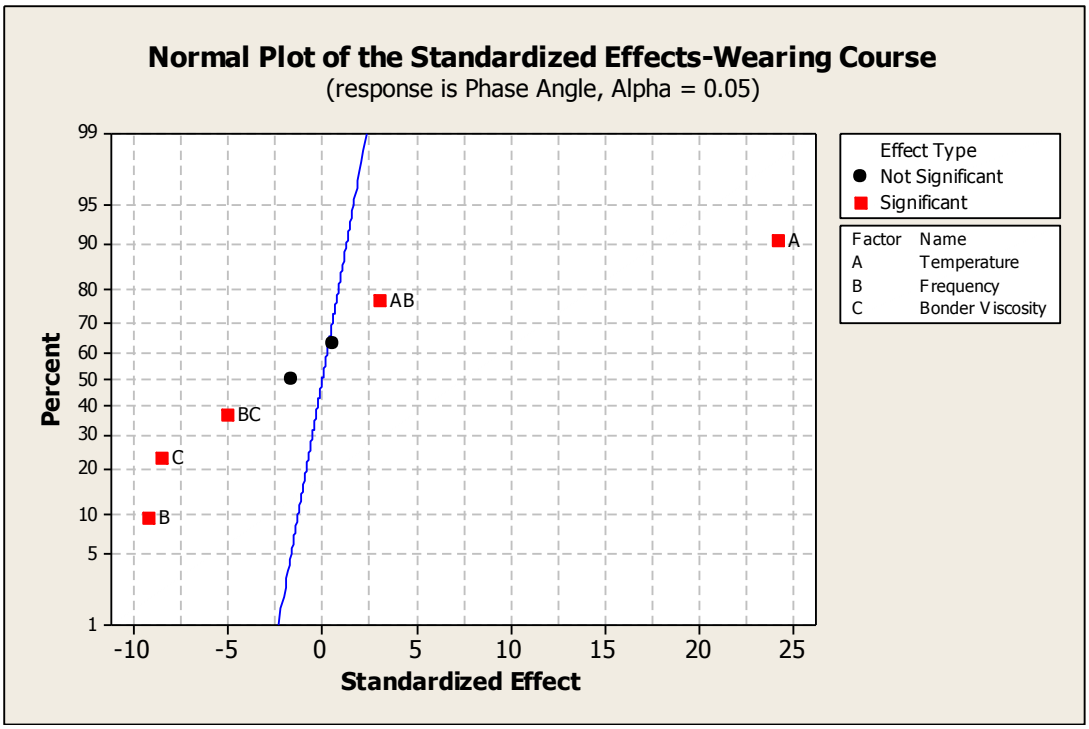

Figure 5.19: Normal Plots- Wearing Course

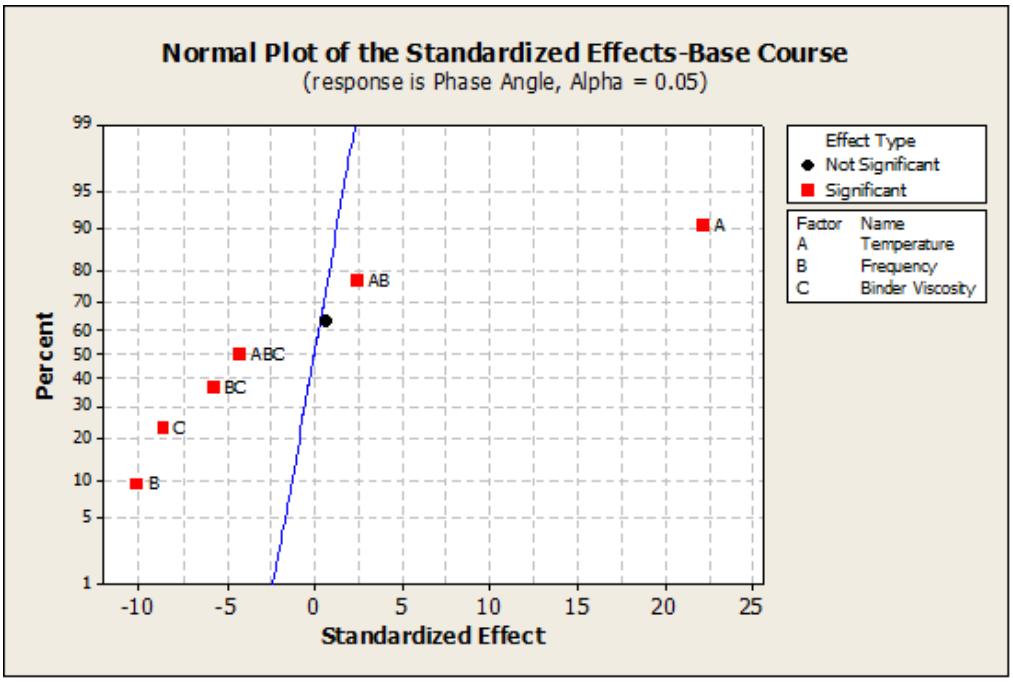

Figure 5.20: Normal Plot- Base Course

Main effects are represented by interaction plots of the main effects. If a line is straight having zero slope, then it has no effect on the response variable. Sharpness of the slope represents the strength of the effect and direction of the slope represents its nature i.e. direct effect or inverse effect. Figure 4.21 and 4.22 represents the main effect plot for the wearing course and base course mixes respectively. In both figures it can be seen that temperature is the most significant factor due to steepest slope of the line and also the positive slope of the temperature line represents that it is having a direct relation with the phase angle i.e. as the temperature increase phase angle increase and vice versa. In the same manner, the lines of other two factors i.e. frequency and binder's viscosity are less steep as compared to temperature line and so they have a comparatively less influence on the phase angle values. the slope of these lines is also negative showing that they are having an inverse relationship with the phase angle i.e. as the viscosity of the binder or the frequency increases the values of phase angle decreases and vice versa.

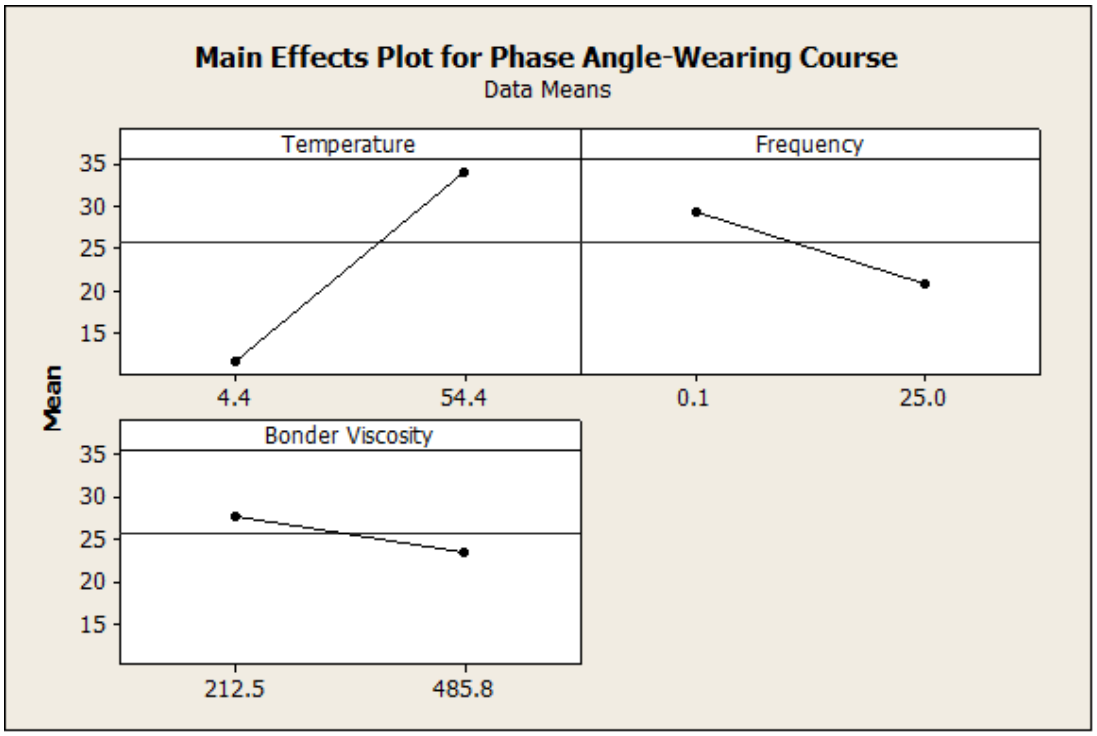

Figure 5.21: Main Effects Plot for Phase Angle-Wearing Course

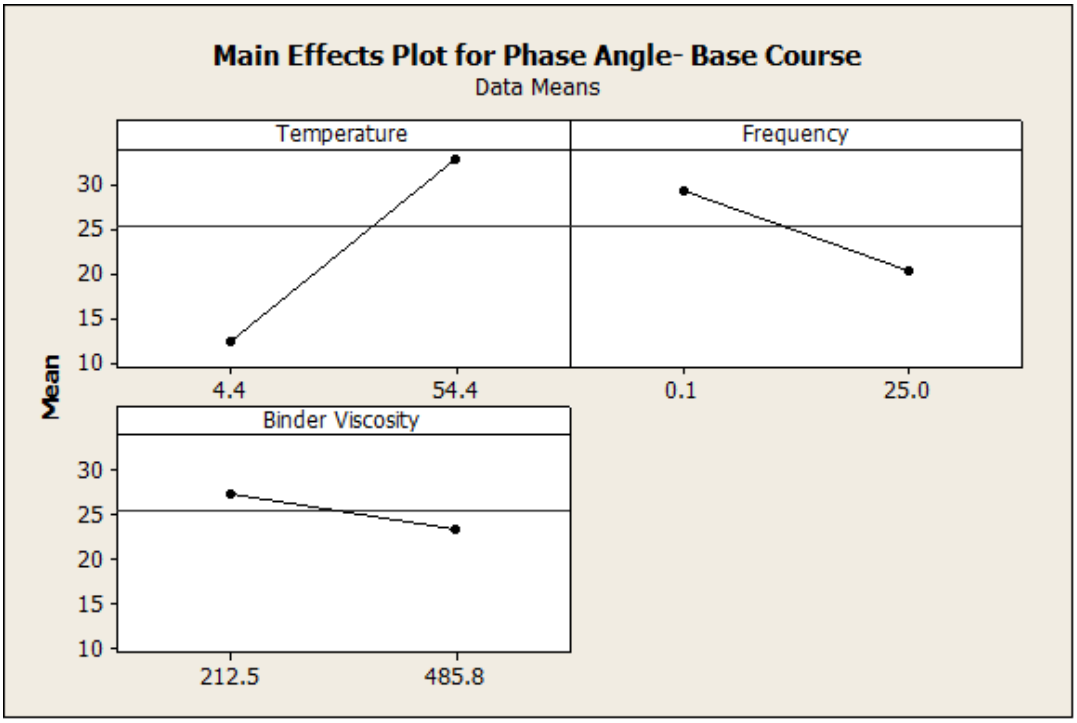

Figure 5.22: Main Effects Plot for the Phase Angle-Base Course

Interaction plots represent the interaction between the different factors. Figure 4.23 and Figure 4.24 represents interaction of phase angle for wearing and base courses respectively.

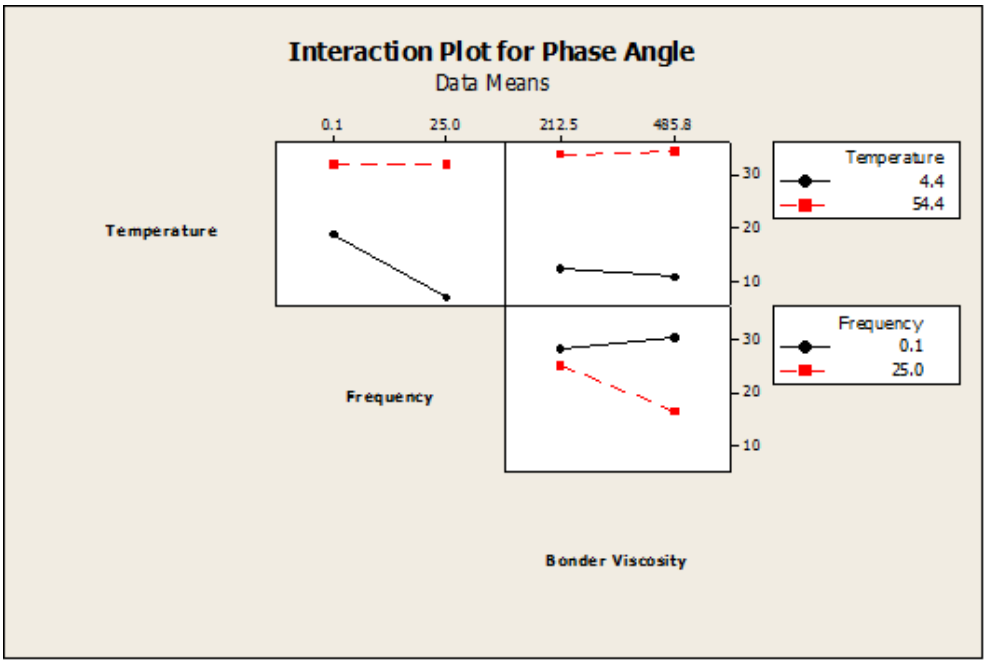

Figure 5.23: Interaction Plots for Phase Angle- Wearing Course

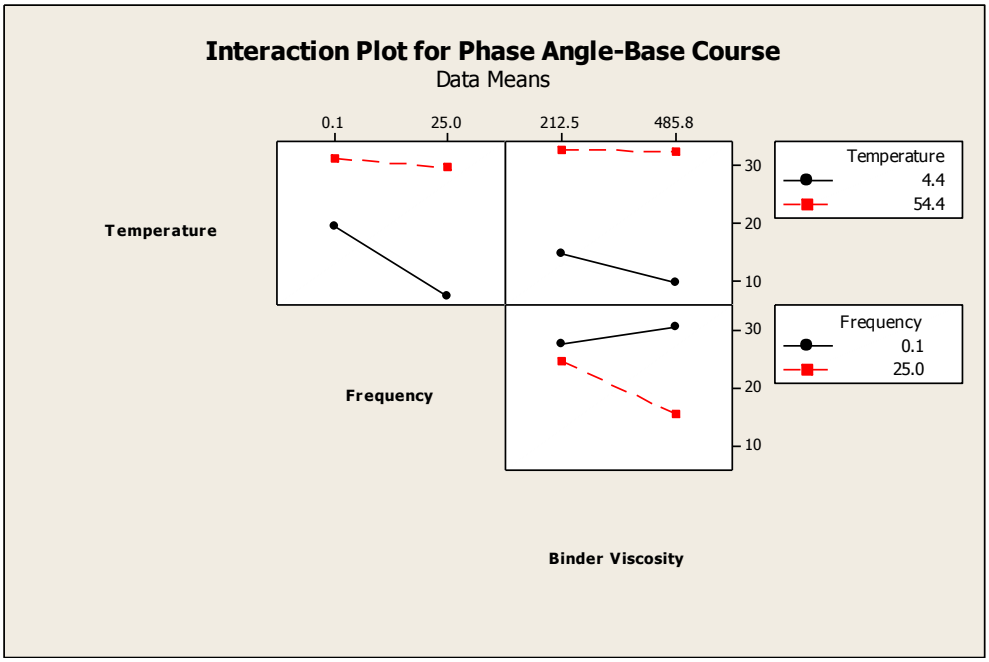

Figure 5.24: Interaction Plots for Phase Angle-Base Course

5.9 FLOW NUMBER TEST RESULTS

Flow Number tests have been performed on the laboratory prepared specimens in order to evaluate rutting susceptibility of the HMA mixes under study. The tests were conducted at 54.4ºC because of increased rutting susceptibility of HMA mixes at higher temperatures. Stress level was chosen as 300 KPa in order to be consistent with the previous studies. And the test termination was set to 50,000 micro strains or 10,000 cycles whichever occurring first. Flow number test is considered to best simulate the field conditions as it allows some rest period between the load applications as in actual pavements. Table 4.12 and 4.13 shows end results of the flow number test for both wearing and base course mixtures respectively. Mixes fabricated with softer 80/100 pen grade binder accumulated more strains and reached the termination strain before completion of load cycles. But mixes fabricated with 40/50 binder accumulated less strains and load cycles were completed first before reaching the termination strains.

Table 5.12: Software Results for Flow Number-Wearing Course

Gradation	Binder	Cycles	Accumulated Strains
NHA A	NRL 40/50	10,000	43711
	ARL 80/100	7792	50,000
SP A	NRL 40/50	10,000	49,945
	ARL 80/100	3170	50,000

Table 5.13: Software Results for Flow Number-Base Course

Gradation	Binder	Cycles	Accumulated Strains
SP B	NRL 40/50	10,000	46491
	ARL 80/100	7460	50,000
DBM	NRL 40/50	10.000	26530
	ARL 80/100	9600	50,000

From the results it is noticeable that the mixtures with 40/50 undergo fewer strains as compared to the mixtures with 80/100 binder. This is due to the fact that40/50 binder is stiffer then ARL 80/100 binder. In the following graphs the four gradations are compared using two binders. Mixtures with 40/50 binder are compared using accumulated axial strains and mixture with 80/100 binder are compared according to their cycles to termination strain limit that is 50,000 micro strains.

Figure 4.25 shows the accumulated axial strains for different wearing course and base course gradation due to the applied 10,000 load cycles. It is clear that in wearing course mixtures, SP A is more rut susceptible due to its greater accumulated axial strains and in base course mixtures DBM accumulated less strains as compared to SP B.

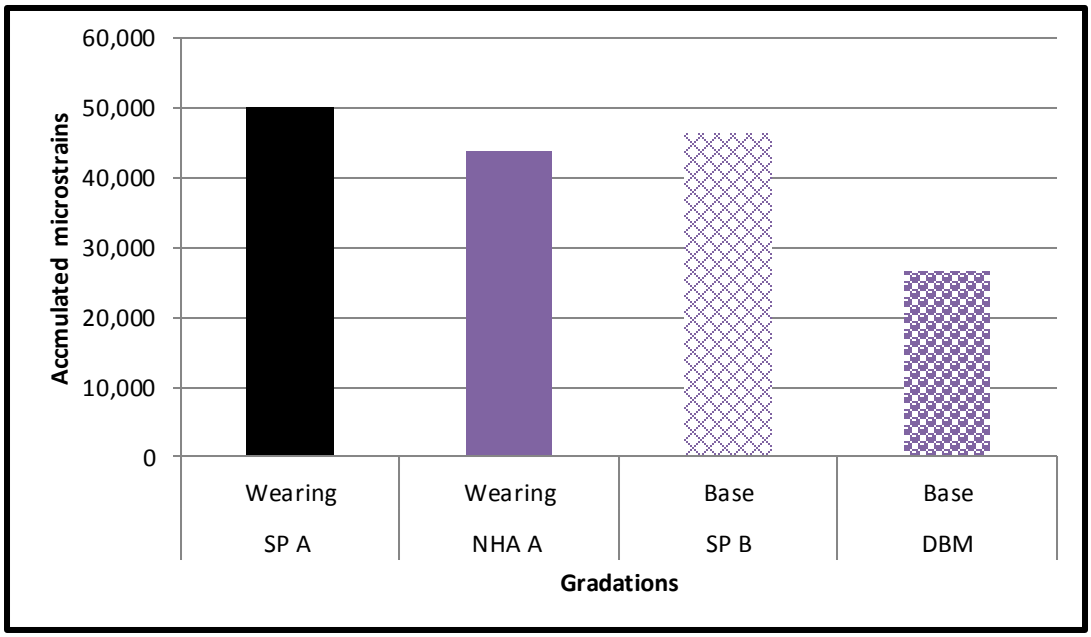

Figure 5.25: Accumulated Strains at Termination Cycle for 40/50

Now the results of mixtures in which 80/100 is used are represented using cycles to termination accumulated axial strains shown in figure 4.26 because in these mixtures termination strains were reached first before the termination cycle. So the following graph shows the cycles to termination strain for different mixtures. Mixtures with greater number of cycles to termination strain offer greater resistance to rutting.

Similar kind of trend is observed in the above graph NHA A and DBM resistance to accumulated strains is greater because they took greater load cycles to reach the termination strain. Output of flow number test includes a load cycle vs accumulated axial strains curve with load cycle on ordinate and strains on abscissa. This curve can be divided into three parts primary, secondary and tertiary flow. In primary flow rate of strain accumulation decreases with time. In secondary flow rate of strain accumulation behaves linearly and in tertiary flow rate of strain accumulation increases again.

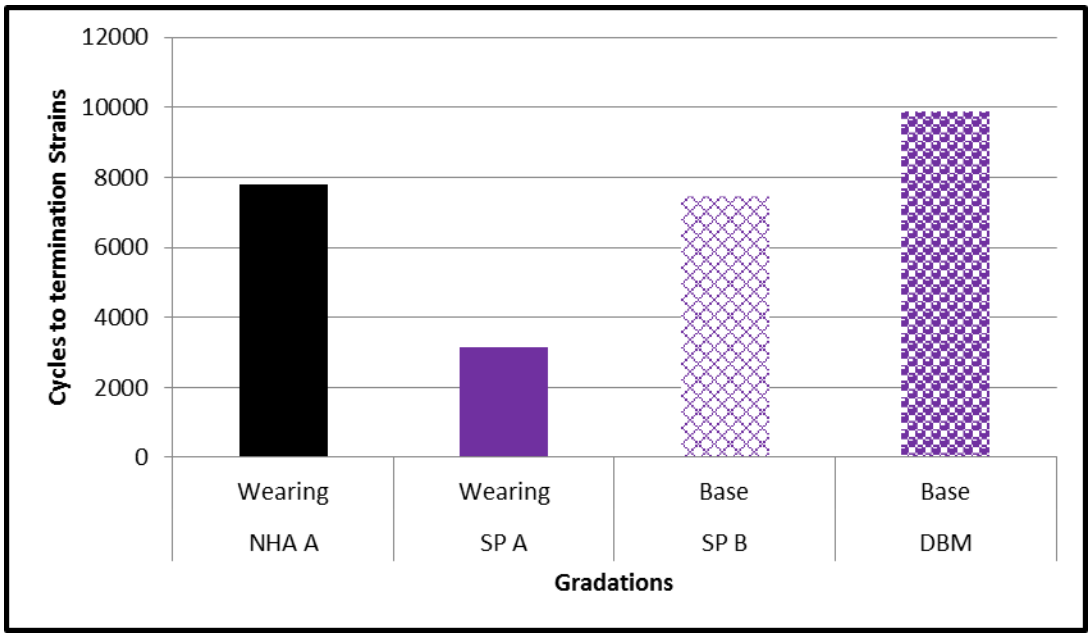

Figure 5.26: Cycles to Termination Strains for 80/100 Binder

Figure 4.27 presented below gives a full picture of accumulated strain against each cycle for wearing course mixtures. The mixtures with 40/50 have a less steep curve and undergo lesser strains as compared to mixtures that are prepared with softer binder 80/100. It is also evident from the figure that the mixtures with 80/100 binder undergone into tertiary state of flow. The mixtures prepared using 40/50 binder are presented using dotted lines whereas the mixtures with 40/50 are presented using solid lines.

Figure 4.28 is a representation of accumulated strains and cycles for wearing course mixtures. SP A with 80/100 is performing low among all the mixture. Due to higher binder content and low NMAS the accumulation of stains is more in SP A wearing course than NHA A. This is due to fact that NHA is well graded with lager NMAS and the induced strains are low.

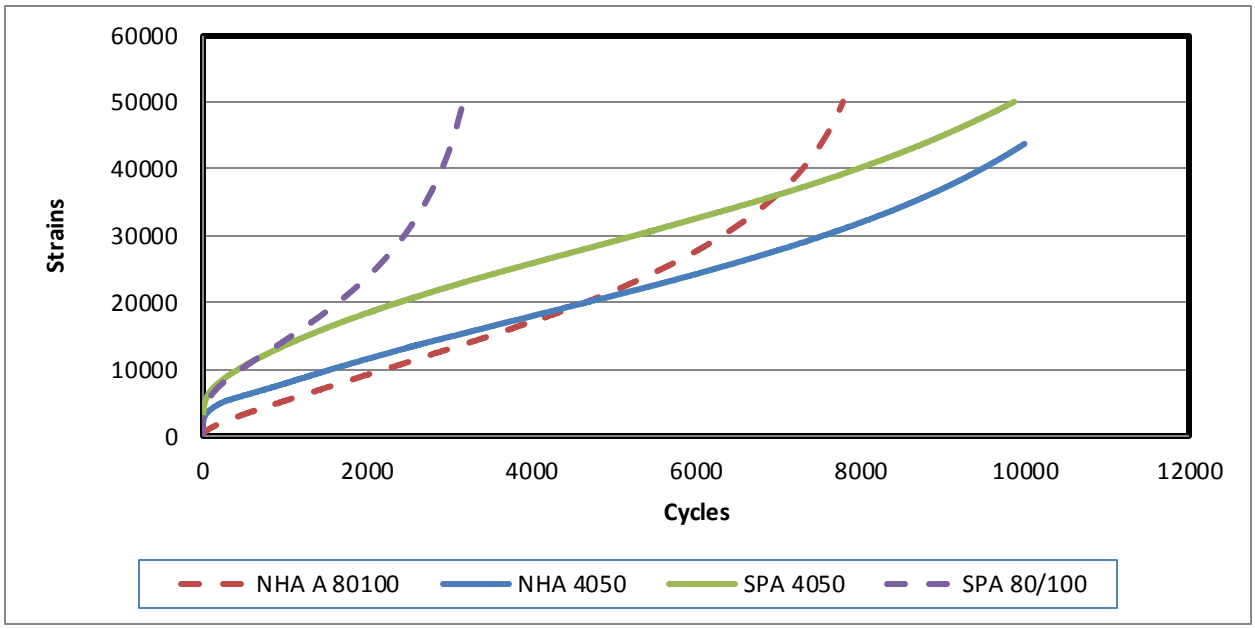

Figure 5.27: Accumulated Axial Strains Vs Cycles- Wearing Course

Figure 4.28 shows a clear picture of load cycles vs accumulated axial micro strains for base course mixtures. It can be seen from the figure that base course mixtures with 40/50 are not showing tertiary flow stage as compared to mixtures with 80/100 binder. This is again due to the higher stiffness of the binder which resists accumulation of strains into the specimen. In case of gradations DBM is performing better as it accumulated fewer strains due to the applied cyclic load. This is because it is densely graded than SP B base course gradation and due to strong interlocking and less voids the accumulation of strains is low.

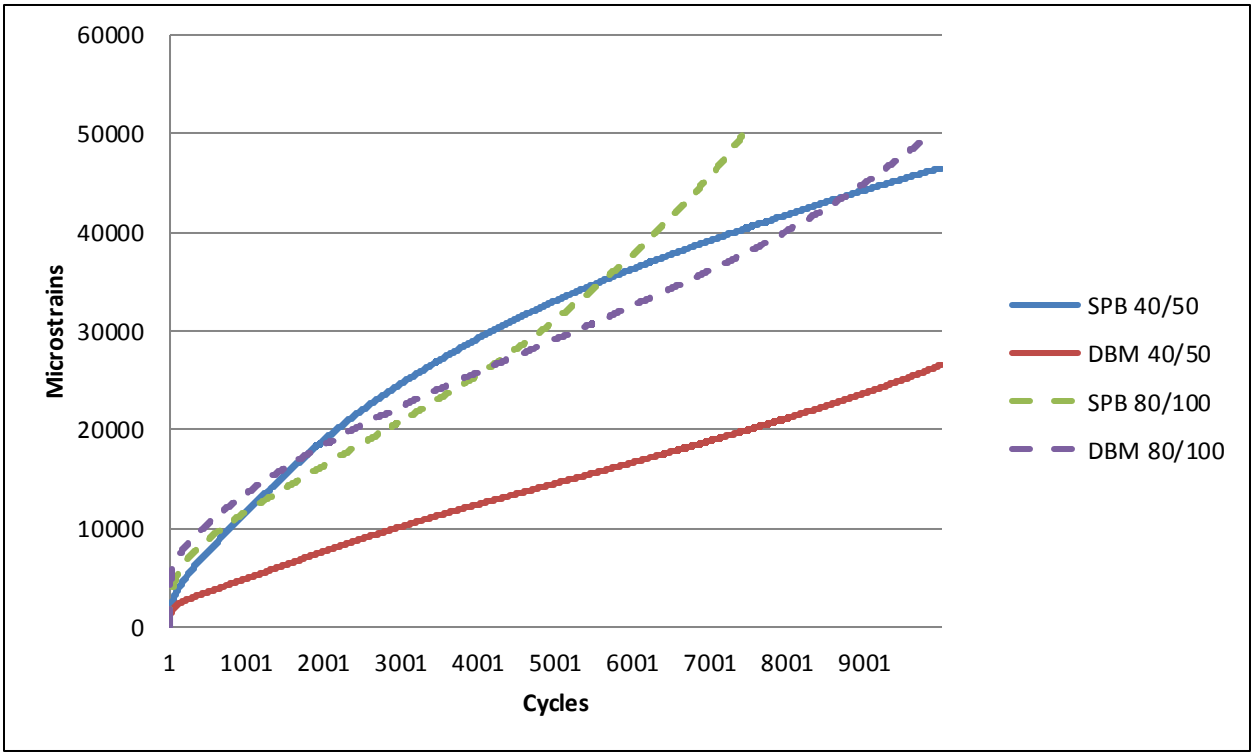

Figure 5.28: Accumulated Axial Strains Vs Cycles- Base Course

The flow number is the load cycle at which rate of change of strain accumulation is minimum or where tertiary flow begins. In AMPT flow number value is not accurate due to resonance in the data. In order to correct the machine results a data smoothing technique is utilized that is five point moving average method. The smoothened strain data is plotted against the load cycles and a 4^{th} order polynomial of the curve is developed using excel sheet. This polynomial was differentiated with respect to time and rate of change of strain accumulation was equalized to zero in order to find the value of load cycle at which rate of strain accumulation is zero also called flow number. Greater the value of flow number lesser the mix is rutting susceptible. Figure 4.29 and 4.30 represents flow number results for wearing and base course mixes respectively and these results are in agreement with the previously established conclusions.

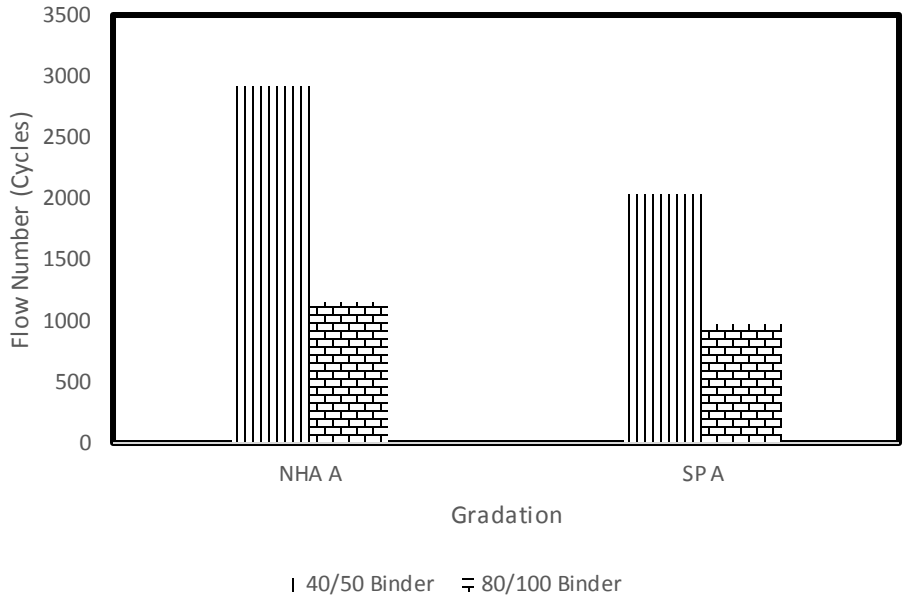

Figure 5.29: Flow Number for wearing course mixtures

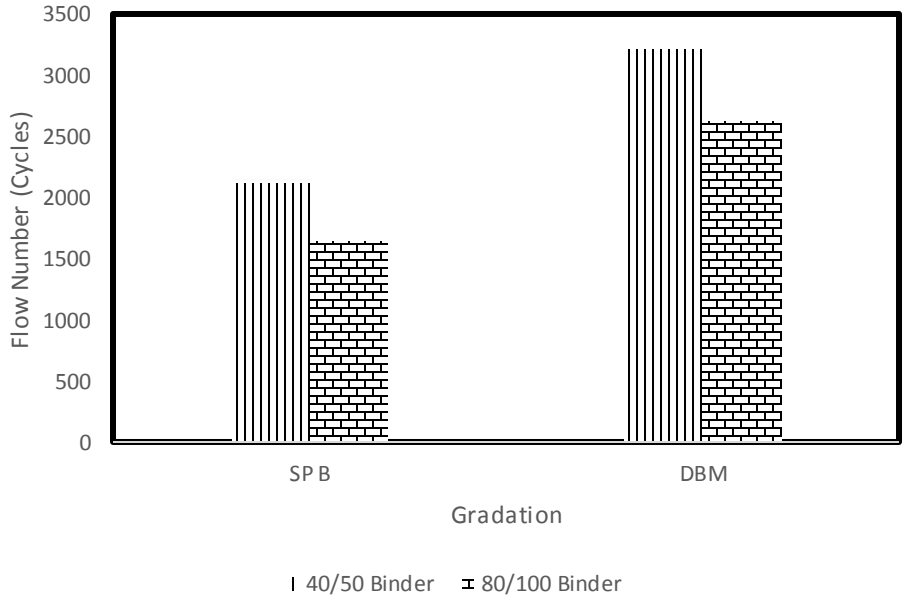

Figure 5.30: Flow Number for wearing course mixtures

Another technique to find rutting susceptibility is to determine compliance parameters.

Compliance parameters are determined from plot of log of compliance vs log of time curve. Basically compliance parameters are regression coefficients 'a' and 'm'. .a' is the intercept and 'm' is the slope of the linear portion of the compliance vs load repetition curve. Compliance parameter for both wearing and base course are presented in Table 4.14.

Table 5.14: Compliance Parameters

Layer Type	Binder	Gradation	40/50 Binder		80/100 Binder	
			Slope	Intercept	Slope	Intercept
Wearing Course	40/50	NHA A	3.69	4046	5.08	5228
		SP A	4.25	8473	9.56	6552
Base Course	40/50	SP B	5.05	5278	5.464	7471
		DBM	2.826	2026	4.43	2613

5.10 FLOW TIME RESULTS

The results obtained from flow time tests shows that no mixture yields the tertiary phase of deformation. Hence, data smoothening is not applied and data obtained from AMPT software is used for further analysis. As mentioned, the tertiary phase of deformation is not observed in any mixture, the analysis is restricted to the comparison of accumulated strain only.

Table 5.15: Time Vs Strains-Wearing Course

Gradation	**Binder**	**Seconds**	**Strains**
NHA A	NRL 40/50	10,000	6051
	ARL 80/100	10,000	6310
SP A	NRL 40/50	10,000	7791
	ARL 80/100	10,000	7832

Table 5.16: Time Vs Strains- Base Course

Gradation	**Binder**	**Seconds**	**Strains**
SP B	NRL 40/50	10,000	4787
	ARL 80/100	10,000	10911
DBM	NRL 40/50	10,000	4633
	ARL 80/100	10,000	6214

The above represented Table 4.15 and Table 4.16 represents the accumulated strains for fixed 10,000 seconds of static loading time for each test binder and gradation combination.

These results in graphed form are presented below in Figure 4.31,

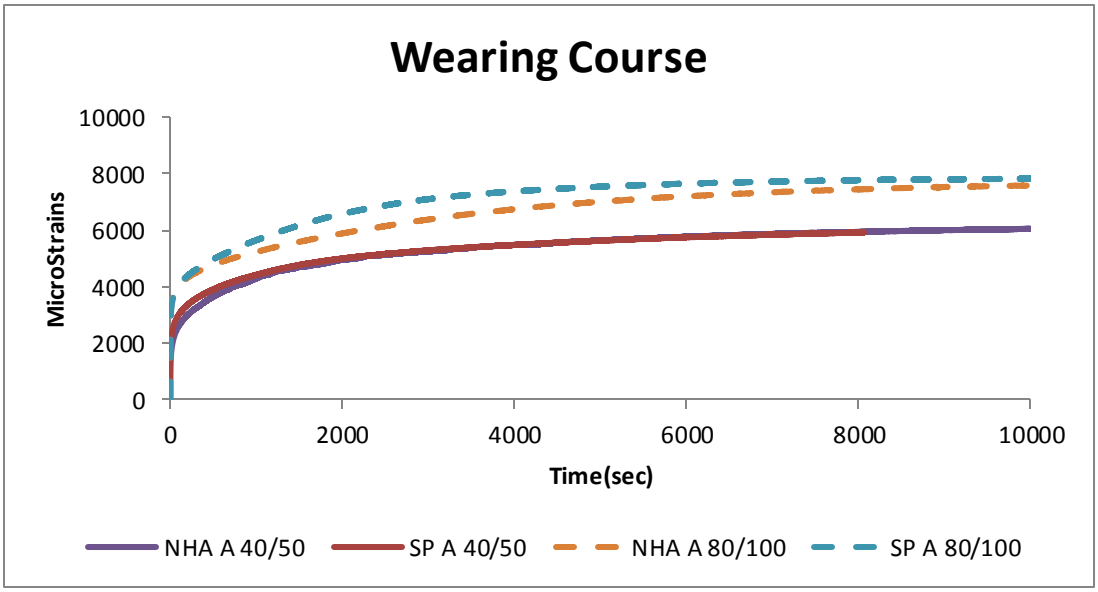

Figure 5.31: Time vs Accumulated Strains- Wearing Course

Both the NHA A and SP A are behaving in the same manner under the statically applied load and when NRL 40/50 binder is used. But the difference in behavior becomes little bit visible when 80/100 binder is used because due to the less stiffness of the 80/100 binder the gradation dependency of HMA increased to take the statically applied loads.

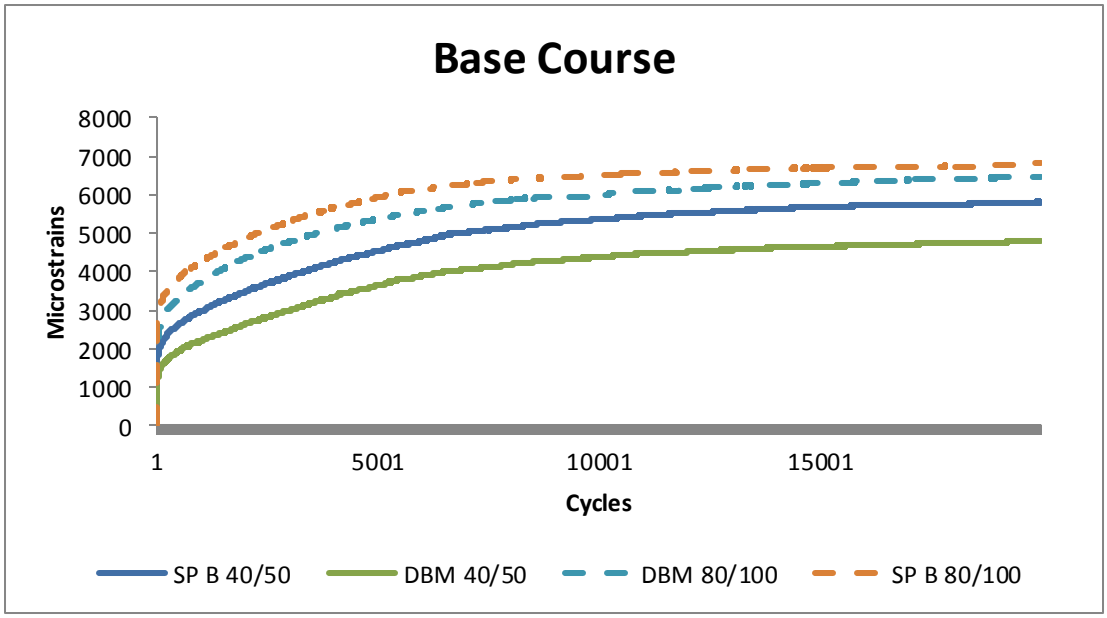

Figure 5.32: Accumulated Strains vs Time- Base Course

Base course mixtures with 40/50 binder accumulated less strains as compares to 80/100 binder. In case of gradations the densely graded DBM accumulated fewer strains as compared to SP B gradation. Figure 4.33 and Figure 4.34 shows accumulated strains at termination for wearing course mixes and base course mixtures respectively,

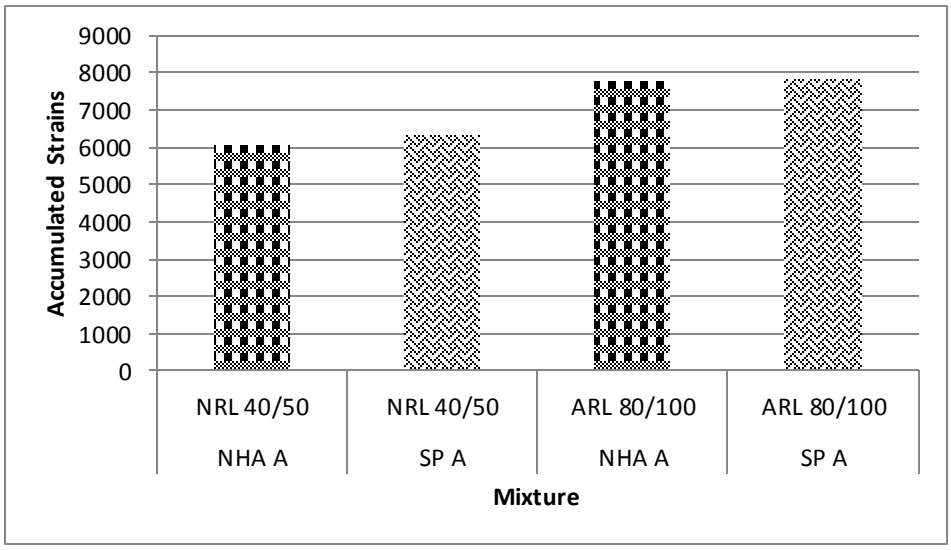

Figure 5.33: Accumulated strains at termination- Wearing Course

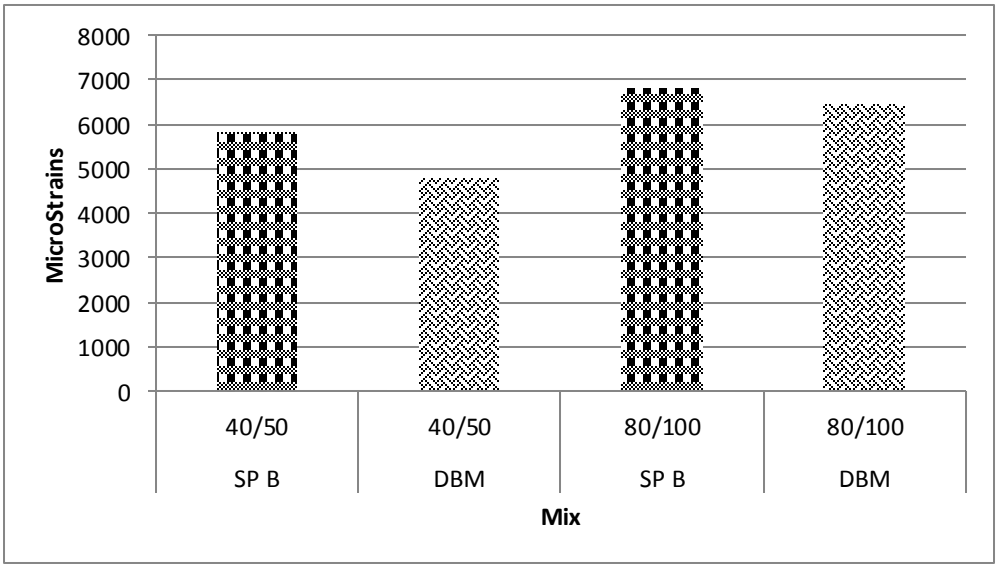

Figure 5.34: Accumulated Strains at Termination- Base Course

It is obvious that NHA A and DBM undergo less permanent strains making them less rut susceptible and as binder stiffness increases rutting susceptibility decreases.

5.11 SUMMARY

In this chapter the results of dynamic modulus, phase angle, flow number and flow time are presented and analyzed. The results from triplicate specimens were averaged and used for further analyses.

Plots of dynamic modulus against frequency and temperature were plotted in order to have clear idea of decrease in the values of dynamic modulus with the increase in temperature and decrease in frequency and also to see that how mixtures fabricated with two different binders develop response at different temperatures and frequencies.

Dynamic modulus master curves were developed using excel solver sheet at a reference temperature of 21.1°C. This was achieved using principle of time temperature superposition. Shift factors were calculated in order to shift data at other temperatures to reference temperature. Master curves were developed both for wearing and base course mixtures and are presented.

Two level factorial design of experiment for dynamic modulus and phase angle results was also a part of this chapter. The factors selected for the design was temperature, frequency and binder's viscosity. The estimated effects of these factors and nature of the effected are presented in tabulated form. Other plots such as main effect plot, cumulative normal probability plots and interaction plots for both the dynamic modulus and phase angle are presented in this chapter. Relation between dynamic modulus and phase angles at different temperatures is plotted and presented for both base course and wearing course. Dynamic modulus values are used to develop fatigue parameters and the results are used to develop the comparison bar plots showing the fatigue parameter of various mixtures at different frequencies. Fatigue parameter is calculated only for a temperature of 21.1°C to determine the fatigue resistance of test mixtures and to see how the change in binder's grade affects the resistance to fatigue. Graphs were plotted represented the fatigue resistance of both the wearing course and base course mixtures at different loading frequencies. Performance modeling was done to develop the equations for predicting the values of dynamic modulus. The resulting regression parameters are tabulated.

The flow number and flow time results are presented showing both the cycles or seconds and accumulated strains. In order to view a clear picture of the results and also to see the comparison between different gradations and binder's different plots of flow number and flow time are also presented in this chapter.

CHAPTER 5

CONCLUSIONS AND RECOMMENDATIONS

6.1 SUMMARY

This research is carried out as a part of Pakistan's National road research project for the improvement of existing mix design technology and to implement new mechanistic empirical pavement design guide (MEPDG). For the implementation of MEPDG we need to characterize HMA mixes using Simple Performance Tests (SPTs). Two wearing course gradations (NHA A and SP A) and two base course gradations (SP B and DBM) were selected for the study and the mixtures were prepared using two bitumen binders having different penetration grades i.e. 40/50 and 80/100 grade. All the specimens were prepared according to the specifications and using Superpave Gyratory Compacter (SGC) which better simulates the field conditions. Three simple performance tests that are Dynamic modulus test |E*|, flow number test (FN) and flow time (FT) test were carried out to evaluate and characterize the performance of these mixtures. Dynamic modulus test was conducted at six different loading frequencies i.e. 25, 10, 5, 1, 0.5, 0.1 Hz and four different temperatures i.e. 4.4, 21.1, 37.7 and 54.4°C. Different frequencies simulate different vehicle speeds and temperature range was selected to characterize HMA mixes for low temperature cracking, medium temperature fatigue cracking and high temperature rutting susceptibility. Dynamic modulus test results were acquired in the form of excel sheets and was used to develop master curves both for wearing course and base course mixtures using the time-temperature superposition principle with the help of nonlinear optimization technique in excel solver add-on. Using this principle data at various temperatures was shifted to the reference temperature of 21°C with respect to reduced loading frequency so that various curves merge into a single smooth curve called master curve. Amount of shift represents temperature dependency of the material. These master curves along with shift factors provide basic material input for MEPDG software. Statistical analysis of the dynamic modulus results also includes the Two Level Factorial Design and Regression Modeling. The factors considered for the analysis included test temperature, loading frequency and binder type. Main effects and interaction effects was presented using the main effect and interaction effects plot and a multi-linear regression model was used to predict dynamic modulus values. Phase angle results were also evaluated

because phase angle is a very important parameter for characterizing viscoelastic properties of HMA. Dynamic modulus and phase angle results were combined to calculate fatigue resistance of HMA mixes using fatigue parameter. Fatigue parameter is calculated at 21.1ºC because of HMA's medium temperature fatigue susceptibility.

The other two performance tests flow number (FN) and flow time (FT) were conducted on triplicate specimens at a temperature of 54.4°C and at a single stress level that is 300Kpa and confining pressure was equalized to zero in order to be consistent with previous studies. These are basic tests to compare rutting resistance of HMA mixes in terms of accumulated strains. FN test is considered to best simulate the field loading conditions because it allows for the recovery time of 0.9 sec for the strains after 0.1 seconds loading. In FT test strains are measured that are produced due to statically applied stress of 300 kpa.

6.2 CONCLUSIONS

This research study presents the results of three simple performance tests on HMA mixes prepared using Marshal Mix Design method with the help of Superpave Gyratory Compactor (SGC). The main purpose was to see effect of binder's penetration grade on stiffness, fatigue and rutting resistance of HMA mixes. During Optimum Binder Content (OBC) determination it was observed that mixes with stiffer binder have a slightly higher OBC value as compared to mixes with softer binder because softer binder becomes more fluid at a given temperature and fill more voids as compared to stiffer 40/50 grade binder. Dynamic modulus testing conducted on various temperature and loading frequencies was used to develop master curves for the HMA mixes prepared using two bitumen binders of different penetration grades. HMA mixes with stiffer binder produced higher dynamic modulus values as compared to HMA mixes with softer binder. But it is observed that at lowest testing temperature which is 4.4ºC the master curves merged at single point with minor difference between dynamic modulus values because at low temperature both the binders are stiffer and resulting dynamic modulus values reached limiting equilibrium values and master curves becomes asymptotic. At intermediate temperatures, mix behavior is governed by combine interaction of binder stiffness and aggregate gradation forming an S shape curve with mixes with 80/100 grade binder showing a sudden decline in dynamic modulus values. At higher temperature binder stiffness is reduced to a point that mix behavior is now

governed by aggregate interlock and dynamic modulus value again reaching a limiting equilibrium values forming lower asymptote of master curve. Using two level factorial design it is observed that Dynamic modulus values are significantly affected by testing temperature, loading frequency and the viscosity of the binder. Among these factors temperature is the most significant factor effecting dynamic modulus values. Other factors like nominal maximum aggregate size, Binder content, VMA and VFA bear no significant effects on the values of dynamic modulus. Nonlinear regression models are developed for both wearing course and base course gradations with R^2 values of 0.84 and 0.86 respectively because it is important for highway agencies being able to predict dynamic modulus values for commonly used HMA mixes because laboratory determination of dynamic modulus is a very laborious work and takes a lot of time.

Phase angle results were analyzed using scatter plots to have an idea about the temperature and gradation dependency of phase angle results for mixes with both binders. Normally HMA mixes with 40/50 binder produced lower phase angle values as compared to mixes with 80/100 binder. For 40/50 binder, phase angle increase with increase in temperature and decrease in frequency from 4.4ºC to 37.8ºC because as the binder stiffness is decrease with increase in temperature, HMA mix behavior changes from elastic to more viscous and the load induced strains taking more time to recover strains resulting in increased phase angle values. After 54.4ºC phase angle values again start decreasing at lower frequencies. This may be due to the reason that at higher temperature binder softens enough and HMA mix viscoelastic behavior is dependent on aggregate interlock resulting in decreased phase angle values. For softer 80/100 binder, this decrease in phase angle values was observed at 21.1ºC instead 54.4ºC.

Fatigue parameter calculated using dynamic modulus and phase angle values depicted that mixes with 80/100 pen grade binder are more fatigue resistant due to their lower fatigue parameter value as compared to mixes with 40/50 pen grade binder because stiffness of mix is good against rutting but stiffer mixes are more prone to fatigue cracking.

Flow number test results showed that HMA mixtures with stiffer binder (40/50) perform better than gradation with softer binder (80/100). The analyses were made by comparing the accumulated axial strains at the termination cycle or cycle number at the termination accumulated axial strains. No mixture with 40/50 exhibited tertiary flow. On the other hand all the mixtures with 80/100 undergo tertiary flow condition.

Flow time results also followed the same trends the mixtures with 40/50 showed lesser accumulated strains as compared to mixtures with softer binders.

In case of aggregate gradation NHA A wearing course gradation and DBM base course gradation produced higher dynamic modulus values and lower FN and FT values as compared to SP A wearing course gradation and SP B base course gradation which are more durable against fatigue cracking due to their lower fatigue parameter values. This is in agreement with previous research study by Ali et.al. (2015).

6.3 CONTRIBUTION TO THE STATE OF THE ART

In order to improve mix design technology of Pakistan, there is a need to shift from empirical pavement design to mechanistic-empirical pavement design. For this we need to develop a database of material characteristics and environmental conditions of Pakistan for software input. Previously studies had been carried out for material characterization. This study is carried out to augment the findings of these studies and fill the testing gaps. It is conducted on a range of bitumen binders manufactured in Pakistani oil refineries. This will help to improve materials database of National road agency and will help pavement designer and engineers in selection of bitumen binder better suited for traffic and environmental conditions of the proposed road site.

6.4 RECOMMENDATIONS

In this research only simple performance tests of HMA were performed but in order to completely characterize the mixtures it is necessary to perform some other tests such as Hamburg Wheel Tracker rutting test and indirect tensile fatigue test. After performing these tests and full characterization of mixtures it is necessary to check the performance of these mixtures in the field by constructing the test sections and exposing them to real traffic loads and environmental conditions of Pakistan and monitor their performance and establish a relationship between field performance and lab performance.

BIBLIOGRAPHY

AASHTO TP 62-07. *Standard Test Method for Determining Dynamic Modulus of Hot Mix Asphalt (HMA)*. American Association of State Highway and Transportation Officials, 2007

Apeagyei, A., K. (2011), *"Rutting as a Function of Dynamic Modulus and Gradation*", Journal of Materials in Civil Engineering, Vol. 23, No. 9, 1302-1310.

American Association of State Highway and Transportation Officials (AASHTO). "*Mechanistic-Empirical Pavement Design Guide: A Manual of Practice*," AASHTO Designation MEPDG-1, Washington, DC, July 2008.

AASHTO. *AASHTO Guide for Design of Pavement Structures*, AASHTO, Washington, DC, 1993.

Ahmad, J., Rahman, M. Y. A., & Hainin, M. R. (2011). *Rutting evaluation of dense graded hot mix asphalt mixture*. International Journal of Engineering & Technology (IJET-IJEN), 11(05), 56-60.

Apeagyei, A. K., Diefenderfer, B. K., & Diefenderfer, S. D. (2012*). Development of dynamic modulus master curves for hot-mix asphalt with abbreviated testing temperatures*. International Journal of Pavement Engineering, 13(2), 98-109..

Ali, Y., Irfan, M., Ahmed, S., Khanzada, S., & Mahmood, T. (2015). *Investigation of factors affecting dynamic modulus and phase angle of various asphalt concrete mixtures*. Materials and Structures, 49(3), 857-868.

Ameri, M., Sheikhmotevali, A. H., & Fasihpour, A. (2014). *Evaluation and comparison of flow number calculation methods*. Road Materials and Pavement Design, 15(1), 182-206.

Bari, J., & Witczak, M. W. (2006). *"Development of a New Revised Version of the Witczak E* Predictive Model for Hot Mix Asphalt Mixtures*". Journal of the Association of Asphalt Paving Technologists from the Proceedings of the Technical Sessions, *75*, 381-423, Savannah, Ga.

Bhasin, A., Button, J.W. and Chowdhury, A. (2003), "*Evaluation of Simple Performance Tests on HMA Mixtures from the South Central United States*" Texas Transportation Institute, The Texas A&M University System, Texas.

Bhasin, A., Button, J.W. and Chowdhury, A. (2005), "*Evaluation of Selected Laboratory Procedures and Development of Databases for HMA*" Texas Transportation Institute, the Texas A&M University System, Texas.

Bonaquist R. F., Christensen D.W. and Stump W. (2003), "*Simple performance Tester for Super pave Mix Design: First article development and Evaluation*" National Cooperative Highway Research Program, NCHRP Report 513, Advanced Asphalt Technologies, LLC.

Bonaquist, R. (2010). *Wisconsin mixture characterization using the asphalt mixture performance tester (AMPT) on historical aggregate structures* (No. WHRP 09-03).

Bonaquist, R. F. (2011). *Precision of the Dynamic Modulus and Flow Number Tests Conducted with the Asphalt Mixture Performance Tester* (Vol. 702). Transportation Research Board.

Bonnaure, F., Gest, G., Gravois, A., & Uge, P. (1977*). A new method of predicting the stiffness of asphalt paving mixtures*.

Bennert, T. A. (2009). *Dynamic Modulus of Hot Mix Asphalt* (No. FHWA-NJ-2009-011).

Christensen Jr, D. W., Pellinen, T., & Bonaquist, R. F. (2003). *Hirsch model for estimating the modulus of asphalt concrete*. Journal of the Association of Asphalt Paving Technologists, 72.

Cross, S. A., & Jakatimath, Y. (2007). *"Determination of Dynamic Modulus Master Curves for Oklahoma HMA Mixtures"*. Oklahoma Department of Transportation: Final report.

Ceylan, H., Gopalakrishnan, K., & Kim, S. (2009). *Looking to the future: the next-generation hot mix asphalt dynamic modulus prediction models*. International Journal of Pavement Engineering, 10(5), 341-352.

Ekingen , E. R. (2004). *"Determining Gradation and Creep Effects in Mixtures Using the Complex Modulus Test"*. ME Thesis: University of Florida, USA.

Faheem, A.F. and Bahia, H.U. (2005), "*Estimating the Results of the Proposed Simple Performance Test for HMA from the Superpave Gyratory Compactor Results*", the Asphalt Pavement Research Group, Department of Civil and Environmental Engineering, the University of Wisconsin, Madison.

Flintsch, G. W., Loulizi, A., & Diefenderfer, B. K. (2007). *"Asphalt MaterialCharacterization in Support of Implementation of Mechanistic Emperical PavementDesign Guide"*. Virginia Transportation Research Council: Final Report.

Gul, H. M. F. (2014). "*Rutting Evaluation Of Hot Mix Asphalt Mixtures Using Static Creep And Repeated Load Tests*". MS Thesis: National University of Science and Technology (NUST) Islamabad Pakistan.

Huang, Y. H. (1993). *Pavement analysis and design.*

Hafeez, I., Kamal, M. A., Ahadi, M. R., Shahzad, Q., & Bashir, N. (2012). Performance prediction of hot mix asphalt from asphalt binders. Pakistan Journal of Engineering and Applied Sciences, 11, 104-113.

Hafeez, I., Kamal, M. A., Ahadi, M. R., & Msawil, M. J. (2011). *Effects of Hydrated Lime on Fatigue and Rutting Behavior of HMA Mixtures in Dynamic Modulus Testing*. Transportation Research, 1(1), 23.

Irfan, M., Waraich, A. S., Ahmed, S., & Ali, Y. (2016). *Characterization of Various Plant-Produced Asphalt Concrete Mixtures Using Dynamic Modulus Test*. Advances in Materials Science and Engineering, 2016.

Khanal, P. P., & Mamlouk, M. S. (1995). *Tensile versus compressive moduli of asphalt concrete*. Transportation Research Record, (1492), 144-150.

Khosravifar, S., Haider, I., Afsharikia, Z., & Schwartz, C. W. (2015). *Application of time–temperature superposition to develop master curves of cumulative plastic strain in repeated load permanent deformation tests*. International Journal of Pavement Engineering, 16(3), 214-223.

Kim, Y. R., King, M., & Momen, M. (2005). *Typical dynamic moduli for North Carolina asphalt concrete mixes* (No. FHWA/NC/2005-03).

Lekarp, F., & Isacsson, U. (2001). The Effects of Grading Scale on Repeated Load Triaxial Test Results. International Journal of Pavement Engineering, 2(2), 85-101.

Kim, H., Lee, K., Kim, N., & Kim, Y. (2006). *Dynamic modulus of asphalt mixtures for development of Korean pavement design guide*. Journal of Testing and Evaluation, 35(2), 1-8.

Miljković, M. and Radenberg, M., (2011), "*Rutting Mechanisms And Advanced Laboratory Testing Of Asphalt Mixtures Resistance Against Permanent Deformation*", series: Architecture and Civil Engineering Vol. 9, No 3, 2011, pp. 407 – 417, University of Nis, The Faculty of Architecture and Civil Engineering, Serbia.

Mohammad, L.N. and Wu, Z. (2005), "*Permanent Deformation Analysis of HMA Mixtures Using Simple Performance Tests And the 2002 Mechanistic-empirical Pavement Design Software*", 85th Transportation Research Board Annual Meeting, Washington, D.C.

Mohammad, L.N., Saadeh, S., Obulareddy, S. and Cooper, S. (2006), "*Characterization of Louisiana Asphalt Mixtures using Simple Performance Test*", 86th Transportation Research Board Annual Meeting, Washington, D.C.

Mohammad, L. N., Wu, Z., Obulareddy, S., Cooper, S., & Abadie, C. (2006). *Permanent Deformation Analysis of HMA Mixtures Using Simple Performance Tests and The 2002 Mechanistic-Empirical Pavement Design Software*.‖ CD-ROM of TRB 85 th Annual Meeting, Washington.

Mu-yu, L., & Shao-yi, W. (2003). *Genetic optimization method of asphalt pavement based on rutting and cracking control*. Journal of Wuhan University of Technology-Mater. Sci. Ed., 18(1), 72-75.

Nega A, Ghadimi B, Nikraz H (2015)," *Developing Master Curves, Binder Viscosity and Predicting Dynamic Modulus of Polymer-Modified Asphalt Mixtures"*. International Journal of Engineering and Technology.

Papazian, H. S. (1962). *"The response of linear viscoelastic materials in the frequency domain with emphasis on asphaltic concrete"*. 1st International Conference on the structural Design of Asphalt Pavements.: pp. 454-463.

Rahman, A. and Tarefder, R. (2014).“*Effect of Binder Performance Grade on the Dynamic Modulus Mastercurves of SP III Superpave Mixes in New Mexico*”. Advanced Characterization of Asphalt and Concrete Materials: pp. 9-16.

Romanoschi, S. A., Dumitru, N. I., Dumitru, O., Fager, G., & Transportation Research Board. (2006). *Dynamic Resilient Modulus and the Fatigue Properties of Superpave HMA Mixes Used in the Base Layer of Kansas Flexible Pavements*. In 85th Annual Meeting of the Transportation Research Board, Washington, DC.

Shen S. and Yu H. (2012), “*An Investigation Of Dynamic Modulus And Flow Number Properties Of Asphalt Mixtures In Washington State*” Washington State Transportation Center (TRAC), Pullman, WA.

Shen S. and Yu H. (2012), “*An Investigation Of Dynamic Modulus And Flow Number Properties Of Asphalt Mixtures In Washington State*” Washington State Transportation Center (TRAC), Pullman, WA.

Sugandh, R., Zea, M., Tandon, V., Smit, A., & Prozzi, J. (2007). *Performance Evaluation of HMA Consisting of Modified Asphalt Binder* (No. FHWA/TX-07/0-4824-2).

Schwartz, C. W., Li, R., Kim, S., Ceylan, H., & Gopalakrishnan, K. (2011). *Sensitivity evaluation of MEPDG performance prediction.*

Seo, J., Kim, Y., Cho, J., & Jeong, S. (2013). *Estimation of in situ dynamic modulus by using MEPDG dynamic modulus and FWD data at different temperatures*. International Journal of Pavement Engineering, 14(4), 343-353.

Rushing, J. F., & Little, D. N. (2013). *Static creep and repeated load as rutting performance tests for airport HMA mix design*. Journal of Materials in Civil Engineering, 26(9), 04014055.

Uzan, J. (2003). *Characterization of asphalt concrete materials for permanent deformation.* International Journal of Pavement Engineering, 4(2), 77-86.

Wu, S., Zhang, K., Wen, H., DeVol, J., & Kelsey, K. (2015). *Performance Evaluation of Hot Mix Asphalt Containing Recycled Asphalt Shingles in Washington State.* Journal of Materials in Civil Engineering, 28(1), 04015088.

Wu, S., Ye, Q., Li, N., & Yue, H. (2007). *Effects of fibers on the dynamic properties of asphalt mixtures.* Journal of Wuhan University of Technology-Mater. Sci. Ed., 22(4), 733-736.

Witczak, M.W. and Kaloush, K. (2002), "*Simple Performance Test for Superpave Mix Design*" National Cooperative Highway Research Program, NCHRP Report 465, Arizona State University, Tempe, AZ.

Wasage, T., Statsna, J., & Zanzotto, L. (2010). Repeated loading and unloading tests of asphalt binders and mixes. Road Materials and Pavement Design, 11(3), 725-744.

Walubita, L. F., Zhang, J., Das, G., Hu, X., Mushota, C., Alvarez, A. E., & Scullion, T. (2012, January). *Comparison of the Hamburg, dynamic modulus, and repeated load tests for evaluation of HMA permanent deformation*. In 91st Transportation Research Board Annual Meeting, Washington DC.

White, T. D., Littlefield, J. C., Pittman, J., Plummer, R. C., Easterling, J. R., & Owens, J. R. (2008*). Hot Mix Asphalt (HMA) Characterization for the 2002 AASHTO Design Guide* (No. FHWA/MS-DOT-RD-07-166).

Ye, Q., Wu, S., & Li, N. (2009). "*Investigation of the dynamic and fatigue properties of fibermodified asphalt mixtures*". International Journal of Fatigue, 31(10), 1598-1602.

Yu, H., & Shen, S. (2012). *An investigation of dynamic modulus and flow number properties of asphalt mixtures in Washington State*. Report No. TNW, 2.

Yu, B., Zhu, H., Gu, X., Ni, F., & Guo, R. (2015). *Modified repeated load tri-axial test for the high-temperature performance evaluation of HMA*. Road Materials and Pavement Design, 16(4), 784-798.

APPENDICES

APPENDIX A

|E*| TEST RESULTS

Table A1: Average Dynamic Modulus for Wearing Course Mixtures

Temperature (°C)	Frequency (Hz)	Average Dynamic Modulus (MPa)			
		NHA A		SP A	
		40/50	80/100	40/50	80/100
4.4	25	28334	26923	23130	17531
	10	27118	25798	21855	15954
	5	26093	24780	20635	14688
	1	23284	22993	17408	11738
	0.5	21125	20963	15685	10408
	0.1	16876	17102	11620	7424
21.1	25	21203	8673	16848	5651
	10	19079	6664	15017	4228
	5	17280	5321	13526	3350
	1	12743	2919	9550	1713
	0.5	10609	2205	7813	1267
	0.1	5978	1143	4299	617
37.7	25	18168	5230	12560	3366
	10	15538	3549	10339	2250
	5	13379	2642	8618	1623
	1	8765	1251	5023	859
	0.5	6142	880	3874	526
	0.1	2966	437	1641	251
54.4	25	10987	2812	5955	3140
	10	8348	2070	4039	2242
	5	6703	1105	2911	1673
	1	3833	767	1245	760
	0.5	2274	384	835	555
	0.1	955	213	467	287

Table A2: Dynamic Modulus Results for Base Course Mixtures

Temperature (°C)	Frequency (Hz)	Average Dynamic Modulus (MPa)			
		SP B		DBM	
		40/50	80/100	40/50	80/100
4.4	25	25806	16922	27773	22356
	10	24859	15592	26144	20375
	5	23991	14519	25413	18693
	1	21284	11578	22314	14999
	0.5	20128	10377	20748	13372
	0.1	16106	7561	16822	9765
21.1	25	17485	7170	21283	8474
	10	14924	5687	19271	6505
	5	12932	4511	17597	5388
	1	8588	2588	13542	3117
	0.5	7112	1775	11835	2390
	0.1	3707	829	7893	1295
37.7	25	12787	5710	16675	7156
	10	10386	4145	14295	5321
	5	8195	3071	12467	4099
	1	4368	1378	8160	2097
	0.5	3059	965	6280	1514
	0.1	1177	441	2812	721
54.4	25	11301	2899	11408	2711
	10	8679	1833	8891	1605
	5	6914	1259	7001	1186
	1	3522	575	3529	554
	0.5	2312	403	2402	387
	0.1	822	217	941	271

APPENDIX B

PHASE ANGLE RESULTS RESULTS

Table B1: Phase Angle Results for Wearing Course Mixtures

Temperature (°C)	Frequency (Hz)	Average Phase Angle (degrees)			
		NHA A		SP A	
		40/50	80/100	40/50	80/100
4.4	25	5.003333	6.803333	6.808333	9.253333
	10	6.033333	7.613333	8.383333	10.56833
	5	6.853333	8.513333	9.548333	11.79333
	1	10.34333	11.19833	13.39833	15.32833
	0.5	11.79833	12.40833	15.30833	17.00833
	0.1	15.82833	16.27333	21.01333	21.74833
21.1	25	11.34333	24.62333	13.36333	28.04833
	10	13.98833	28.20833	16.19333	30.50833
	5	16.20333	29.66833	18.65833	31.92833
	1	22.65833	32.23333	25.72333	34.37333
	0.5	25.33333	32.45833	28.60833	34.59833
	0.1	33.08833	32.09333	35.61333	33.93333
37.7	25	15.42833	31.17833	20.23833	33.97833
	10	18.87333	33.33833	24.45333	35.61833
	5	21.40833	33.89333	27.33833	36.29333
	1	28.28833	33.90333	33.87333	36.60333
	0.5	31.08833	33.26333	35.64333	35.82333
	0.1	35.27833	29.99333	37.28833	32.21333
54.4	25	27.16333	34.34833	32.63833	34.42833
	10	31.35833	35.17333	36.98833	35.59333
	5	33.24333	34.90833	38.32333	35.74833
	1	35.67333	33.07833	39.35833	35.61833
	0.5	35.73333	31.44833	37.95833	34.56333
	0.1	31.60833	27.78833	34.11333	33.85333

Table B2: Phase Angle Results for Base Course Mixtures

Temperature (^{O}C)	Frequency (Hz)	Average Phase Angle (degrees)			
		SP B		DBM	
		40/50	80/100	40/50	80/100
4.4	25	5.9150	8.85	6.4050	10.100
	10	7.4200	10.31	7.5000	11.440
	5	8.3900	11.8	7.7400	12.665
	1	11.6200	15.99	10.7100	16.390
	0.5	13.2850	17.58	11.9200	17.865
	0.1	18.7200	22.87	16.4750	22.260
21.1	25	17.2200	25.69	11.2150	25.620
	10	20.9050	28.77	13.4550	29.200
	5	23.8000	30.25	15.5900	29.975
	1	31.6850	32.95	21.1100	31.575
	0.5	34.0800	33.01	23.6500	31.300
	0.1	38.5750	31.34	30.4350	30.585
37.7	25	23.6300	28.16	16.3800	29.140
	10	28.1000	30.48	19.7950	31.275
	5	30.9800	31.96	22.2150	31.785
	1	36.5200	34.02	29.0700	32.455
	0.5	37.8800	33.03	31.8150	32.095
	0.1	38.1800	29.3	36.1300	30.890
54.4	25	26.1050	34.45	23.6900	35.805
	10	30.8250	34.82	29.1200	35.970
	5	33.3000	34.21	31.9150	35.425
	1	37.7050	30.8	36.5200	33.170
	0.5	38.7100	29.02	37.6950	31.540
	0.1	37.4650	24.8	36.1250	27.595

APPENDIX C

MEPDG INPUT CATALOGUE

Table C1: MEPDG Input -NHA A 4050

Temp C	Temp F	Frequency Hz	Shift Factor	Reduced Frequency	E* ksi	E* MPa
-10.0	14	25	1.794321	1556.902	3312.9	22848.8
-10.0	14	10	1.794321	622.7607	3287.1	22670.8
-10.0	14	5	1.794321	311.3804	3258.7	22475.6
-10.0	14	1	1.794321	62.27607	3145.6	21695.4
-10.0	14	0.5	1.794321	31.13804	3066.0	21146.5
-10.0	14	0.1	1.794321	6.227607	2765.9	19076.3
4.4	40	25	0.910953	203.6539	3236.4	22321.3
4.4	40	10	0.910953	81.46155	3170.6	21867.5
4.4	40	5	0.910953	40.73078	3099.7	21378.7
4.4	40	1	0.910953	8.146155	2829.7	19516.5
4.4	40	0.5	0.910953	4.073078	2651.8	18289.5
4.4	40	0.1	0.910953	0.814616	2062.1	14222.4
21.1	70	25	-0.00057	24.96702	3035.3	20934.8
21.1	70	10	-0.00057	9.986808	2874.1	19822.5
21.1	70	5	-0.00057	4.993404	2708.6	18681.3
21.1	70	1	-0.00057	0.998681	2150.2	14829.6
21.1	70	0.5	-0.00057	0.49934	1837.8	12675.3
21.1	70	0.1	-0.00057	0.099868	1054.6	7273.8
37.8	100	25	-0.81439	3.833064	2634.1	18167.4
37.8	100	10	-0.81439	1.533226	2323.4	16024.4
37.8	100	5	-0.81439	0.766613	2035.2	14036.9
37.8	100	1	-0.81439	0.153323	1259.0	8683.5
37.8	100	0.5	-0.81439	0.076661	935.0	6448.5
37.8	100	0.1	-0.81439	0.015332	379.8	2619.3
54.4	130	25	-1.54542	0.712067	2002.1	13808.7
54.4	130	10	-1.54542	0.284827	1564.9	10792.9
54.4	130	5	-1.54542	0.142413	1223.1	8436.0
54.4	130	1	-1.54542	0.028483	553.8	3819.5
54.4	130	0.5	-1.54542	0.014241	362.4	2499.4
54.4	130	0.1	-1.54542	0.002848	126.7	873.6

Table C2: MEPDG Input -NHA A 80/100

Temp C	Temp F	Frequency Hz	Shift Factor	Reduced Frequency	E* ksi	E* MPa
-10.0	14	25	3.433924	67899.06	3421.7	23599.5
-10.0	14	10	3.433924	27159.62	3400.6	23453.9
-10.0	14	5	3.433924	13579.81	3376.9	23290.7
-10.0	14	1	3.433924	2715.962	3279.1	22616.0
-10.0	14	0.5	3.433924	1357.981	3208.2	22126.7
-10.0	14	0.1	3.433924	271.5962	2931.3	20217.1
4.4	40	25	1.743357	1384.512	3210.5	22142.6
4.4	40	10	1.743357	553.8049	3077.0	21221.9
4.4	40	5	1.743357	276.9025	2935.8	20248.3
4.4	40	1	1.743357	55.38049	2434.3	16789.3
4.4	40	0.5	1.743357	27.69025	2138.9	14752.0
4.4	40	0.1	1.743357	5.538049	1350.9	9317.3
21.1	70	25	-0.0011	24.93692	2090.7	14419.7
21.1	70	10	-0.0011	9.974769	1643.8	11337.0
21.1	70	5	-0.0011	4.987385	1300.0	8966.2
21.1	70	1	-0.0011	0.997477	642.9	4434.4
21.1	70	0.5	-0.0011	0.498738	456.3	3146.8
21.1	70	0.1	-0.0011	0.099748	215.3	1485.1
37.8	100	25	-1.55857	0.690836	536.5	3700.6
37.8	100	10	-1.55857	0.276334	341.3	2353.9
37.8	100	5	-1.55857	0.138167	247.5	1707.2
37.8	100	1	-1.55857	0.027633	136.6	941.9
37.8	100	0.5	-1.55857	0.013817	113.9	785.9
37.8	100	0.1	-1.55857	0.002763	86.6	597.5
54.4	130	25	-2.95758	0.027565	136.5	941.3
54.4	130	10	-2.95758	0.011026	108.4	747.7
54.4	130	5	-2.95758	0.005513	95.4	657.7
54.4	130	1	-2.95758	0.001103	79.2	546.2
54.4	130	0.5	-2.95758	0.000551	75.6	521.4
54.4	130	0.1	-2.95758	0.00011	70.9	489.3

Table C3: MEPDG Input -SP A 4050

Temp C	Temp F	Frequency Hz	Shift Factor	Reduced Frequency	E* ksi	E* MPa
-10.0	14	25	2.135113	3412.348	3218.1	22195.4
-10.0	14	10	2.135113	1364.939	3161.2	21802.9
-10.0	14	5	2.135113	682.4697	3104.3	21410.4
-10.0	14	1	2.135113	136.4939	2908.5	20060.1
-10.0	14	0.5	2.135113	68.24697	2788.8	19234.4
-10.0	14	0.1	2.135113	13.64939	2406.6	16598.3
4.4	40	25	1.083968	303.3251	3018.4	20817.7
4.4	40	10	1.083968	121.33	2889.9	19931.6
4.4	40	5	1.083968	60.66501	2766.0	19076.8
4.4	40	1	1.083968	12.133	2372.5	16363.2
4.4	40	0.5	1.083968	6.066501	2155.3	14865.1
4.4	40	0.1	1.083968	1.2133	1565.9	10800.0
21.1	70	25	-0.00068	24.96076	2568.1	17712.2
21.1	70	10	-0.00068	9.984305	2314.2	15961.3
21.1	70	5	-0.00068	4.992152	2089.4	14410.8
21.1	70	1	-0.00068	0.99843	1490.3	10278.8
21.1	70	0.5	-0.00068	0.499215	1223.9	8441.0
21.1	70	0.1	-0.00068	0.099843	680.6	4694.1
37.8	100	25	-0.96907	2.684539	1867.9	12883.0
37.8	100	10	-0.96907	1.073816	1518.6	10473.6
37.8	100	5	-0.96907	0.536908	1251.4	8631.0
37.8	100	1	-0.96907	0.107382	701.5	4838.2
37.8	100	0.5	-0.96907	0.053691	519.7	3584.3
37.8	100	0.1	-0.96907	0.010738	242.1	1669.5
54.4	130	25	-1.83894	0.362245	1104.5	7617.9
54.4	130	10	-1.83894	0.144898	791.8	5460.8
54.4	130	5	-1.83894	0.072449	593.5	4093.5
54.4	130	1	-1.83894	0.01449	279.9	1930.8
54.4	130	0.5	-1.83894	0.007245	200.2	1380.7
54.4	130	0.1	-1.83894	0.001449	96.9	668.3

Table C4: MEPDG Input –SP A 80/100

Temp C	Temp F	Frequency Hz	Shift Factor	Reduced Frequency	E* ksi	E* MPa
-10.0	14	25	3.362375	57585.69	3234.0	22305.1
-10.0	14	10	3.362375	23034.28	3172.9	21883.2
-10.0	14	5	3.362375	11517.14	3108.7	21440.4
-10.0	14	1	3.362375	2303.428	2873.0	19815.1
-10.0	14	0.5	3.362375	1151.714	2721.9	18773.2
-10.0	14	0.1	3.362375	230.3428	2228.3	15368.3
4.4	40	25	1.707032	1273.422	2746.0	18939.2
4.4	40	10	1.707032	509.3687	2497.3	17224.1
4.4	40	5	1.707032	254.6843	2265.0	15621.5
4.4	40	1	1.707032	50.93687	1607.7	11088.0
4.4	40	0.5	1.707032	25.46843	1305.9	9006.8
4.4	40	0.1	1.707032	5.093687	698.3	4816.4
21.1	70	25	-0.00107	24.93824	1296.9	8944.7
21.1	70	10	-0.00107	9.975294	927.5	6396.7
21.1	70	5	-0.00107	4.987647	691.9	4771.8
21.1	70	1	-0.00107	0.997529	327.0	2255.2
21.1	70	0.5	-0.00107	0.498765	238.0	1641.3
21.1	70	0.1	-0.00107	0.099753	126.5	872.3
37.8	100	25	-1.52609	0.744473	285.4	1968.1
37.8	100	10	-1.52609	0.297789	190.6	1314.6
37.8	100	5	-1.52609	0.148895	145.4	1003.0
37.8	100	1	-1.52609	0.029779	89.7	619.0
37.8	100	0.5	-1.52609	0.014889	77.5	534.5
37.8	100	0.1	-1.52609	0.002978	61.7	425.3
54.4	130	25	-2.89596	0.031767	91.1	628.6
54.4	130	10	-2.89596	0.012707	75.3	519.3
54.4	130	5	-2.89596	0.006353	67.5	465.7
54.4	130	1	-2.89596	0.001271	57.2	394.8
54.4	130	0.5	-2.89596	0.000635	54.8	377.8
54.4	130	0.1	-2.89596	0.000127	51.4	354.4

Table C5: MEPDG Input –SP B 4050

Temp C	Temp F	Frequency Hz	Shift Factor	Reduced Frequency	E* ksi	E* MPa
-10.0	14	25	2.170991	3706.215	3312.0	22842.7
-10.0	14	10	2.170991	1482.486	3289.2	22685.8
-10.0	14	5	2.170991	741.2431	3265.3	22520.6
-10.0	14	1	2.170991	148.2486	3175.1	21898.9
-10.0	14	0.5	2.170991	74.12431	3114.7	21481.7
-10.0	14	0.1	2.170991	14.82486	2895.4	19969.8
4.4	40	25	1.102183	316.3171	3224.8	22241.8
4.4	40	10	1.102183	126.5268	3162.7	21813.2
4.4	40	5	1.102183	63.26342	3098.4	21369.7
4.4	40	1	1.102183	12.65268	2866.2	19768.5
4.4	40	0.5	1.102183	6.326342	2718.9	18752.5
4.4	40	0.1	1.102183	1.265268	2237.4	15431.6
21.1	70	25	-0.00069	24.9601	2980.8	20558.7
21.1	70	10	-0.00069	9.984041	2819.6	19446.8
21.1	70	5	-0.00069	4.992021	2660.7	18351.0
21.1	70	1	-0.00069	0.998404	2149.6	14825.5
21.1	70	0.5	-0.00069	0.499202	1870.7	12902.5
21.1	70	0.1	-0.00069	0.09984	1160.3	8002.8
37.8	100	25	-0.98535	2.585747	2476.4	17080.0
37.8	100	10	-0.98535	1.034299	2162.9	14917.7
37.8	100	5	-0.98535	0.517149	1885.6	13005.2
37.8	100	1	-0.98535	0.10343	1175.7	8109.0
37.8	100	0.5	-0.98535	0.051715	886.1	6111.1
37.8	100	0.1	-0.98535	0.010343	379.1	2614.7
54.4	130	25	-1.86984	0.337366	1701.7	11736.8
54.4	130	10	-1.86984	0.134946	1293.0	8918.0
54.4	130	5	-1.86984	0.067473	993.7	6853.3
54.4	130	1	-1.86984	0.013495	443.6	3059.4
54.4	130	0.5	-1.86984	0.006747	291.4	2010.0
54.4	130	0.1	-1.86984	0.001349	102.4	706.2

Table C6: MEPDG Input –SP B 80/100

Temp C	Temp F	Frequency Hz	Shift Factor	Reduced Frequency	E* ksi	E* MPa
-10.0	14	25	2.541122	8690.843	3081.9	21255.8
-10.0	14	10	2.541122	3476.337	2971.7	20495.6
-10.0	14	5	2.541122	1738.169	2863.5	19749.4
-10.0	14	1	2.541122	347.6337	2509.2	17305.9
-10.0	14	0.5	2.541122	173.8169	2307.1	15911.8
-10.0	14	0.1	2.541122	34.76337	1735.4	11969.2
4.4	40	25	1.290093	487.5659	2596.8	17910.0
4.4	40	10	1.290093	195.0264	2342.7	16157.7
4.4	40	5	1.290093	97.51318	2116.2	14595.6
4.4	40	1	1.290093	19.50264	1509.1	10408.3
4.4	40	0.5	1.290093	9.751318	1238.7	8543.6
4.4	40	0.1	1.290093	1.950264	690.2	4760.2
21.1	70	25	-0.00081	24.95331	1606.1	11077.0
21.1	70	10	-0.00081	9.981323	1247.7	8605.2
21.1	70	5	-0.00081	4.990661	991.5	6838.5
21.1	70	1	-0.00081	0.998132	517.5	3569.3
21.1	70	0.5	-0.00081	0.499066	377.7	2604.8
21.1	70	0.1	-0.00081	0.099813	180.6	1245.7
37.8	100	25	-1.15335	1.756279	660.7	4557.0
37.8	100	10	-1.15335	0.702512	441.8	3047.4
37.8	100	5	-1.15335	0.351256	320.9	2213.2
37.8	100	1	-1.15335	0.070251	155.2	1070.3
37.8	100	0.5	-1.15335	0.035126	117.2	808.2
37.8	100	0.1	-1.15335	0.007025	68.8	474.7
54.4	130	25	-2.18863	0.161925	224.4	1547.5
54.4	130	10	-2.18863	0.06477	150.0	1034.2
54.4	130	5	-2.18863	0.032385	113.6	783.5
54.4	130	1	-2.18863	0.006477	67.3	464.4
54.4	130	0.5	-2.18863	0.003238	56.8	391.6
54.4	130	0.1	-2.18863	0.000648	42.7	294.4

Table C7: MEPDG Input –DBM 40/50

Temp C	Temp F	Frequency Hz	Shift Factor	Reduced Frequency	E* ksi	E* MPa
-10.0	14	25	2.406749	6378.064	3324.3	22927.6
-10.0	14	10	2.406749	2551.226	3303.1	22781.2
-10.0	14	5	2.406749	1275.613	3279.2	22616.6
-10.0	14	1	2.406749	255.1226	3179.9	21931.9
-10.0	14	0.5	2.406749	127.5613	3107.6	21433.3
-10.0	14	0.1	2.406749	25.51226	2824.6	19481.0
4.4	40	25	1.221874	416.6908	3218.6	22199.0
4.4	40	10	1.221874	166.6763	3138.3	21644.7
4.4	40	5	1.221874	83.33817	3050.5	21039.5
4.4	40	1	1.221874	16.66763	2713.8	18717.2
4.4	40	0.5	1.221874	8.333817	2494.6	17205.5
4.4	40	0.1	1.221874	1.666763	1806.8	12461.5
21.1	70	25	-0.00077	24.95577	2819.2	19444.4
21.1	70	10	-0.00077	9.98231	2556.5	17632.1
21.1	70	5	-0.00077	4.991155	2300.6	15867.3
21.1	70	1	-0.00077	0.998231	1553.8	10716.2
21.1	70	0.5	-0.00077	0.499115	1214.3	8374.9
21.1	70	0.1	-0.00077	0.099823	578.3	3988.4
37.8	100	25	-1.09236	2.021072	1899.6	13101.8
37.8	100	10	-1.09236	0.808429	1449.0	9994.0
37.8	100	5	-1.09236	0.404214	1115.7	7694.8
37.8	100	1	-1.09236	0.080843	518.5	3576.3
37.8	100	0.5	-1.09236	0.040421	360.9	2489.0
37.8	100	0.1	-1.09236	0.008084	167.6	1155.7
54.4	130	25	-2.07289	0.211372	837.8	5778.1
54.4	130	10	-2.07289	0.084549	530.7	3660.6
54.4	130	5	-2.07289	0.042274	369.4	2547.7
54.4	130	1	-2.07289	0.008455	170.7	1177.4
54.4	130	0.5	-2.07289	0.004227	130.9	903.1
54.4	130	0.1	-2.07289	0.000845	85.0	586.5

Table C8: MEPDG Input –DBM 80/100

Temp C	Temp F	Frequency Hz	Shift Factor	Reduced Frequency	E* ksi	E* MPa
-10.0	14	25	2.635534	10801.24	3197.5	22053.2
-10.0	14	10	2.635534	4320.495	3123.7	21544.5
-10.0	14	5	2.635534	2160.247	3048.1	21022.5
-10.0	14	1	2.635534	432.0495	2780.8	19179.0
-10.0	14	0.5	2.635534	216.0247	2616.0	18042.4
-10.0	14	0.1	2.635534	43.20495	2103.1	14505.1
4.4	40	25	1.338025	544.4586	2828.5	19508.3
4.4	40	10	1.338025	217.7834	2618.1	18057.0
4.4	40	5	1.338025	108.8917	2419.6	16687.9
4.4	40	1	1.338025	21.77834	1837.5	12673.2
4.4	40	0.5	1.338025	10.88917	1554.1	10718.8
4.4	40	0.1	1.338025	2.177834	928.6	6404.8
21.1	70	25	-0.00084	24.95157	1891.8	13047.8
21.1	70	10	-0.00084	9.98063	1518.2	10471.1
21.1	70	5	-0.00084	4.990315	1237.2	8532.7
21.1	70	1	-0.00084	0.998063	684.8	4723.3
21.1	70	0.5	-0.00084	0.499031	513.3	3540.3
21.1	70	0.1	-0.00084	0.099806	263.9	1819.9
37.8	100	25	-1.1962	1.591265	824.4	5685.9
37.8	100	10	-1.1962	0.636506	568.6	3921.8
37.8	100	5	-1.1962	0.318253	424.4	2926.9
37.8	100	1	-1.1962	0.063651	222.6	1535.4
37.8	100	0.5	-1.1962	0.031825	175.4	1209.4
37.8	100	0.1	-1.1962	0.006365	114.2	787.4
54.4	130	25	-2.26994	0.134276	296.8	2046.7
54.4	130	10	-2.26994	0.05371	209.4	1444.2
54.4	130	5	-2.26994	0.026855	166.2	1146.2
54.4	130	1	-2.26994	0.005371	110.2	760.2
54.4	130	0.5	-2.26994	0.002686	97.2	670.6
54.4	130	0.1	-2.26994	0.000537	79.8	550.1

APPENDIX D

REGRESSION MODEL OUTPUTS

Iteration History for Wearing Course Mixtures[b]

Iteration Number[a]	Residual Sum of Squares	Parameter			
		a	b	c	d
1.0	4.095E10	.100	.100	.100	.100
1.1	1.667E189	6.982	15.995	23.548	12.172
1.2	3.931E20	.792	1.702	2.459	1.314
1.3	4.094E10	.169	.260	.336	.221
2.0	4.094E10	.169	.260	.336	.221
2.1	4.093E10	.194	.294	.383	.247
3.0	4.093E10	.194	.294	.383	.247
3.1	4.091E10	.228	.334	.438	.277
4.0	4.091E10	.228	.334	.438	.277
4.1	4.088E10	.271	.377	.496	.310
5.0	4.088E10	.271	.377	.496	.310
5.1	4.082E10	.323	.420	.555	.343
6.0	4.082E10	.323	.420	.555	.343
6.1	4.071E10	.385	.464	.614	.376
7.0	4.071E10	.385	.464	.614	.376
7.1	4.049E10	.459	.508	.672	.409
8.0	4.049E10	.459	.508	.672	.409
8.1	4.009E10	.546	.551	.728	.441
9.0	4.009E10	.546	.551	.728	.441
9.1	3.935E10	.647	.593	.784	.473
10.0	3.935E10	.647	.593	.784	.473
10.1	3.809E10	.762	.633	.837	.504
11.0	3.809E10	.762	.633	.837	.504
11.1	3.593E10	.906	.674	.891	.536
12.0	3.593E10	.906	.674	.891	.536
12.1	3.301E10	1.084	.713	.945	.569
13.0	3.301E10	1.084	.713	.945	.569
13.1	3.140E10	1.340	.700	.962	.613
14.0	3.140E10	1.340	.700	.962	.613

	14.1	3.050E10	1.588	.620	.924	.651
	15.0	3.050E10	1.588	.620	.924	.651
	15.1	2.843E10	2.086	.465	.861	.734
	16.0	2.843E10	2.086	.465	.861	.734
	16.1	2.279E10	3.038	.153	.746	.924
	17.0	2.279E10	3.038	.153	.746	.924
	17.1	8.078E9	4.901	-.329	.384	1.304
	18.0	8.078E9	4.901	-.329	.384	1.304
	18.1	1.412E10	14.638	-.425	.054	1.172
	18.2	4.388E9	6.595	-.399	.093	1.414
	19.0	4.388E9	6.595	-.399	.093	1.414
	19.1	4.886E9	11.969	-.462	.146	1.284
	19.2	3.734E9	8.672	-.460	.146	1.365
	20.0	3.734E9	8.672	-.460	.146	1.365
	20.1	3.787E9	13.078	-.451	.146	1.285
	20.2	3.592E9	10.605	-.450	.147	1.331
	21.0	3.592E9	10.605	-.450	.147	1.331
	21.1	3.518E9	14.530	-.452	.147	1.274
	22.0	3.518E9	14.530	-.452	.147	1.274
	22.1	3.316E9	18.533	-.453	.148	1.239
	23.0	3.316E9	18.533	-.453	.148	1.239
	23.1	3.294E9	26.553	-.456	.147	1.175
	24.0	3.294E9	26.553	-.456	.147	1.175
	24.1	3.038E9	30.602	-.458	.148	1.163
	25.0	3.038E9	30.602	-.458	.148	1.163
	25.1	2.963E9	38.679	-.459	.147	1.122
	26.0	2.963E9	38.679	-.459	.147	1.122
	26.1	2.860E9	46.772	-.461	.147	1.093
	27.0	2.860E9	46.772	-.461	.147	1.093
	27.1	2.816E9	62.964	-.464	.147	1.040
	28.0	2.816E9	62.964	-.464	.147	1.040
	28.1	2.670E9	79.173	-.467	.147	1.007

	29.0	2.670E9	79.173	-.467	.147	1.007
	29.1	2.687E9	111.593	-.470	.146	.946
	29.2	2.592E9	94.066	-.469	.146	.982
	30.0	2.592E9	94.066	-.469	.146	.982
	30.1	2.563E9	123.854	-.471	.146	.933
	31.0	2.563E9	123.854	-.471	.146	.933
	31.1	2.462E9	153.650	-.474	.146	.902
	32.0	2.462E9	153.650	-.474	.146	.902
	32.1	2.499E9	213.242	-.478	.145	.843
	32.2	2.410E9	177.181	-.476	.146	.881
	33.0	2.410E9	177.181	-.476	.146	.881
	33.1	2.393E9	224.243	-.479	.145	.840
	34.0	2.393E9	224.243	-.479	.145	.840
	34.1	2.343E9	271.308	-.482	.145	.812
	35.0	2.343E9	271.308	-.482	.145	.812
	35.1	2.386E9	365.438	-.485	.144	.759
	35.2	2.317E9	301.200	-.484	.145	.797
	36.0	2.317E9	301.200	-.484	.145	.797
	36.1	2.310E9	360.984	-.486	.144	.766
	37.0	2.310E9	360.984	-.486	.144	.766
	37.1	2.295E9	420.770	-.488	.144	.742
	38.0	2.295E9	420.770	-.488	.144	.742
	38.1	2.290E9	480.555	-.490	.144	.722
	39.0	2.290E9	480.555	-.490	.144	.722
	39.1	2.287E9	494.142	-.491	.144	.719
	40.0	2.287E9	494.142	-.491	.144	.719
	40.1	2.287E9	495.401	-.492	.144	.719
	41.0	2.287E9	495.401	-.492	.144	.719
	41.1	2.287E9	495.496	-.492	.144	.719
	42.0	2.287E9	495.496	-.492	.144	.719
	42.1	2.287E9	495.522	-.492	.144	.718

Derivatives are calculated numerically.

a. Major iteration number is displayed to the left of the decimal, and minor iteration number is to the right of the decimal.

b. Run stopped after 92 model evaluations and 42 derivative evaluations because the relative reduction between successive residual sums of squares is at most SSCON = 1.00E-008.

Parameter Estimates

Parameter		Estimate	Std. Error	95% Confidence Interval	
				Lower Bound	Upper Bound
dimension0	a	495.522	123.956	251.534	739.510
	b	-.492	.016	-.523	-.460
	c	.144	.009	.126	.161
	d	.718	.041	.637	.800

Correlations of Parameter Estimates

	a	b	c	d
a	1.000	-.131	-.057	-.988
b	-.131	1.000	.000	.000
c	-.057	.000	1.000	.000
d	-.988	.000	.000	1.000

ANOVA[a]

Source	Sum of Squares	df	Mean Squares
Regression	3.866E10	4	9.666E9
Residual	2.287E9	284	8051236.532
Uncorrected Total	4.095E10	288	
Corrected Total	1.717E10	287	

Dependent variable: DynamicModulus

a. R squared = 1 - (Residual Sum of Squares) / (Corrected Sum of Squares) = .867.

Iteration History for Base Course Mixtures[b]

Iteration Number[a]	Residual Sum of Squares	Parameter			
		a	b	c	d
1.0	4.095E10	.100	.100	.100	.100
1.1	5.237E184	6.668	15.302	22.461	14.261
1.2	9.831E19	.760	1.630	2.348	1.523
1.3	4.094E10	.166	.253	.325	.242
2.0	4.094E10	.166	.253	.325	.242
2.1	4.093E10	.192	.288	.374	.274
3.0	4.093E10	.192	.288	.374	.274
3.1	4.092E10	.226	.330	.430	.311
4.0	4.092E10	.226	.330	.430	.311
4.1	4.089E10	.269	.373	.489	.350
5.0	4.089E10	.269	.373	.489	.350
5.1	4.084E10	.321	.417	.549	.389
6.0	4.084E10	.321	.417	.549	.389
6.1	4.074E10	.383	.462	.608	.428
7.0	4.074E10	.383	.462	.608	.428
7.1	4.055E10	.457	.506	.666	.466
8.0	4.055E10	.457	.506	.666	.466
8.1	4.019E10	.544	.549	.723	.503
9.0	4.019E10	.544	.549	.723	.503
9.1	3.953E10	.645	.592	.779	.539
10.0	3.953E10	.645	.592	.779	.539
10.1	3.838E10	.762	.633	.833	.575
11.0	3.838E10	.762	.633	.833	.575
11.1	3.660E10	.893	.672	.882	.608
12.0	3.660E10	.893	.672	.882	.608
12.1	3.385E10	1.060	.711	.935	.644
13.0	3.385E10	1.060	.711	.935	.644

	13.1	3.155E10	1.301	.737	.980	.688
	14.0	3.155E10	1.301	.737	.980	.688
	14.1	3.087E10	1.548	.671	.947	.722
	15.0	3.087E10	1.548	.671	.947	.722
	15.1	2.943E10	2.030	.540	.891	.796
	16.0	2.943E10	2.030	.540	.891	.796
	16.1	2.593E10	2.939	.286	.800	.960
	17.0	2.593E10	2.939	.286	.800	.960
	17.1	1.742E10	4.487	-.125	.597	1.282
	18.0	1.742E10	4.487	-.125	.597	1.282
	18.1	1.326E10	10.523	-.389	-.069	1.559
	19.0	1.326E10	10.523	-.389	-.069	1.559
	19.1	7.908E9	17.492	-.463	.125	1.438
	20.0	7.908E9	17.492	-.463	.125	1.438
	20.1	8.259E9	31.845	-.409	.148	1.275
	20.2	7.316E9	23.221	-.408	.148	1.367
	21.0	7.316E9	23.221	-.408	.148	1.367
	21.1	7.171E9	34.819	-.412	.151	1.281
	22.0	7.171E9	34.819	-.412	.151	1.281
	22.1	6.657E9	46.467	-.410	.152	1.237
	23.0	6.657E9	46.467	-.410	.152	1.237
	23.1	6.467E9	69.767	-.412	.153	1.152
	24.0	6.467E9	69.767	-.412	.153	1.152
	24.1	5.916E9	93.091	-.412	.154	1.108
	25.0	5.916E9	93.091	-.412	.154	1.108
	25.1	5.697E9	139.741	-.415	.153	1.023
	26.0	5.697E9	139.741	-.415	.153	1.023
	26.1	5.122E9	186.404	-.416	.154	.980
	27.0	5.122E9	186.404	-.416	.154	.980
	27.1	4.890E9	279.729	-.420	.154	.896
	28.0	4.890E9	279.729	-.420	.154	.896
	28.1	4.308E9	373.060	-.423	.155	.853

	29.0	4.308E9	373.060	-.423	.155	.853
	29.1	4.091E9	559.723	-.428	.153	.770
	30.0	4.091E9	559.723	-.428	.153	.770
	30.1	3.529E9	746.389	-.434	.154	.728
	31.0	3.529E9	746.389	-.434	.154	.728
	31.1	3.370E9	1119.721	-.442	.152	.645
	32.0	3.370E9	1119.721	-.442	.152	.645
	32.1	2.869E9	1493.054	-.450	.151	.604
	33.0	2.869E9	1493.054	-.450	.151	.604
	33.1	2.825E9	2239.721	-.461	.149	.521
	34.0	2.825E9	2239.721	-.461	.149	.521
	34.1	2.437E9	2613.055	-.468	.149	.511
	35.0	2.437E9	2613.055	-.468	.149	.511
	35.1	2.380E9	3359.723	-.475	.146	.461
	36.0	2.380E9	3359.723	-.475	.146	.461
	36.1	2.311E9	4106.391	-.485	.145	.429
	37.0	2.311E9	4106.391	-.485	.145	.429
	37.1	2.288E9	4611.898	-.490	.144	.411
	38.0	2.288E9	4611.898	-.490	.144	.411
	38.1	2.287E9	4666.778	-.492	.144	.411
	39.0	2.287E9	4666.778	-.492	.144	.411
	39.1	2.287E9	4673.509	-.492	.144	.411
	40.0	2.287E9	4673.509	-.492	.144	.411
	40.1	2.287E9	4673.755	-.492	.144	.411
	41.0	2.287E9	4673.755	-.492	.144	.411
	41.1	2.287E9	4673.940	-.492	.144	.411

Derivatives are calculated numerically.

a. Major iteration number is displayed to the left of the decimal, and minor iteration number is to the right of the decimal.

b. Run stopped after 85 model evaluations and 41 derivative evaluations because the relative reduction between successive residual sums of squares is at most SSCON = 1.00E-008.

Parameter Estimates

Parameter	Estimate	Std. Error	95% Confidence Interval	
			Lower Bound	Upper Bound
a	4673.940	581.655	3529.039	5818.841
b	-.492	.016	-.523	-.460
c	.144	.009	.126	.161
d	.411	.024	.364	.457

Correlations of Parameter Estimates

	a	b	c	d
a	1.000	-.263	-.114	-.951
b	-.263	1.000	.000	.000
c	-.114	.000	1.000	.000
d	-.951	.000	.000	1.000

ANOVA[a]

Source	Sum of Squares	df	Mean Squares
Regression	3.866E10	4	9.666E9
Residual	2.287E9	284	8051236.533
Uncorrected Total	4.095E10	288	
Corrected Total	1.717E10	287	

Dependent variable: Dynamic Modulus

a. R squared = 1 - (Residual Sum of Squares) / (Corrected Sum of Squares) = .867.